

Instrumenting and Validating a Vibrotactile Device to Assess and Rehabilitate Dynamic Seated  
Balance

by

Andrew D. Williams

A thesis submitted in partial fulfillment of the requirements for the degree of

Master of Science

Department of Biomedical Engineering

University of Alberta

© Andrew D. Williams, 2017

## Abstract

Tools that effectively assess and train dynamic seated balance are critical for enhancing functional independence and reducing risk of secondary health complications in the elderly and individuals with neuromuscular impairments. On the one hand, current assessment tools quantify changes in the integrity of the postural control system by measuring biomechanical characteristics of balance during postural perturbations. On the other hand, current training tools augment inherent sensory systems with encoded sensory cues that pertain to balance performance. However, these methods are complex or costly and, thus, have limited potential to serve as clinical assessment or training tools. The objective of this thesis research was to devise and validate a portable tool for assessing and training dynamic sitting balance. An instrumented wobble board was designed and constructed that can: (1) elicit multidirectional perturbations in seated individuals; (2) quantify seated balance proficiency; and (3) provide kinematics-based vibrotactile feedback. Interchangeable, curved bases were designed to elicit modular levels of seated instability in all tilt directions. An embedded, inertial measurement unit was used to estimate the tilt angle and direction, whereas eight vibrating tactors displayed feedback cues on the sitting surface. A microprocessor encoded the vibrotactile stimulation based on the wobble board's tilt angle and speed, similar to sensory augmentation devices that improve balance-impaired standing. After performing a technical validation study to compare kinematic wobble board measurements against a gold-standard motion capture system, twelve non-disabled participants performed a dynamic sitting task using the wobble board. Posturographic analyses in time and frequency domain as well as stabilogram diffusion analyses were used to characterize sitting balance for three different conditions: (1) with eyes open and closed; (2) with two different levels of seated instability; and (3) with vibrotactile feedback on and off. Our results demonstrate that the tilt angle measurements were highly accurate throughout the range of

wobble board dynamics. Furthermore, the posturographic analyses for the dynamic sitting task revealed that the wobble board can effectively discriminate between the three conditions of perturbed balance, demonstrating the potential for the wobble board to serve as a clinical tool for the assessment and training of seated balance. Unlike similar instrumented tools, the wobble board is portable, requires no laboratory equipment, and can be adjusted to meet the user's balance abilities. While future work is warranted, this thesis contributes to the knowledge of assessment and training techniques for seated balance. Obtained findings will aid in effective translation of such techniques to a clinical setting, which has the potential to enhance diagnosis and prognosis for individuals with seated balance impairments.

## Preface

Some of the research conducted for this thesis forms part of a research collaboration, led by Assistant Professor Albert H. Vette at the University of Alberta. The technical apparatus described in Chapter 3 was developed by efforts of the undergraduate design group *Pivotal Solutions*, Quinn Boser, Animesh Kumawat, Kshitij Agarwal, Albert Vette, and myself. The experimental validation in Chapter 4 and concluding analysis in Chapter 5 are my original work, as well as the literature review in Chapter 2. A modified version of Chapter 3 has been accepted as a special session manuscript at the upcoming *2017 IEEE International Conference on Systems, Man, and Cybernetics* (IEEE SMC 2017). A modified version of Chapter 4, including the technical description and validation from Chapter 3, will be submitted as: *AD Williams, QA Boser, A Kumawat, K Agarwal, H Rouhani, and AH Vette, "An instrumented wobble board for assessing and training dynamic sitting balance"* to the *ASME Journal of Biomechanical Engineering*. I was responsible for the apparatus assembly, motion measurement implementation, vibrotactile feedback implementation, development of the user interface, experimental protocol design, experimental data collection and analysis, and manuscript conceptualization and preparation. Quinn Boser was responsible for production of the structural components and contributed to manuscript revisions. Animesh Kumawat selected the factors for providing vibrational feedback. Kshitij Agarwal selected the inertial measurement unit for motion measurement and contributed to manuscript revisions. Albert Vette was the supervisory author and was involved in concept formation, device development, and manuscript preparation. The human research described in Chapter 4 received human research ethics approval from the Health Research Ethics Board of the University of Alberta, Project Name "Use of Stochastic Resonance for Improving Postural Control in the Elderly and Individuals Post-Stroke", HREB Pro00039437, June 24, 2013.

## Acknowledgments

I owe my sincere thanks to all those individuals who have contributed to my scientific, professional, and personal development over the last two and a half years.

The most important mentor in my academic and personal ambitions of the last three years is undoubtedly my MSc supervisor, Dr. Albert Vette. He challenged me to perform excellent research and continuously empowered my efforts to do so, providing invaluable guidance, encouragement, and criticism whenever necessary. His example of mindful intelligence and impassioned ethic is one I strive to emulate. I could not be more fortunate and grateful to have spent the last three years under Albert's mentorship.

I appreciate the other half of my supervisory committee, Dr. Hossein Rouhani, who provided scientific feedback and professional support. I thank those colleagues who were instrumental to my personal development and the research presented here: Austin Azar, Kshitij Agarwal, Alireza Noamani, Quinn Boser, Fatemeh Gholibeigian, Brad Roberts, McNiel Keri, Hosein Bahari, Jeremy Hall, and Animesh Kumawat. I also thank all members of the Glenrose Rehabilitation Hospital Research Centre, who provided me with a vision for improving public health through research, and of the Neuromuscular Control and Biomechanics Laboratory, who provided a wealth of expertise in topics such as signal processing and kinematic analysis.

I am grateful for the funding support provided by the Discovery Grant from the Natural Sciences & Engineering Research Council of Canada.

Finally, I thank my parents, for expecting and supporting my best effort in all aspects of life.

# Table of Contents

<b>Preface</b> .....	<b>iv</b>
<b>Acknowledgments</b> .....	<b>v</b>
<b>Table of Contents</b> .....	<b>vi</b>
<b>List of Tables</b> .....	<b>x</b>
<b>List of Figures</b> .....	<b>xii</b>
<b>1 Introduction</b> .....	<b>1</b>
1.1 Motivation.....	1
1.2 Quantitative Assessment of Dynamic Seated Stability.....	2
1.3 Training of Dynamic Sitting Stability via Sensory Augmentation.....	3
1.4 Thesis Objective.....	4
1.5 Thesis Outline .....	4
<b>2 Literature Review</b> .....	<b>6</b>
2.1 Overview.....	6
2.2 Dynamics and Control of Upright Sitting.....	6
2.2.1 Role of Vision in Balance Control.....	10
2.2.2 Role of Auditory System in Balance Control .....	11
2.2.3 Role of Vestibular System in Balance Control.....	11
2.2.4 Role of Proprioception in Balance Control.....	12
2.2.5 Effect of Cognitive Load on Balance Control .....	12
2.3 Methods for Assessing Seated Balance .....	13
2.3.1 Traditional Assessment Methods.....	13
2.3.2 Quantitative Assessment Methods.....	13
2.3.3 Dynamic Sitting Assessment Methods .....	15

2.4	Sensory Augmentation Methods for Improving Seated Balance.....	21
2.4.1	Traditional Seated Balance Therapies .....	21
2.4.2	Sensory Augmentation Methods.....	22
2.5	Conclusions.....	25
<b>3</b>	<b>Development of an Instrumented Device to Assess and Train Seated Balance.....</b>	<b>27</b>
3.1	Introduction.....	27
3.2	Methods.....	27
3.2.1	Design of the Instrumented Wobble Board .....	27
3.2.2	Validation of Kinematic Measurements .....	35
3.3	Results.....	37
3.3.1	Validity of the IMU Measurements .....	37
3.4	Discussion.....	39
3.4.1	Potential of Dynamic Sitting Assessment Device .....	39
3.4.2	Potential of Vibrotactile Feedback Device .....	41
3.5	Conclusions.....	42
<b>4</b>	<b>Utility of Instrumented Wobble Board for Balance Assessment and Sensory Augmentation during Balance Training.....</b>	<b>44</b>
4.1	Introduction.....	44
4.2	Methods.....	44
4.2.1	Participants.....	44
4.2.2	Experimental Protocol .....	45
4.2.3	Data Processing.....	47
4.2.4	Posturographic Analysis .....	48
4.2.5	Statistical Analysis.....	48
4.3	Results.....	49
4.3.1	Response of Vibrotactile Display .....	49

4.3.2	Sample Characteristics.....	50
4.3.3	Correlation of Posturographic Measures .....	51
4.3.4	Effects of Participant Anthropometry on Posturographic Measures .....	53
4.3.5	Effects of Base Curvature on Posturographic Measures.....	53
4.3.6	Effects of Eye Condition on Posturographic Measures .....	56
4.3.7	Effects of Vibrotactile Feedback on Posturographic Measures.....	56
4.3.8	Effects of Learning and Fatigue on Posturographic Measures .....	61
4.4	Discussion.....	61
4.4.1	Sensitivity and Independence of Posturographic Measures.....	62
4.4.2	Modularity of Unstable Sitting Task.....	64
4.4.3	Quantitative Assessment of Conditioned Responses.....	64
4.4.4	Potential for Enhancement of Training by Vibrotactile Feedback .....	66
4.5	Conclusions.....	67
<b>5</b>	<b>Conclusion.....</b>	<b>68</b>
5.1	Future Directions .....	69
	<b>References.....</b>	<b>71</b>
	<b>Appendices.....</b>	<b>A1</b>
	Appendix A: Selection and Calculation of Posturographic Measures .....	A1
	Selecting Posturographic Measures .....	A4
	Calculating Selected Measures .....	A6
	Appendix B: Bill of Materials.....	A11
	Appendix C: Estimating Tilt Angles from Motion Capture Measurements .....	A14
	Cardan Angle Method.....	A15
	Projection Method.....	A15
	Comparison.....	A16
	Appendix D: Preliminary Protocol .....	A17

Method .....	A17
Results.....	A18
Discussion.....	A20
Appendix E: Filtering Kinematic Time Series.....	A21

## List of Tables

Table 1-1: Prevalence of neuromuscular disorders that may impair trunk stability in Canada (Statistics Canada, 2012). .....	1
Table 3-1: Geometrical properties of the interchangeable bases from most stable (Base #1) to least stable (Base #5). .....	28
Table 3-2: Accuracy results for the IMU tilt angle measurements from twelve displacement tests and their mean and standard deviation (SD).....	38
Table 4-1: Participant characteristics.....	45
Table 4-2: Schedule of 30-s trials in one exemplary block of ten trials (shown: base #2 with eyes closed). In random order, four blocks were attempted: one for each unique combination of base and eye conditions. The horizontal line between trials 4 and 5 represents the end of the familiarization trials. In trials 5 through 10, the vibration condition was randomized so that exactly 3 trials were control (no feedback) trials.....	46
Table 4-3: Summary of explanatory variables used in mixed linear model of balance trials.....	49
Table 4-4: Summary of completed balance trials in each task condition. Trials in bold were excluded from the analysis because the participant lost balance in half or more of the balance trials for that task condition (in the case of Participant 11, all trials were excluded because the participant lost balance in half or more trials in all but one of the task conditions, so comparisons between conditions were unreliable). .....	51
Table 4-5: Matrix of correlation coefficients for posturographic measures derived from AP, ML, and TM tilt angles (coefficients greater than 0.60 are in bold).....	52
Table 4-6: Correlation coefficients for the weight and height of each participant and the average of their posturographic measures from trials on base #2. ....	53

Table 4-7: Posturographic measures derived from AP and ML tilts during upright sitting trials under each experimental condition. Average measures and their standard deviation were calculated for each participant, then averaged per condition across all participants. Shown in brackets is the average of within-participant standard deviations. .... 55

Table 4-8: Estimated effect of experimental conditions on posturographic measures derived from tilt angles in each direction. Effects include: base (BASE: the estimated change in the posturographic measure when the radius of curvature is decreased, i.e., when the surface is less stable), eye (EYE: the estimated change in the posturographic measure when visual input is removed, i.e., when eyes are closed), vibration (VIB: the estimated change in the posturographic measure when the vibrotactile feedback is provided, i.e., compared to control trials with no feedback), and trials since last rest (TR: the estimated change in the posturographic measure when progressing from one trial to the next). Shown are the estimated coefficients of the linear mixed models, their standard error, and the probability that the F-statistic derived from the ANOVA in the mixed-effects model is observed under the hypothesis that the factor has no effect on the posturographic measure. Effects in bold are considered significant after a Bonferroni correction for multiple comparisons ( $\alpha_{\text{adjusted}} = 0.0014$ ). .... 57

## List of Figures

Figure 2-1: A simplified linkage of body segments. The purple segment indicates an upright configuration of the HAT segment. The center of mass (COM), center of pressure (COP), sagittal joint torque and support surface reaction are labelled. ....	8
Figure 2-2: A basic model of seated balance control. From a control perspective, the reactive balance control system consists of a plant, monitored by sensory systems, actuated by muscular tissue and controlled by the central nervous system. Human body dynamics are modelled by an inverted pendulum model. The input is the sum of torques generated by passive dynamics, neuromuscular controlled active dynamics, and external perturbations. The output is the deviation of the COM from a reference posture, sensed by proprioceptive, visual, and vestibular systems affected by sensory perturbations. Adapted from [80], with permission (© 2014 - American Medical Directors Association, Inc.) .....	10
Figure 2-3: Stabilograms, showing the planar trajectory of the centre of pressure (COP) for a non-disabled, young individual during 15-s of sitting (SI) and standing (ST). Mediolateral (ML) and anteroposterior (AP) COP displacements are plotted along the x-axis and y-axis, respectively. Reprinted from [64], with permission (© 2009 IPEM). ....	14
Figure 2-4: A two-segment model (green: upper body; blue: lower body and support surface) of unstable sitting on a central pivot device. Reprinted from [69], with permission (© 2009 Elsevier Ltd).....	17
Figure 2-5: An unstable sitting apparatus with one degree of freedom for fundamental investigations of seated balance. Reprinted from [111], with permission (© 2014 Elsevier Ltd). ....	18
Figure 2-6: An unstable sitting device using a pivot and springs to elicit multidirectional perturbations and investigate postural stability during dynamic sitting. Reprinted from [35], with permission (© 2007 Elsevier Ltd).....	19

Figure 2-7: An unstable sitting apparatus with a hemispherical base that elicits multidirectional perturbations for fundamental investigations of dynamic sitting. Reprinted from [33], with permission (© 2015 Elsevier Inc). ..... 21

Figure 2-8: A participant equipped with inertial measurement unit and vibrating factors. Reprinted from [126], with permission (© 2001 IEEE). ..... 24

Figure 2-9: Sensor (top right), processor (top left) and vibrotactile display array (bottom) for balance training in vestibulopathic participants. Reprinted from [56] with permission (© 2008 IOS Press and the authors)..... 25

Figure 3-1: Schematic of the wobble board components, including: (1) the platform surface with holes for 8 holes for vibrotactile interfaces; (2) a steel extrusion for footrest attachment; (3) two clevis pins to secure the footrest; (4) a footrest module of adjustable height; and (5) one of five curved base modules. .... 29

Figure 3-2: Top view photograph of the wobble board with footrest attached (bottom) and the lid removed to reveal electronic instrumentation. Shown are: an inertial measurement unit housed by a custom-printed enclosure (center); a microprocessing board with universal serial bus connection (left); eight electronic vibrators held in custom-printed enclosures (mid-region); and a steel bar (top) to counterbalance the footrest..... 31

Figure 3-3: Two-part mounting enclosure for vibrating factors. A mounting hole in the factor enclosure (top) fitted loosely on a locating pin in the platform attachment (bottom) to minimize vibration dampening. .... 32

Figure 3-4: Schematic of the wobble board hardware and software integration. The inertial measurement unit and vibrotactile elements interface with an on-board microprocessor that, in turn, interfaces with custom-built LabVIEW software via USB. .... 33

Figure 3-5: Schematic of factor activation thresholds. Three factors are activated when the anteroposterior (AP) or mediolateral (ML) control signal surpasses the two-sided threshold in either direction. If both AP and ML control signals exceed respective thresholds simultaneously, five factors are activated. The cueing scheme is repulsive rather than attractive; factors are activated in the same direction as the tilt control signal. .... 34

Figure 3-6: LabVIEW interface for monitoring balance assessments, selecting vibrotactile feedback thresholds, and recording all time series and parametric data. The length and direction of the vector are proportional to the magnitude and direction of the feedback control signal, respectively. The rectangle on the graph visualizes the two feedback thresholds: when the vector moves outside of the rectangle (as shown here), vibrotactile cues are delivered to the sitting surface (here: via the three anterior tactors). ..... 35

Figure 3-7: ML (left) and AP (right) tilt angles measured by the gold-standard motion capture system (bold gray lines) and the inertial measurement unit (thin black lines) during five seconds of fast, multidirectional displacements, after demeaning and time synchronization. .... 38

Figure 4-1: Control signal time series in AP (top) and ML (bottom) directions during one 30-s balance trial (Participant 4, base #2, eyes open) with vibrotactile feedback. The gray time series represent the control signals (tilt angle plus one half of tilt velocity), whereas the black horizontal lines represent the two-sided thresholds for vibrotactile feedback. Bold lines indicate that tactors were active in the corresponding direction (front for positive AP, rear for negative AP, right for positive ML, left for negative ML). The vibrators were active (in at least one direction) for approximately 4.8 seconds, or 15.1% of the depicted balance trial. .... 50

Figure 4-2: Response of time-domain measures derived from AP (top) and ML (bottom) tilts to changes in base (decreased stability), eye (elimination of visual input), and vibration (addition of vibrotactile feedback) conditions. Circles indicate the estimated effect. Bars indicate the confidence intervals for effects, based on the Bonferroni-corrected confidence level ( $1 - \alpha_{\text{adjusted}} = 0.9986$ ). Black bars represent measures that are significantly different between conditions. .... 59

Figure 4-3: Response of frequency-domain measures derived from AP (top) and ML (bottom) tilts to changes in base (decreased stability), eye (elimination of visual input), and vibration (addition of vibrotactile feedback) conditions. Circles indicate the estimated effect. Bars indicate the confidence intervals for effects, based on the Bonferroni-corrected confidence level ( $1 - \alpha_{\text{adjusted}} = 0.9986$ ). Black bars represent measures that are significantly different between conditions. .... 60

Figure 4-4: Response of stabilogram diffusion measures derived from AP (top) and ML (bottom) tilts to changes in base (decreased stability), eye (elimination of visual input), and vibration

(addition of vibrotactile feedback) conditions. Circles indicate the estimated effect. Bars indicate the confidence intervals for effects, based on the Bonferroni-corrected confidence level ( $1 - \alpha_{\text{adjusted}} = 0.9986$ ). Black bars represent measures that are significantly different between conditions..... 61

# 1 Introduction

## 1.1 Motivation

During sitting, the human trunk relies on the integrity of the neuromuscular control system to maintain balance against the destabilizing effect of gravity and other challenges, such as those of manipulating objects with the hands or riding a train as it accelerates. Therefore, any pathology affecting sensorimotor control and output, including spatial orientation, degrades balance control [1]. Maintaining balance during sitting can pose a major challenge for individuals with spinal cord injury [2]–[4], a history of stroke [5]–[7], vestibular loss [8], or other neuromuscular impairment (Table 1-1), as well as many elderly individuals [9], [10]. Poor seated stability may reduce functional independence [2], increase the risk of falling [6], and lead to secondary health complications such as kyphosis, respiratory dysfunction, or pressure sores [3], [11]. The importance of stable sitting is reflected in the plethora of scientific and clinical efforts that attempt to: (1) characterize seated stability; and (2) improve sensorimotor function in individuals who have difficulties in maintaining seated balance.

**Table 1-1:** Prevalence of neuromuscular disorders that may impair trunk stability in Canada (Statistics Canada, 2012).

	Household Population 2010-2011	Institutional Population 2010-2011
Multiple Sclerosis	93,535	3,831
Cerebral Palsy	42,679	4,309
Muscular Dystrophy	23,350	496
Dystonia	13,328	625
Parkinson’s Disease	54,897	12,514
Effects of a Stroke	319,354	39,795
Brain Injury	133,812	5,504
Spinal Cord Injury	117,799	1,187

## 1.2 Quantitative Assessment of Dynamic Seated Stability

Traditional assessments of seated balance rely on subjective and qualitative measurements [9], [10], [12]–[14] and often fail to reliably identify the specific deficiencies and needs of a balance-impaired individual [15]–[17]. Conversely, advanced assessment tools can quantify seated posture by measuring biomechanical characteristics of the postural control system, e.g., the magnitude and location of forces exerted on the support surface [18]–[21] or the angular displacements of body segments in space [22]–[24]. In these cases, *posturographic measures* can then be used to summarize the variation of these biomechanical characteristics over time and frequency [25]. Such measures have been demonstrated to reliably detect changes in postural control effort and output and, hence, the quasi-static integrity of the postural control system during quiet, i.e., unperturbed upright sitting [19], [26]. While parameters measured in the absence of external perturbations can quantify stability in clinical populations [19]–[21], they may fail to assess the integrity of the postural control system that comes into play when reacting to external challenges such as an unstable support surface (e.g., when riding on a bus) or an altered sensory environment (e.g., in dim lighting) [26], [27]. In these cases, seated balance relies more heavily on the complex interactions of passive forces (primarily due to stiffness and damping of joints and connective tissue), sensory feedback, and active neuromuscular control. As such, artificial *postural perturbations* are needed to assess the function of control efforts that, while dormant during quasi-static sitting, are critical for preventing injury in more dynamic activities of daily living as described above [28].

Postural perturbations disturb mechanical or sensory environments to elicit a reactive response from the postural control system. The response can then be used to characterize the integrity or impairment of the system. A common approach is to destabilize the support surface, causing loss of balance unless corrected by dynamic response [23], [24], [29]–[46]. Near the limits of stability, individuals rely on reactive control to maintain upright sitting, allowing trunk control deficits to be identified. For example, stroke survivors exhibit degraded postural control compared to non-disabled, older adults *only while sitting on an unstable surface*; no differences between groups can be observed during quasi-static sitting [26].

On the one hand, unstable support surfaces are commonly used to investigate *fundamental* aspects of human postural control – for example, to characterize the role of visual input in

maintaining seated balance [30]. On the other hand, unstable surfaces could be used to assess dynamic sitting ability in a *clinical* setting. Such methodology is commonly used to also assess dynamic standing ability; for example, the Motor Control Test using the EquiTest device (NeuroCom International, Clackamas, OR, USA) perturbs the standing surface [47] and has been used to objectively assess balance proficiency in stroke survivors [48] and quantify the effects of novel balance aids [49] by measuring parameters such as latency and velocity of body displacement. However, many of the tools used to evaluate balance focus on standing and walking rather than seated balance [50]. Supported by the findings in stroke survivors mentioned above [26], it could be argued that unstable sitting tasks could enhance the sensitivity and reliability of posturographic assessments in pathological populations [44]. Van Dieen et al. explored posturographic measures obtained from in-lab force plate measurements during unstable sitting and found that many of the observed metrics were redundant, but reliable measures of balance performance in non-disabled individuals [37]. Lariviere et al. identified inertial sensor-based posturographic measures that were reliable across different sessions of unstable sitting assessment in non-disabled individuals when performed on different days [23]. These studies, however, demonstrate a significant limitation in the desire to optimize quantitative assessments for seated balance rehabilitation – as the need for cumbersome and costly laboratory equipment (e.g., sitting apparatus, force plates) significantly impedes the practical potential of respective technologies to serve as clinical assessment tools.

### 1.3 Training of Dynamic Sitting Stability via Sensory Augmentation

Beyond seated balance assessment, unstable support surfaces have proven useful in balance rehabilitation paradigms by safely challenging balance of impaired individuals to enhance postural proficiency [51] with or without balance aids such as sensory augmentation devices. These devices stimulate sensory receptors with an encoded pattern that the central nervous system (CNS) can use to partially or fully recover balance functions via neuroplasticity or other means [52]. In general, sensory augmentation devices consist of a *sensor* to measure physical biomechanical features of balance, a *display* to stimulate sensory receptors, and a *processor* to control the feedback loop from sensor to display [53]. In the context of balance training, devices can stimulate vision, hearing, proprioception, and other senses [54]. Technological advances

have especially proposed vibrotactile factors as a non-invasive, compact, and relatively inexpensive means to display sensory feedback to muscle spindles and cutaneous receptors [54], [55]. In fact, vibrotactile feedback has already demonstrated the potential to improve stance control in neurologically impaired individuals [49], [56]–[61] and older adults [62], [63]. Despite biomechanical and neuromuscular similarities between sitting and standing postures [64], [65], vibrotactile feedback for augmenting and training reactive balance control in dynamic sitting has not been fully explored.

## 1.4 Thesis Objective

Based on the above considerations, the objectives of this thesis research were to: (1) develop a portable device for perturbing seated posture, including on-board instrumentation that accurately quantifies postural proficiency and delivers real-time vibrotactile feedback to the user; and (2) evaluate the feasibility of using the device to assess and train sensorimotor function during continuous, multidirectional perturbations by assessing and training a sample of non-disabled volunteers under experimental conditions.

## 1.5 Thesis Outline

Chapter 2 provides a general background coverage of relevant research in balance control, assessment, and training. The biomechanics of upright sitting are described, followed by a summary of relevant investigations regarding unstable surfaces and sensory augmentation as tools to understand, assess, and train seated posture. In Chapter 3, the development of a novel perturbation and feedback apparatus for sitting, called the ‘instrumented wobble board,’ is described. The accuracy of the instrumented wobble board’s measurement tools is validated via a technical experiment and the potential benefits of the overall apparatus are discussed. In Chapter 4, the utility of the wobble board for assessing and training seated balance is demonstrated in a sample of non-disabled participants. An experiment was conducted to measure the tilt kinematics of the wobble board under different combinations of balance difficulty, visual feedback (eyes open or closed), and vibrotactile augmentation conditions. The results and implications of this

study are discussed. Chapter 5 provides concluding remarks on the contributions of this thesis to the domain of seated stability research. A proposition of future work is included.

## 2 Literature Review

### 2.1 Overview

Non-disabled individuals can maintain upright seated balance even when performing manipulations with their arms, or experiencing external challenges such as an unstable support surface (e.g., riding a bus) or an altered sensory environment (e.g., dim lighting). However, how does the human trunk in the absence of any sensorimotor impairments remain upright during sitting despite the destabilizing effect of gravity and transient perturbations? Moreover, how can the degree of seated stability be assessed and associated impairments rehabilitated? These questions demonstrate that a thorough understanding of the mechanisms underlying balance control is essential for advancing assessment and rehabilitation strategies for individuals experiencing seated instability. This chapter explores literature and knowledge in three salient domains: (1) the mechanistic foundation of upright sitting from a dynamic systems approach; (2) methods for assessment of seated balance and the role of unstable surfaces in human sitting research; and (3) methods for improving seated stability through balance training, particularly with the assistance of sensory augmentation techniques.

### 2.2 Dynamics and Control of Upright Sitting

A significant body of literature is dedicated to understanding the underlying mechanisms responsible for the maintenance of upright sitting. The approach generally involves measurement or modelling of variables that characterize some aspect of upright sitting, and their response to challenges or impairments. For example, electromyography (EMG) has been used to measure the activity of muscles, revealing that coordinated activation patterns contribute to upper body stability [66], [67]. The forces exerted on the support surface (measured by a force plate) and the displacement of body segments (measured by potentiometers, inertial units, or motion capture) are also variables of interest, as they correspond to inputs and outputs, respectively, of the dynamic system comprising the human body. Biomechanical models are often used to study the relationship between variables and characteristics of the system. In addition, they provide a

useful context for depicting and understanding the various mechanisms that contribute to upright sitting.

From a basic biomechanics perspective, a seated human behaves as a linkage of rigid, inertial segments – each with its own inertial properties, and each connected by joints with one or more degrees of freedom. Consider the following simple model for seated posture: the head, arms, and trunk (HAT) form one lumped segment, represented as an inverted pendulum with two degrees of freedom (sagittal and frontal plane rotation; sagittal plane shown in Figure 2-1). The lower body is assumedly fixed in space, due to reaction forces from the support surface. The average location of the reaction force on the horizontal plane is defined as the center of pressure (COP). The center of mass (COM) of the HAT is defined as the average location of all its mass in three-dimensional (3D) space, with respect to the joint between the fourth and fifth lumbar vertebrae (L4/L5 joint). Considering the equations of motion that describe the inverted pendulum model, the joint torques required to stabilize the HAT segment can be calculated via inverse dynamics using measurements or estimates of the HAT segment's mass and COM location. The estimated joint torques are sensitive to changes in underlying function of upright sitting that may be obscured in the kinematic data alone [68]. Simple biomechanical models can therefore be used to identify joint torques and other characteristics of the postural control system, all of which may contribute to the enhancement of seated balance assessment and therapy techniques.

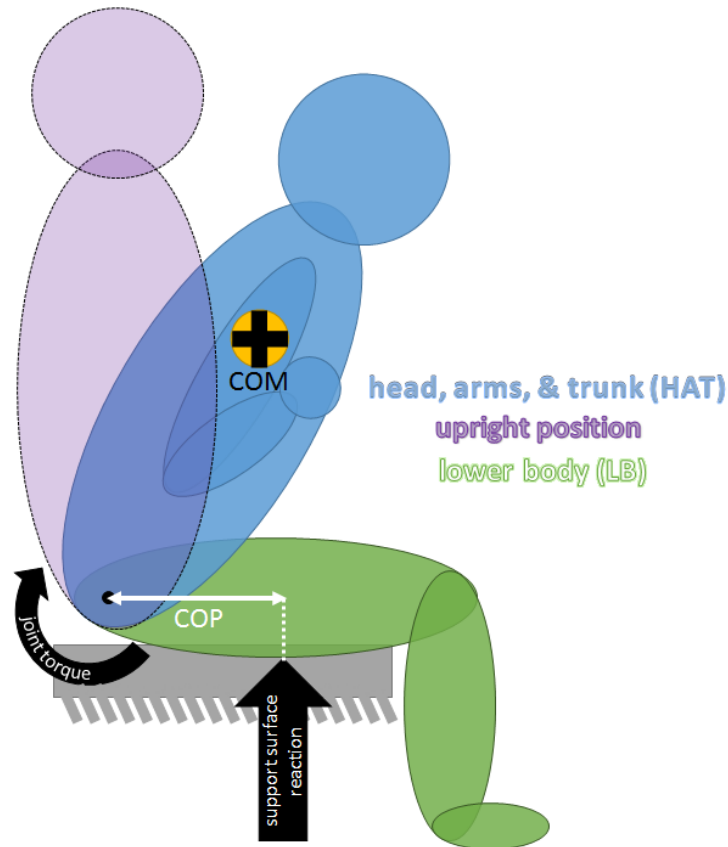


Figure 2-1: A simplified linkage of body segments. The purple segment indicates an upright configuration of the HAT segment. The center of mass (COM), center of pressure (COP), sagittal joint torque and support surface reaction are labelled.

Two general mechanisms produce joint torques during sitting: *passive* dynamics of viscoelastic tissues and *active* dynamics of contractile muscular tissue. Passive joint torque results from the combined stiffness and damping effects of intervertebral joints, inactive muscle-tendon complexes, viscoelastic properties of other tissues surrounding the trunk, and intraabdominal pressure. Active joint torque is generated by the neutrally regulated contraction of muscular tissue.

Joint torques represent the inputs to the plant of a classic movement control model whose output is the motion of the body segments. A closed-loop control model of upright sitting (Figure 2-2) provides useful context for understanding the process by which muscles, sensors, and control

schemes interact to maintain seated stability during dynamic sitting. Passive mechanisms are represented by a torsional spring and damper system at the joint (or joints, in multi-segment models of upright sitting [69]). While passive mechanisms certainly contribute to the required corrective joint torque, feedback control of muscle-produced joint torques is required to ensure stability against gravity and other disturbances [70], [71]. Feedback is provided by sensory receptors, and after a neural processing delay, the central nervous system issues and adjusts motor commands accordingly.

In contrast to *reactive* control strategies, *anticipatory* control strategies elicit motor commands based on the expectation of an impending perturbation or intended body displacement. Anticipatory control strategies rely on previous experience in addition to sensory information to produce motor commands that minimize the impact of a predictable and imminent disturbance. During sitting, co-contraction (the simultaneous activation of antagonist, i.e., opposing muscle groups) have been shown to increase the stiffness of the trunk [72], e.g., before an expected perturbation [46], but was insufficient to stabilize the trunk during dynamic sitting [22]. If perturbations are randomly delivered to the body (i.e., unexpectedly), the response can be measured and used to identify the dynamics of the reactive system [73]. For example, by measuring the muscle response during discrete perturbations of the sitting surface, Forssberg and Hirschfield observed that direction-specific activation of agonist-antagonist muscle pairs restored stable posture after unexpected perturbations in the sagittal plane [74]. Known perturbations are used to identify characteristics of the balance control model to advance our fundamental understanding of balance control, and to facilitate assessment and training paradigms [75]–[77]. In some cases, sensory systems are also artificially perturbed, as is necessary for accurate estimation of closed-loop dynamics [75] and for revealing the relative contributions from the various sensory modalities [78]. Whether anticipatory or reactive, active control relies on continuous integration of sensory information by the CNS to produce and/or optimize corrective motor commands [78]. Inherent feedback systems that provide information about the current state of the body include the visual, auditory, and vestibular systems, but also muscle receptors, joint receptors, and cutaneous receptors (proprioception) [79].

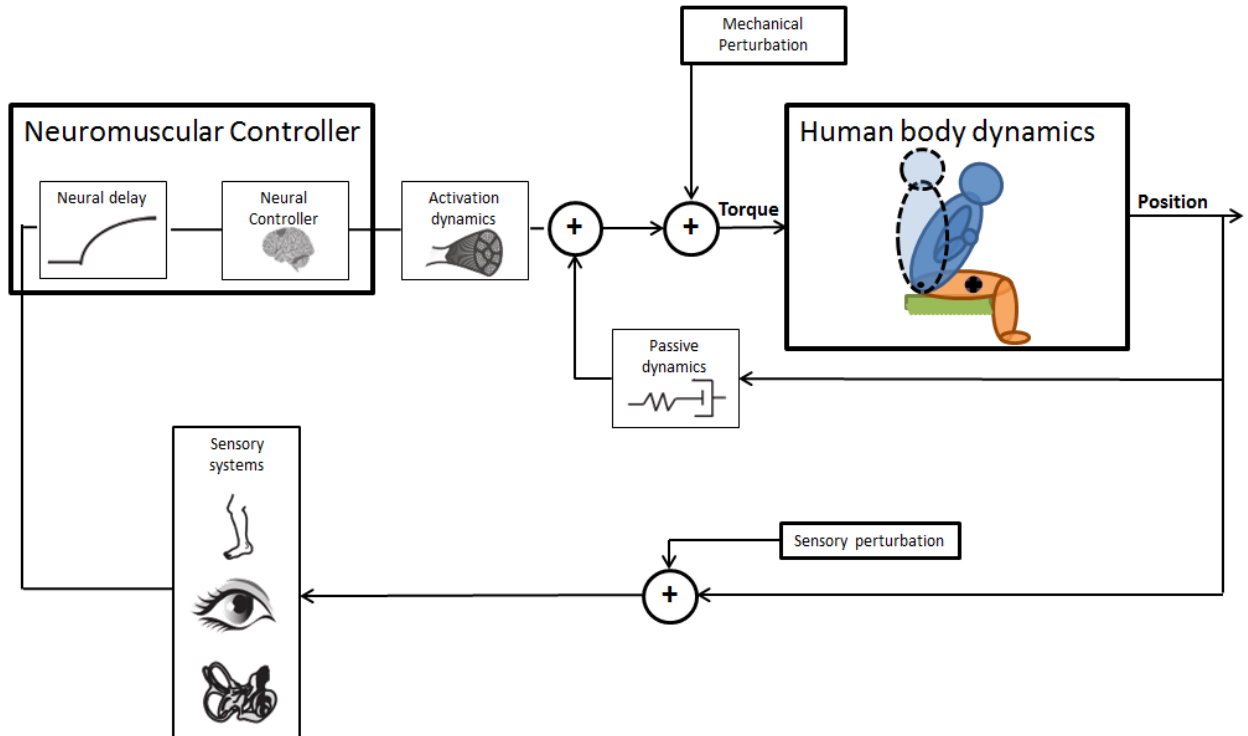


Figure 2-2: A basic model of seated balance control. From a control perspective, the reactive balance control system consists of a plant, monitored by sensory systems, actuated by muscular tissue and controlled by the central nervous system. Human body dynamics are modelled by an inverted pendulum model. The input is the sum of torques generated by passive dynamics, neuromuscular controlled active dynamics, and external perturbations. The output is the deviation of the COM from a reference posture, sensed by proprioceptive, visual, and vestibular systems affected by sensory perturbations. Adapted from [80], with permission (© 2014 Elsevier).

### 2.2.1 Role of Vision in Balance Control

Vision provides sensory feedback in the obvious sense: we can look at our limbs and torso to know their position in space. In addition, vision provides feedback of a proprioceptive nature in that the position of the head can be inferred from the movement of our optical array. When the eye moves through space, the light rays received by the retina (termed *optical array*) move correspondingly. The movement of the optical array specifies a distinct movement of the eyes with respect to the environment. The movement of the eyes (and, thus, the person's head) can be

reconstructed from the continuous changes of these angles. For example, consider a stationary object perceived as two light rays in the optical array. If the angle between these rays is increasing, the eye must be moving towards the object. In this way, vision can be used to provide information about movements of the head [79]. It is therefore also not surprising that postural sway increased when seated participants were asked to close their eyes [30]. To further explore the role of vision in balance control, investigators have used a “visual surround” apparatus (or moving room paradigm) that allows the participant’s visual environment to be perturbed. This perturbation has no mechanical influence on the body, but may alter the participant’s visual perception of their surroundings. For example, moving the visual surround towards the participant gives the visual perception of falling forward, causing a compensatory backward movement [81]. This type of response has been observed approximately 100 ms after the visual perturbation takes place, indicating a relatively automatic response without the processing times required for high level recognition and identification of visual inputs [82].

### 2.2.2 Role of Auditory System in Balance Control

Just as the orientation of visual flow indicates the position of the head with respect to the environment, the location of auditory stimuli in the environment indicates the orientation of the head with respect to those stimuli. For example, a delay between a planar sound wave striking the left ear and the right ear indicates that the source is located somewhere on the left side of the head. Auditory feedback is processed faster than visual feedback, but is less rich in its usefulness for balance [79].

### 2.2.3 Role of Vestibular System in Balance Control

Each inner ear contains three semicircular canals that are oriented in the three major planes of the body (frontal, sagittal, and horizontal) and respond to acceleration in each plane. Together with the vestibular apparatus, the semicircular canals provide sensation of the head’s orientation in space with respect to gravity, which is essential for balance [83]. Individuals with vestibular loss are significantly more reliant on vision; as such, in dim lighting, they become unstable [84]. Peterka et al. used a visual surround that oscillated with increasing amplitude and frequency to challenge the stability of standing participants. As the amplitude increased, vestibular-absent

participants swayed more until they fell, whereas control participants swayed no more after a threshold amplitude was reached, demonstrating that the vestibular system plays a major role in the control of standing balance [85].

#### 2.2.4 Role of Proprioception in Balance Control

Muscle receptors (muscle spindles and Golgi tendon organs) signal changes in the length and force output of muscles [79]. Joint receptors sense, to some extent, the position of joints [79]. Cutaneous receptors provide information about touch and pressure exerted on a certain area of the skin, in addition to many other signals that are not pertinent to movement control [79]. The ensemble of information from these proprioceptors provides sensation of the position, movement, and force exertion of body segments [79]. Forssberg and Hirschfield theorize that reactive control during sitting is most likely comprised of two levels: early co-contraction triggered by proprioception of pelvic tilt in the early stages of the perturbation, followed by precise muscle activation in response to multisensory integration of vestibular, proprioceptive, and visual feedback [74].

#### 2.2.5 Effect of Cognitive Load on Balance Control

Attentiveness contributes to the control of balance; for example, the COP trajectories of non-disabled, standing individuals became more regular (as quantified by sample entropy, a parameter produced by nonlinear time series analysis [86]) when eyes were closed and more irregular when performing a cognitive dual task [87]. The cognitive load factor should be considered when designing training tools that may increase or decrease cognitive load [88], or when extrapolating balance assessment results from simple task conditions to everyday conditions where simultaneous tasks may demand attention [63].

## 2.3 Methods for Assessing Seated Balance

### 2.3.1 Traditional Assessment Methods

There are at least 30 measurement tools in practice that clinicians use to evaluate human balance [89]. Some tools measure the ability to complete a functional balance task (e.g., reach test [90], [91] or arm raise test during sitting [92]). Other measurement tools use a rating structure to quantify balance ability over a range of functional tasks (e.g., Berg Balance Scale [10], Trunk Impairment Scale [93], or Brunel Balance Assessment [94]). These traditional assessments rely on subjective and qualitative measurements [9], [10], [12]–[14]. In addition, they often fail to reliably identify the specific deficiencies and needs of a balance-impaired individual [15], [16]. Some traditional assessments also rely on standing tasks for validity [15], [94] and, as a result, may be impractical for individuals with no standing ability [50]. For assessments of seated stability to be objective and sensitive over a broad range of function in balance-impaired individuals, quantitative methods are preferred to subjective tools [50].

### 2.3.2 Quantitative Assessment Methods

Clinicians and scientists use measurement tools that quantify time-varying, biomechanical features of balance. For example, force plates quantify the body's exertion of forces on a support surface during functional balance tasks [18]–[21], [64] and produce an estimate of the body's COP, typically as a pair of anteroposterior (*AP*) and mediolateral (*ML*) displacements. The location of body segments in three-dimensional space can be measured by motion capture or other means and similarly resolved into *AP* and *ML* displacements. Temporal fluctuations of COM and COP displacements reflect the orientation and acceleration of body segments during postural control, respectively, and, thus, contain information regarding balance control mechanisms [68]. Patterns in COM and COP fluctuations are used to characterize motor functions, such as during upright sitting. Figure 2-3 shows the *AP* and *ML* components of COP displacements during standing and sitting, plotted over time in a stabilogram. Stabilograms are a simple tool for visual analysis of postural stability, but ignore dynamic characteristics such as the magnitude of displacements between adjacent points [95]. Metrics used to summarize the COP or segment displacement time series are known as *posturographic measures*. Such measures are valued because they can quantitatively detect changes in postural control effort and

output and, hence, the integrity of the mechanisms that control balance [19], [26], [96]. However, there is not always a clear interpretation of each measure as pertaining to the integrity of underlying balance systems [97]. Appendix A overviews several posturographic measures, including those produced by analyses in time and frequency domain, stabilogram diffusion analysis, recurrence quantification analysis, dimensionality analysis, and divergence analysis.

COP-based posturographic measures are established tools for assessing *standing* balance [25], [56], [98], [99], and can also characterize *seated* balance, e.g., to assess stability after neurological impairment [19], [20], [50], [96], [100] as motivated above. Vette et al. explored the relationship between quiet standing and quiet sitting as quantified by posturographic measures, and reported that many COP-based posturographic measures were similar between sitting and standing, and that some of their differences, including the relative stability of sitting compared to standing, could be attributed to biomechanical factors and differences in control strategy for the two postures [64].

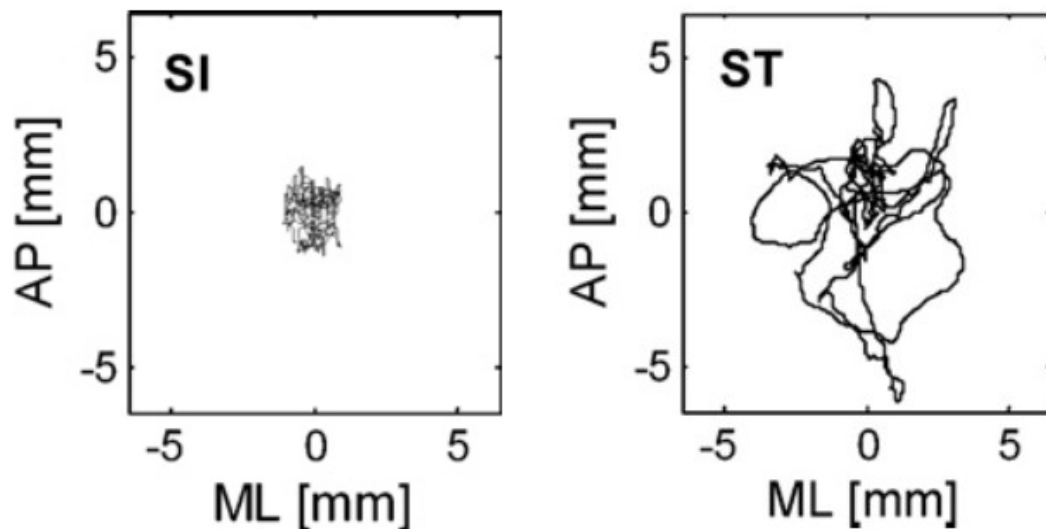


Figure 2-3: Stabilograms, showing the planar trajectory of the centre of pressure (COP) for a non-disabled, young individual during 15-s of sitting (SI) and standing (ST). Mediolateral (*ML*) and anteroposterior (*AP*) COP displacements are plotted along the x-axis and y-axis, respectively. Reprinted from [64], with permission (© 2009 Elsevier).

In addition to force plate measurements of the COP, seated balance can be quantified by inertial sensors [57], [63] or optoelectronic systems [23], [101] that measure displacements of the body

or support surface. For example, the tilt angle of an unstable sitting surface can be resolved into *AP* and *ML* components, and these angles were correlated with COP displacements during functional sitting tests [23]. Posturographic measures based on support surface tilt angles have proven reliable across different sessions of unstable sitting assessment in non-disabled individuals [23].

Posturographic measures have some limitations in their ability to provide reliable, discriminatory balance assessments. Over the duration of a trial, and from one trial to the next, practice and fatigue can have time-varying effects on the inertial or kinematic measurements, confounding the correlation of posturographic measures with clinical performance and the risk of falling in daily life [17]. Posturographic measures may correlate with weight, height, strength, flexibility, reaction speed, or other parameters that vary for each individual, making between-participant comparisons difficult [23]. A first step to validate posturographic measures, derived from kinematic or kinetic measurements during any given balance protocol, is to verify that they can detect changes in non-disabled individuals that undergo changes in balance conditions (e.g., mechanical or sensory perturbation).

### 2.3.3 Dynamic Sitting Assessment Methods

While posturographic measures are useful to characterize the integrity of balance systems during quasi-static sitting or voluntary movements, postural perturbations (i.e., alterations to the mechanical, sensory, or cognitive environment) are necessary to characterize the contributions of reactive systems to balance control [28] and pinpoint the functional integrity of sensory, central, and motor contributions to balance [1]. It is common practice to differentiate *dynamic* and *static* assessments as those with and without postural perturbations, respectively, despite the observation that unperturbed posture is not completely static, only relatively so [17]. Dynamic assessments are facilitated by various perturbation techniques, including: rotation, translation, or destabilization of the support surface (mechanical), application of a transient force to one or more of the body segments (mechanical), disturbance of the visual surroundings (sensory), electrical stimulation of vestibular nerves (sensory), vibration of sensory receptors underlying skin tissue (sensory), and addition of a dual task (cognitive) [1]. Dynamic sitting assessments also include those protocols where individuals are instructed to complete voluntary movements [102].

One method to induce dynamic sitting is to apply mechanical perturbations to a seated individual using cables and a harness, and measure characteristics of the postural response [103], [104]. Using this method, both the EMG response [103] and trunk COM response [104] to sudden perturbations have been characterized in eight horizontal directions. High variability in the experimenter-produced perturbation force limits the reliability of such methods [103], [104]. Using a portable and automated postural perturbation system [73], Vette et al. induced perturbations to seated posture that were small in amplitude, so to elicit only passive trunk stiffness and damping, and recorded the trunk COM response [105]. The trunk undergoing small perturbations resembled a second-order, underdamped system, for which the stiffness and damping coefficients were estimated [105]. These findings are relevant to the development of a neuroprosthesis using functional electrical stimulation (FES) to rehabilitate upright sitting following spinal cord injuries [103]–[105]. Harness perturbation tools and methods could also be used to perform quantitative, dynamic assessments of seated balance [73].

Another commonly used approach is to rotate, translate, or destabilize the support surface on which an individual is sitting. On the one hand, rotation and translation perturbations are *actively* elicited by actuators in the sitting apparatus [74], [106], [107]. On the other hand, unstable sitting surfaces *passively* elicit dynamic sitting [18], [22], [23], [29], [34], [35], [37], [39], [44]. Actively elicited perturbations (of both a chest harness and the support surface) can be designed to resemble postural perturbations experienced during sitting in daily life [108]. Usually, rapid and brief perturbations are applied in order to characterize the immediate postural response [109]. In contrast, slow and continuous perturbations can capture the low-frequency characteristics of balance control, thereby validating the time-invariance assumption that is needed for advanced quantification methods [75]. While passive techniques do not afford the luxury of prescribing a known perturbation to the upright sitting posture, they hold the advantage of requiring less power and machinery. Furthermore, unstable support surfaces can be designed to facilitate the assessment of the full directional range of reactive control that may be required to maintain upright sitting during everyday challenges – whereas actively elicited perturbation techniques are limited to the discrete directionalities of the actuating mechanisms.

All mechanical and sensory perturbation techniques are relevant to the study and assessment of postural stability. In this thesis, the objective was to develop a dynamic assessment method that could produce quantitative metrics pertaining to the integrity of seated balance control, without

the requirement of advanced laboratory equipment or a cumbersome apparatus. To this end, a passive perturbation method was desired.

For passively eliciting dynamic sitting by destabilizing the support surface, there are several methods described in the literature. Continuous, multidirectional instability of the support surface can be implemented by attaching it to a hemispherical base [18], [22], [29], [37], [39], [44] or a central pivot [23], [34], [35]. This unstable sitting method elicits instability in two rotational dimensions and continuously perturbs balance as long as balance is maintained. A two-segment model of the unstable sitting methodology (Figure 2-4) has been used to show that feedback control of the torque between segments produces stable segment positions and velocities [69]. Unstable sitting devices have been used to carry out many *fundamental* investigations into the nature of dynamic, seated balance control [18], [22], [24], [29]–[36], [38]–[43], [45], [46]. Some studies have also demonstrated the potential for unstable sitting methods to be used in seated balance *assessment* paradigms in clinical populations by challenging stability within a safe range [23], [24], [36]–[38], [41], [42], [110].

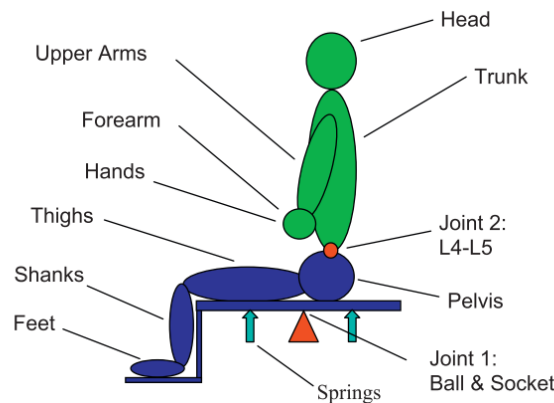


Figure 2-4: A two-segment model (green: upper body; blue: lower body and support surface) of unstable sitting on a central pivot device. Reprinted from [69], with permission (© 2009 Elsevier).

### 2.3.3.1 Single Degree of Freedom Surfaces

Freddolini et al. developed a sitting apparatus with sagittal plane instability facilitated by a hinge in the support surface (Figure 2-5). By comparing non-disabled participant behaviour to a

biomechanical model, they estimated the parameters of a rotational spring and damper that act at the hip joint. Their results suggest that trunk stiffness was higher in participants with lower back pain, which may be a compensatory strategy to decrease pain and risk of further injury in this population [40]. They later compared estimated hip torques to EMG data collected from the hip musculature, finding that individuals with low back pain exhibited larger reaction times and increased co-contraction compared to non-disabled individuals during unstable sitting [46]. Freddolini et al. also observed increased muscle activity before the start of an unstable sitting trial, suggesting that participants were preparing for the perturbation [46]. Preuss et al. used a hemicylindrical-based sitting surface with free rotation in the sagittal plane to differentiate those muscles that co-contract from those that are asymmetrically activated during dynamic sitting balance [22]. Pérennou et al. used a similar one degree of freedom apparatus to demonstrate a relationship between an injury to the sensory cortex and impaired seated balance [42] and to show that transcutaneous electric nerve stimulation improved dynamic balance in stroke survivors with spatial neglect [41].



Figure 2-5: An unstable sitting apparatus with one degree of freedom for fundamental investigations of seated balance. Reprinted from [111], with permission (© 2014 Elsevier).

### 2.3.3.2 Multidirectional Pivot Surfaces

Slota et al. developed an unstable sitting apparatus with multidirectional instability achieved by attaching the support surface to four springs surrounding a central pivot (Figure 2-6). The radial

displacement of the springs could be adjusted to increase the angular stiffness of the platform and, thus, mitigate the confounding effect of between-participant, anthropometric differences on postural performance. This methodology was used to demonstrate that non-disabled individuals were less stable when being perturbed with a constant force by a chest harness [34] and when whole-body vibration was applied [35], which may be contributing factors to injuries of the lower back. Using a similar methodology, Lariviere et al. demonstrated that an inertial sensor could measure the support surface kinematics to provide valid posturographic measures [23], although these measures were not sensitive to the presence of lower back pain, perhaps due to low reliability [24].

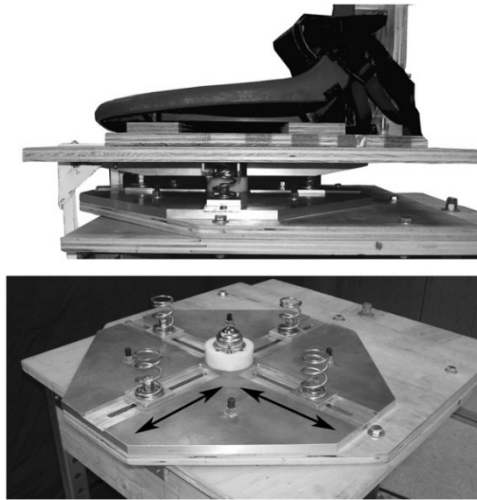


Figure 2-6: An unstable sitting device using a pivot and springs to elicit multidirectional perturbations and investigate postural stability during dynamic sitting. Reprinted from [35], with permission (© 2007 Elsevier).

### 2.3.3.3 Hemispherical Base Surfaces

Cholewicki et al. developed an unstable sitting apparatus with adjustable instability achieved by modulating the diameter of polyester resin hemispheres attached to the bottom of the seat (Figure 2-7). Non-disabled individuals sat on the seat and exhibited reliable COP displacements as summarized by short-term diffusion coefficients and other posturographic measures [29]. This methodology has been used to identify trunk motor control impairments in individuals with lower back pain [18], [32], [33], for example, to demonstrate that their response to the

continuous, multidirectional perturbations was slower than in individuals with no back pain [18]. Non-disabled participants sitting on the apparatus demonstrated closed-loop control behaviour that improved when their eyes were open [30], degraded when trunk stiffness was actively increased (as verified by EMG measurements), and remained unaffected with increased passive stiffness (by wearing a lumbosacral brace) [31]. A hemispherical base apparatus was also used by Van Daele et al. to demonstrate that individuals with low back pain exhibited larger angular deviations and higher correlations between pelvic and trunk displacements than non-disabled participants, probably due to trunk-pelvis stiffness [36]. Test-retest reproducibility of time domain measures for unstable sitting were only moderate, probably due to learning effects [110]. Using a similar device, van der Burg et al. observed differences in COP and trunk angle patterns during unstable sitting between non-disabled participants and those with Parkinson's disease, which could be linked to the prevalence of falls in the latter population [43]. Hemispherical bases have also been used in the assessment of standing balance, e.g., by Cimadoro et al. [112].

Van Dieën et al. also used a hemispherical base protocol to identify reliable posturographic measures that correlate with loss of balance [37] and demonstrated that some of these measures could differentiate between individuals with recent and current low back pain [38]. Furthermore, EMG recordings revealed differences in muscle activation levels during unstable sitting between non-disabled individuals and those with low back pain [39]. Barbado et al. used a sitting apparatus with a hemispherical base to demonstrate that higher-level judo athletes were not more stable than lower-level judokas [45].



Figure 2-7: An unstable sitting apparatus with a hemispherical base that elicits multidirectional perturbations for fundamental investigations of dynamic sitting. Reprinted from [33], with permission (© 2015 Elsevier).

## 2.4 Sensory Augmentation Methods for Improving Seated Balance

### 2.4.1 Traditional Seated Balance Therapies

Physical therapies are widely used, and often effective, to improve seated balance and overall trunk stability [51], [113]. Physical therapies include functional balance training (e.g., reaching while sitting, sit-to-stand tasks), trunk training exercises (selective movements of the trunk in supine and sitting positions), and sitting on unstable surfaces or with eyes closed [51]. Traditional balance therapies often employ *terminal* (i.e., post-movement) feedback where a trained observer gives feedback regarding overall performance or specific movements after completion of a balance task. In contrast, *concurrent* feedback provides real-time information about balance performance. Mudie et al. studied the effects of four post-stroke training protocols for seated balance and observed that treatments incorporating concurrent feedback or guidance were more effective to reduce seated asymmetry than task-specific or standard physiotherapy

[114]. Concurrent feedback may be provided by a trained therapist, haptic guide, or technical apparatus.

Haptic guides are a simple and effective means to augment sensory information for balance. Non-disabled participants exhibited reduced postural sway when exerting light fingertip touch on a cane compared to control trials where no cane was used [115]. While, in Jeka et al.'s experiment, the applied force was too small to provide physical stabilization, postural sway was reduced to the same degree as in trials where the cane was used as physical support. In the haptic guide condition, the cane provides haptic feedback that can be interpreted by the central nervous system (CNS) to more precisely control standing posture [115]. The capacity of haptic feedback to rehabilitate balance disorders has been demonstrated in many other paradigms and balance-impaired samples [116].

## 2.4.2 Sensory Augmentation Methods

Sensory augmentation techniques vary in design and purpose. Sensory augmentation has long been utilized to enhance or restore sensorimotor function; e.g., tactile feedback improved an aviator's approach and land task [117]. In the context of balance control, sensory augmentation can supplement inherent senses with information regarding the dynamic state of the body. Various sensors exist for measuring biomechanical parameters related to postural control: e.g., force plates measure COP displacements, inertial measurement units (IMUs) measure body position and movement, or EMG electrodes measure muscle activity [118]. A controller processes the measurements and determines the level of feedback to display. Visual, auditory, electrotactile, vestibular, and vibrotactile modalities are available for display [119].

Visual feedback of COP displacement has become a popular modality for sensory augmentation [120], [121]. Shumway-Cook et al. compared visual feedback of COP displacement to traditional therapies for reducing standing asymmetry in hemiplegic individuals. A control group spent the same amount of time in traditional therapy (including visual, verbal, and haptic cues from a trained therapist), but achieved significantly less postural improvement than the participants who received objective display of COP displacements during therapy [122]. Lee et al. provided a group of stroke survivors with visual feedback of COP during a four-week sitting rehabilitation program, and observed significant improvements compared to a control group that did not

receive visual feedback during rehabilitation [123]. Dozza et al. designed an audio-feedback system where volume and balance were based on accelerations of the COM in *AP* and *ML* directions, respectively. Individuals with bilateral vestibular loss donned the apparatus while standing on a foam layer to induce postural instability and a force plate to measure displacements of the COP. Over a series of 1-minute trials, participants spent more time within the one-degree feedback range, and their COP fluctuation was displaced less from the mean in comparison with control trials where no feedback was provided. The results suggest that audio-feedback improved stance stability in individuals with bilateral vestibular loss [124]. Barros et al. developed a device to provide tongue-interfaced electrotactile feedback corresponding to head accelerations that improved postural control in participants with vestibular loss who did not benefit from conventional vestibular rehabilitation [125].

Since 2001, significant research has been dedicated to the study of vibrotactile feedback interfaces for improved balance in various populations [54], [55]. Vibrating tactors, being compact, non-invasive, inexpensive, and relatively easy to implement, are a particularly useful feedback modality for balance tasks. In fact, vibrotactile feedback has already demonstrated the potential to improve stance control in neurologically impaired individuals [49], [56]–[61] and older adults [62], [63]. Wall et al. developed a sensory augmentation apparatus that measures *ML* head tilt and feeds back 100-ms pulses of vibrating tactors placed on each shoulder or side of the trunk (Figure 2-8). As the magnitude of head tilt deviated further from zero, the pulse rate of the tactor on the corresponding side of the body was increased. Non-disabled individuals who used the apparatus produced less overall head tilt during 30-s trials of standing in the Romberg position, compared to control trials without the apparatus [126]. The participants also exhibited COP displacements with less variability during trials with vibrotactile feedback: even less so when the tactors were placed on the trunk than on the shoulders. In a subsequent study, the inertial sensor was placed on the participant's lower back to estimate body tilt, and the tactors were placed in columns of three, which was suggested to be the resolution threshold for improved performance of a control task [127]. When the apparatus provided vibrotactile feedback, vestibular-deficient individuals performed standing tasks (e.g., standing with sway-referenced visual surround) with more stability, as quantified by RMS of COP displacements and body tilts [58]. Improved stability was also evident when the support surface was perturbed during the balance tasks [49]. Stability was increased further when the vibrators were actuated

based on tilt magnitude and rate (i.e., a proportional plus derivative signal) rather than magnitude or rate alone [59].



Figure 2-8: A participant equipped with inertial measurement unit and vibrating factors. Reprinted from [126], with permission (© 2001 IEEE).

Subsequent studies expanded the vibrotactile apparatus to include vibrating factors in multiple directions (Figure 2-9). Vestibulopathic participants donned the apparatus and exhibited improved stability as quantified by COP displacements during perturbed standing [56], analysis of transfer functions between pseudorandom platform motion and body sway [57], and less time to recover from discrete, directional surface perturbations [61]. In a subsequent study, visual feedback was more effective than the vibrotactile apparatus in improving stability [128]. Vibrotactile feedback, however, holds the advantage of remaining useful in eyes closed conditions or when the balance task requires head movements. The vibrotactile feedback device also improved stability during locomotion tasks [129]–[131] and dual tasking [88].

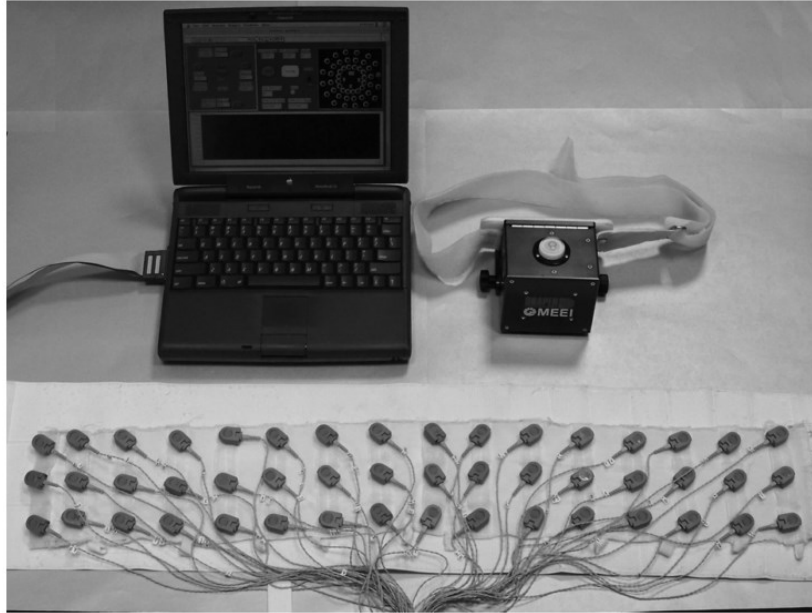


Figure 2-9: Sensor (top right), processor (top left) and vibrotactile display array (bottom) for balance training in vestibulopathic participants. Reprinted from [56] with permission (© 2008 IOS Press and the authors)

Portable devices that deliver sensory feedback have been made viable by advances in the size and performance of IMUs. Lee et al. utilized a smart phone-embedded IMU to develop a bi-directional vibrotactile feedback apparatus that decreased postural sway in non-disabled and vestibulopathic participants [132]. Other vibrotactile feedback devices and their potential application as a standing rehabilitation device in various clinical populations are presented in [53], [133].

## 2.5 Conclusions

As outlined in the beginning of this chapter, a significant population of elderly or neurologically impaired individuals may struggle even to maintain seated posture, let alone perform standing or locomotion tasks. Despite biomechanical and neuromuscular similarities between sitting and standing postures, there are few clinical tools for perturbing and assessing dynamic seated balance such as those available for standing. Most current methods for perturbing seated posture and quantifying a postural response depend on laboratory settings and equipment, which may be

one reason why current methods have not translated into clinical practice. Furthermore, the capacity of vibrotactile feedback to augment and train reactive balance control has not been fully explored. A portable device that challenges seated stability to a customizable degree while providing concurrent, vibrotactile feedback could provide the same benefits for seated balance assessment and training as have been demonstrated for standing.

## 3 Development of an Instrumented Device to Assess and Train Seated Balance

### 3.1 Introduction

Chapter 2 revealed a significant limitation in the desire to optimize quantitative assessments for seated balance rehabilitation – as the need for complex and costly laboratory equipment significantly impedes the practical potential of respective technologies to serve as clinical assessment tools. The main objective of the research presented in this chapter was to develop a device for perturbing seated posture, including on-board instrumentation, that accurately quantifies postural proficiency and delivers vibrotactile feedback to the user. The device also had to be portable so that balance can be assessed and trained in any convenient environment.

### 3.2 Methods

#### 3.2.1 Design of the Instrumented Wobble Board

To meet the stated objective, a ‘wobble board’ was designed that can passively elicit continuous, multidirectional perturbations during sitting as needed for dynamic balance assessment and training. The wobble board consisted of: (1) a sitting surface connected to interchangeable hemispherical bases with increasing radii of curvature to elicit different levels of seated instability; (2) electronic instrumentation to measure the wobble board’s kinematics and apply vibrotactile stimuli to the seated user; and (3) circuitry and software to monitor and record the wobble boards’ kinematics and allow real-time adjustment of the vibrotactile feedback parameters. See Appendix B for the complete bill of materials.

##### 3.2.1.1 Wobble Board Mechanics

The main structural components of the wobble board are depicted in Figure 3-1. A cylindrical platform was constructed from low-density polyethylene and its surface lined with grip tape to

provide a non-slip sitting surface (diameter: 485 mm; height: 40.8 mm). The platform lid (1) can be easily removed to access the electronics and counterweight housed within the platform (Figure 3-2). A steel extrusion (2) and two clevis pins (3) connect a foot rest module of adjustable height (4) for balance paradigms that require the lower limbs to be supported. Five hemispherical bases (5) were manufactured from high-density polyethylene, each with a unique radius of curvature (Table 3-1). The height of each base is 62.5 mm; thus, the total distance from the wobble board surface to the underlying support surface is 103.3 mm. The curved bases can be mounted interchangeably onto a cylindrical extrusion on the inferior side of the platform. A base with a larger radius of curvature generates a more stable surface for sitting [29]. The device weighs 9.4 kg without the footrest, or 15.0 kg with the footrest (2.0 kg) attached and a steel bar (3.6 kg) inserted 10 cm posterior of the medial-lateral axis (Figure 3-2; top) to counterbalance the footrest. All mechanical components can be easily disassembled to facilitate transportation of the wobble board.

Table 3-1: Geometrical properties of the interchangeable bases from most stable (Base #1) to least stable (Base #5).

<b>Base #</b>	<b>Radius of Curvature (cm)</b>
<b>1</b>	<b>25</b>
<b>2</b>	<b>20</b>
<b>3</b>	<b>15</b>
<b>4</b>	<b>13</b>
<b>5</b>	<b>11</b>

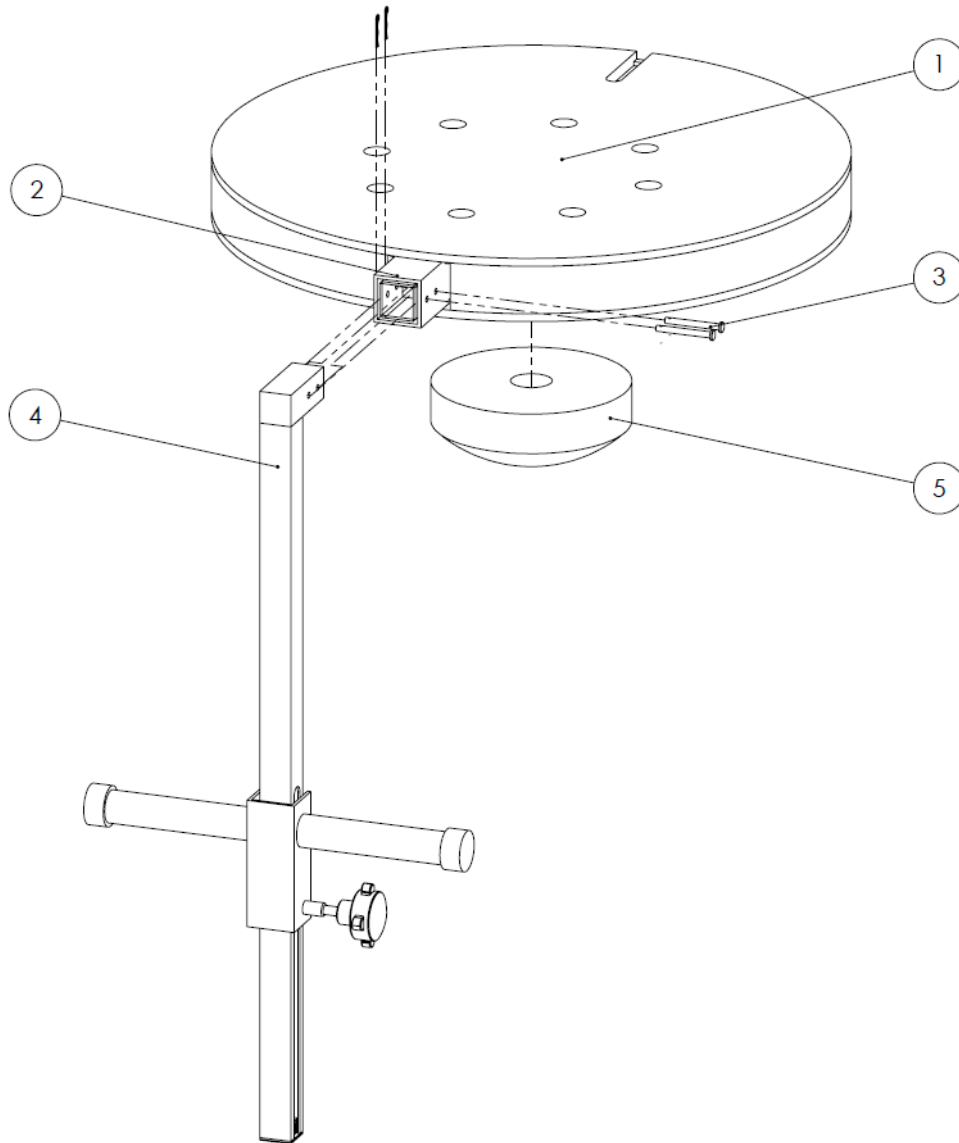


Figure 3-1: Schematic of the wobble board components, including: (1) the platform surface with holes for 8 holes for vibrotactile interfaces; (2) a steel extrusion for footrest attachment; (3) two clevis pins to secure the footrest; (4) a footrest module of adjustable height; and (5) one of five curved base modules.

### 3.2.1.2 Inertial Measurement Unit

An inertial measurement unit (IMU) was selected for low cost and high accuracy (x-IMU, x-io Technologies Limited, Bristol, UK). The IMU comprises a gyroscope, an accelerometer, and a

magnetometer, with an on-board sensor fusion algorithm converting respective raw data into angular displacements. The axes of the IMU were aligned with those of the wobble board such that rotation about the IMU x-axis corresponds to wobble board tilt in the anteroposterior (*AP*) direction (anterior: positive tilt), and rotation about the IMU y-axis corresponds to wobble board tilt in the mediolateral (*ML*) direction (right: positive tilt). The IMU was held firmly at the center of the board by a custom-printed electronic enclosure to keep it from moving during use (Figure 3-2; center). The tilt angles were acquired digitally by a MEGA 2560 microprocessing board (Arduino, Somerville, MA, USA), also housed beneath the platform lid (Figure 3-2; left). The microprocessor and its connecting wires rest in custom-cut troughs to ensure that the platform lid does not rest on any electronic components. A laptop computer was connected via Universal Serial Bus (USB) connection to facilitate data transfer and supply 5 Volts of power to the microprocessor.

### 3.2.1.3 Vibrotactile Elements

The microprocessor delivers a digital signal (0 V or 5 V) to each of eight LilyPad Vibe Boards (Sparkfun Electronics, Boulder, CO, USA) that vibrate with a frequency of 200 Hz when the 5 Volts signal is received [134]. The vibrating tactors are exposed to the seated body via eight holes in the wobble board surface. Each tactor is held flush with the wobble board surface in a custom-printed enclosure. This ensured that as much skin as possible was stimulated, while avoiding mechanical interference with the human body and minimizing the risk of damage. The tactors are arranged around a 22-cm diameter circle to allow directional cueing (Figure 3-2; mid-region). Based on the notion that the degree of directional resolution of vibrotactile feedback affects the usefulness of vibrotactile feedback [57], the eight enclosures are arranged to accommodate two-, four-, or eight-directional configurations. Each enclosure was attached to the board by a mounting hole that fits loosely on a locating pin to minimize vibration dampening (Figure 3-3).

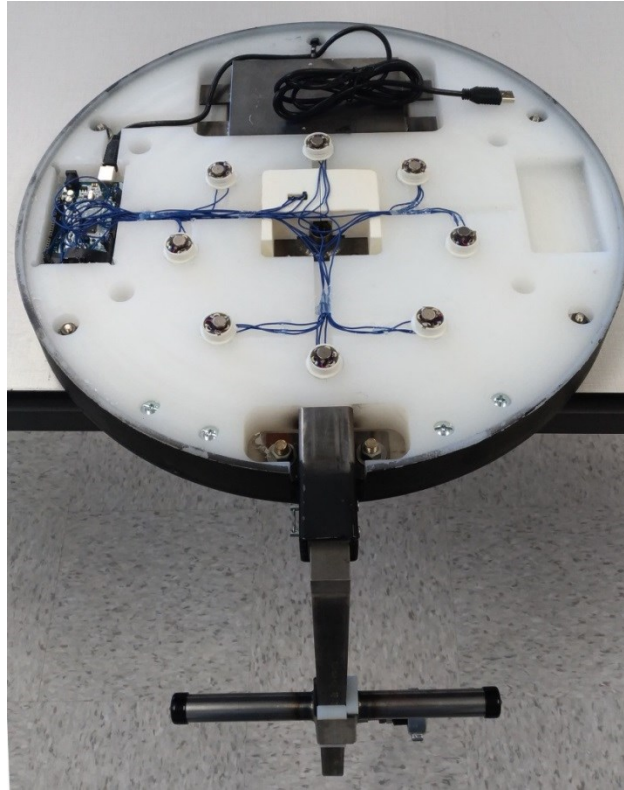


Figure 3-2: Top view photograph of the wobble board with footrest attached (bottom) and the lid removed to reveal electronic instrumentation. Shown are: an inertial measurement unit housed by a custom-printed enclosure (center); a microprocessing board with universal serial bus connection (left); eight electronic vibrators held in custom-printed enclosures (mid-region); and a steel bar (top) to counterbalance the footrest.

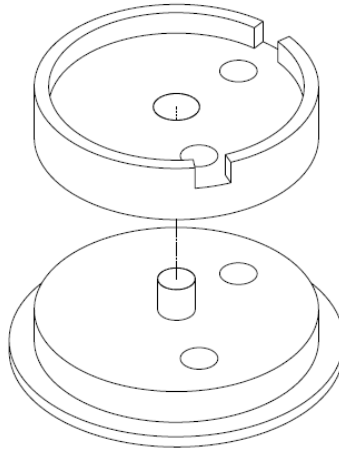


Figure 3-3: Two-part mounting enclosure for vibrating tactors. A mounting hole in the tactor enclosure (top) fitted loosely on a locating pin in the platform attachment (bottom) to minimize vibration dampening.

#### 3.2.1.4 Data Acquisition Software

The MEGA 2560 microprocessor also interfaced with a custom LabVIEW software program (National Instruments, TX, USA). A schematic of the wobble board hardware and software integration is shown in Figure 3-4.

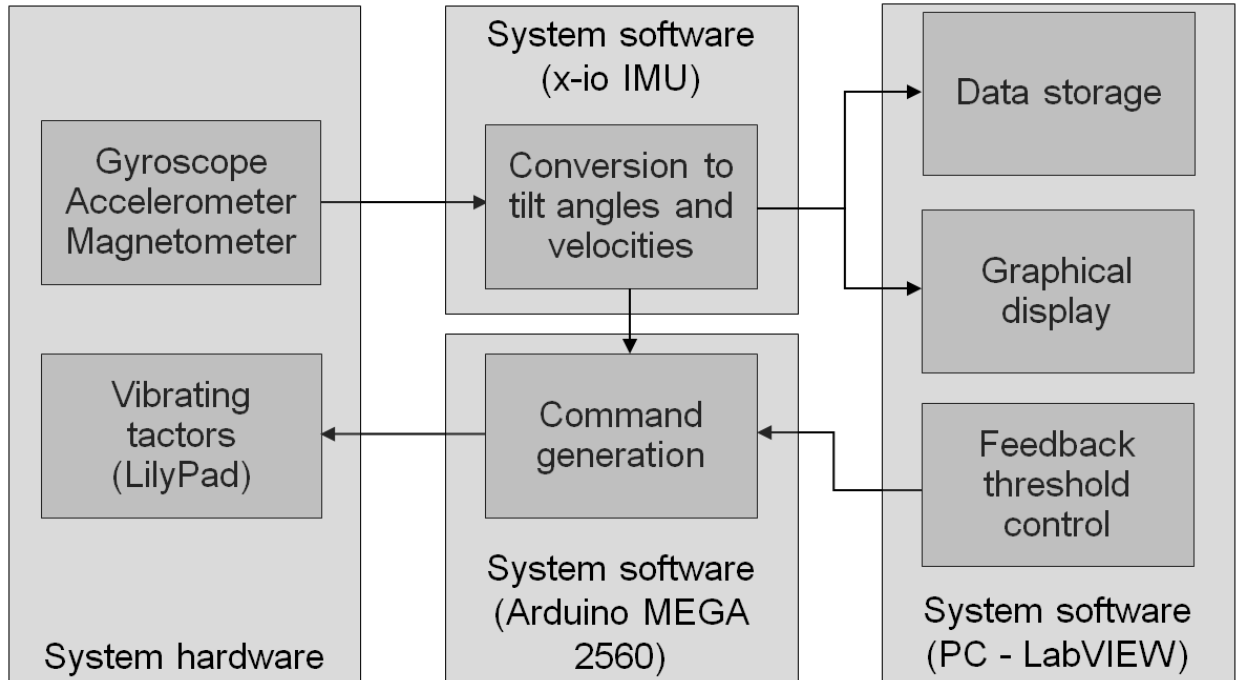


Figure 3-4: Schematic of the wobble board hardware and software integration. The inertial measurement unit and vibrotactile elements interface with an on-board microprocessor that, in turn, interfaces with custom-built LabVIEW software via USB.

Vibrotactile cues were generated based on a feedback control signal that represents a weighted sum of tilt angle and velocity [59]: if the control signal exceeds the feedback threshold in either the *AP* or *ML* tilt direction, the three vibrating factors corresponding to the direction of tilt angle and velocity are activated (Figure 3-5). This activation scheme was based on the notion that added directional resolution (beyond the four cardinal directions) is only as effective as a four-directional factor configuration for vibrotactile feedback during standing balance [57], [61]. None of the factors are active when the control signal is below the threshold in both directions (i.e., in the no-feedback zone).

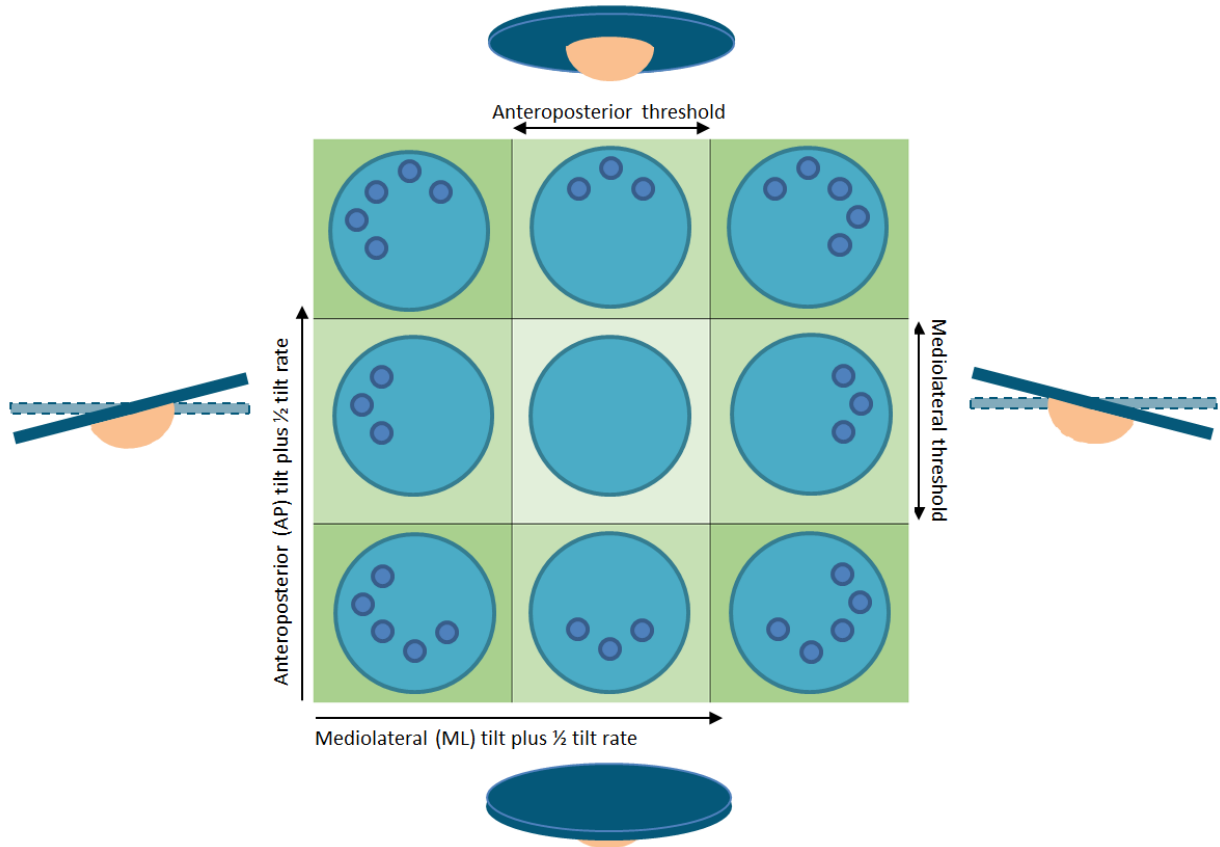


Figure 3-5: Schematic of factor activation thresholds. Three factors are activated when the anteroposterior (*AP*) or mediolateral (*ML*) control signal surpasses the two-sided threshold in either direction. If both *AP* and *ML* control signals exceeded respective thresholds simultaneously, five factors are activated. The cueing scheme is repulsive rather than attractive; factors are activated in the same direction as the tilt control signal.

During each dynamic sitting trial, the control signals are displayed graphically as an arrow with its length and direction corresponding to the vector sum of the *AP* and *ML* control signals (Figure 3-6, bottom). The two-sided thresholds are displayed as a rectangle on the graph. The tilt angles and the vibrotactile feedback status (on or off) are stored in a text file along with other parameters of the balance trial (Figure 3-6, top right). The GUI also displays the third quartile of the positive *AP* and the positive *ML* control signals for the most recent trial recording (Figure 3-6, top left), which may be used to select feedback thresholds for future trials (e.g., after a customization trial; see *Chapter 4 Utility of Instrumented Wobble Board for Balance Assessment and Sensory Augmentation during Balance Training*).

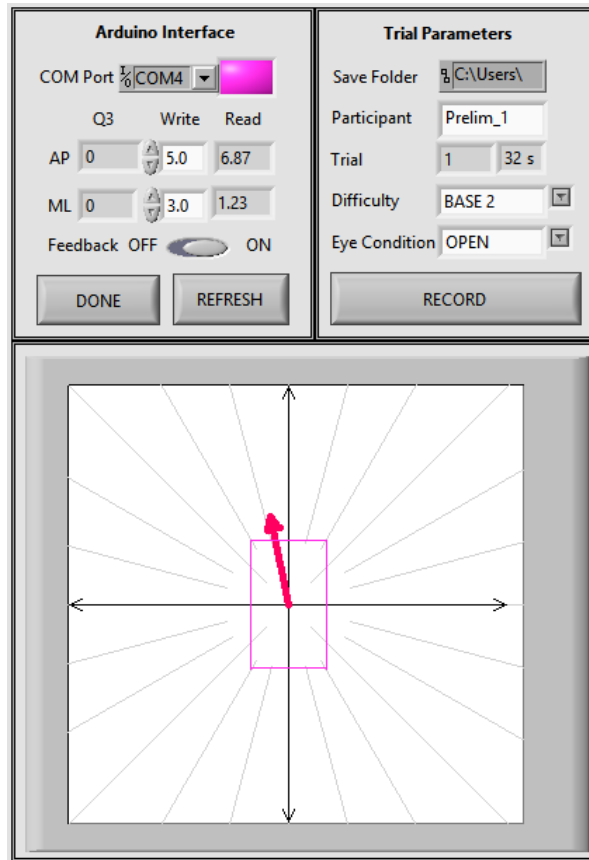


Figure 3-6: LabVIEW interface for monitoring balance assessments, selecting vibrotactile feedback thresholds, and recording all time series and parametric data. The length and direction of the vector are proportional to the magnitude and direction of the feedback control signal, respectively. The rectangle on the graph visualizes the two feedback thresholds: when the vector moves outside of the rectangle (as shown here), vibrotactile cues are delivered to the sitting surface (here: via the three anterior factors).

### 3.2.2 Validation of Kinematic Measurements

The IMU is housed within the wobble board to provide built-in, real-time measurements of the wobble board's kinematics. However, a technical validation experiment was required using a gold-standard optoelectronic motion capture system to validate the accuracy of the IMU measurements during multidirectional movements of the wobble board.

### 3.2.2.1 Angular Displacement Tests

Four reflective markers were attached to the wobble board: two in line with its *AP* axis (ANT and POST) and two in line with its *ML* axis (LEFT and RIGHT). Eight motion capture cameras (Motion Analysis Inc., Santa Rosa, CA, USA) sampled each marker's 3D coordinates at a sampling frequency of 64 Hz. Concurrently, the on-board IMU sampled the wobble board's *AP* and *ML* tilt angles at 32 Hz.

During each trial in a series of 12 trials, an experimenter manually displaced the wobble board for 1 minute. The *AP* and *ML* tilts had a range and frequency of up to  $\pm 17$  degrees and 0.5 Hz, respectively, to encompass the full extent of wobble board motions expected during balance applications [39]. At the beginning of each trial, a 6-Volt push button signal was delivered to both the motion capture system and the custom LabVIEW software to facilitate time synchronization of the kinematic data streams from the two different data acquisition systems.

### 3.2.2.2 Data Processing and Analysis

Data were processed using MATLAB 2017a (Mathworks, Natick, MA, USA). The motion capture data were down-sampled to match the sampling frequency of the IMU data (32 Hz). An orthonormal coordinate system,  $R$ , was derived from the position vectors from RIGHT to LEFT and from POST to ANT (Equations (1)-(4)).

$$\vec{r}_y = ANT - POST \quad (1)$$

$$\vec{r}_z = \vec{r}_y \times (RIGHT - LEFT) \quad (2)$$

$$\vec{r}_x = \vec{r}_z \times \vec{r}_y \quad (3)$$

$$R = \{\vec{r}_x, \vec{r}_y, \vec{r}_z\} \quad (4)$$

This local coordinate system was then used to obtain a rotation matrix defining the time-varying orientation of the wobble board in the global coordinate system of the laboratory. The *AP* and *ML* tilt angles were extracted using a Cardan angle sequence with the following order of rotations: (1) anteroposterior flexion/extension, (2) lateral flexion, and (3) axial rotation [135]. See Appendix C for further details regarding the estimation of angular displacements from motion capture data.

The accuracy of the IMU measurements was quantified by the coefficient of determination,  $R^2$ , which calculates the proportion of the variability in IMU tilt angles that was accounted for by the actual deviations in tilt angles as measured by motion capture [73]. First, data preceding the push button onset in each time series were truncated, thereby time-synchronizing the subsequent measurements. Then, the mean difference between the two data sets (DC offset) was removed. Next,  $R^2$  was calculated according to (5), where  $i = 1:N$  denotes the sample numbers in a time series,  $y$  are IMU measurements, and  $m$  are motion capture measurements. Finally,  $R^2$  values from individual trials were averaged across all trials.

$$R^2 = 1 - \frac{\sqrt{\sum_i (y_i - m_i)^2}}{\sqrt{\sum_i (m_i - \sum_i m_i / N)^2}} \quad (5)$$

### 3.3 Results

#### 3.3.1 Validity of the IMU Measurements

The results of one angular displacement test are shown in Figure 3-7. During all tests and in both *AP* and *ML* directions, the residuals between motion capture and IMU measurements were relatively small, as indicated by the accuracy measures ( $R^2$ ) listed in Table 3-2. The observed  $R^2$  values were similar for both *ML* and *AP* comparisons (mean  $R^2$ : 99.4 %). The poorest accuracy observed was during the fifth trial in the *AP* direction ( $R^2_{AP} = 98.1$  %). The offset between motion capture and IMU measurements was consistent across trials, with mean and standard deviation of  $-1.54 \pm 0.04$  degrees in the *AP* direction and  $0.38 \pm 0.08$  degrees in the *ML* direction, indicating a systematic bias that was potentially caused by imperfect alignment of the IMU axes with the wobble board axes. The suggested calibration procedure is to remove the curved base and rest the wobble board on a level surface, and subtract the measured *AP* and *ML* tilt angles from all subsequent, respective data.

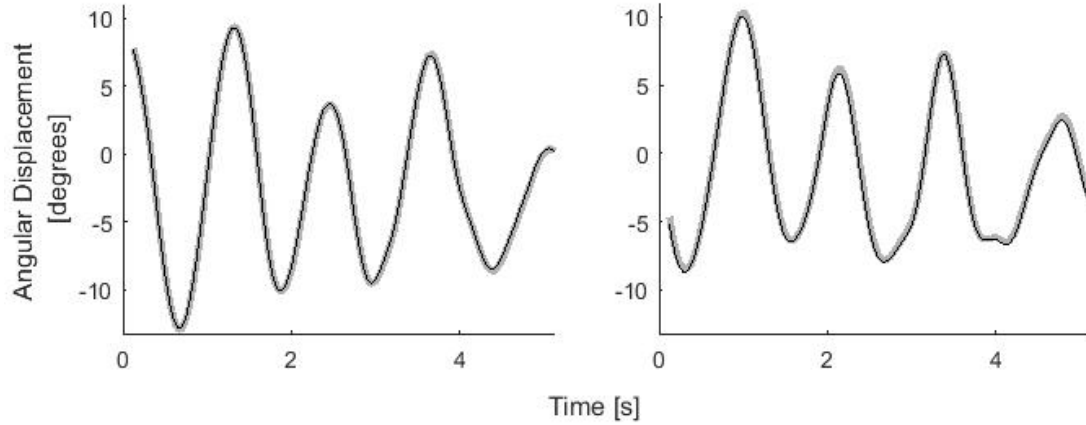


Figure 3-7: *ML* (left) and *AP* (right) tilt angles measured by the gold-standard motion capture system (bold gray lines) and the inertial measurement unit (thin black lines) during five seconds of fast, multidirectional displacements, after demeaning and time synchronization.

Table 3-2: Accuracy results for the IMU tilt angle measurements from twelve displacement tests and their mean and standard deviation (SD).

Displacement Test	Mean Offset [degrees]		Coefficient of Determination, $R^2$ [%]	
	AP	ML	AP	ML
1	-1.50	0.43	99.8	99.7
2	-1.49	0.41	99.9	99.9
3	-1.50	0.39	99.9	99.9
4	-1.58	0.33	99.7	99.8
5	-1.53	0.23	98.4	98.8
6	-1.50	0.24	96.2	97.0
7	-1.58	0.45	99.9	99.8
8	-1.53	0.42	99.9	99.9
9	-1.57	0.43	99.9	99.9
10	-1.60	0.49	99.9	99.9
11	-1.54	0.30	99.6	99.8
12	-1.56	0.38	98.7	99.1
Mean	-1.54	0.38	99.3	99.5
SD	0.04	0.08	1.1	0.8

## 3.4 Discussion

### 3.4.1 Potential of Dynamic Sitting Assessment Device

The objective of the research presented in this chapter was to develop a portable device for perturbing seated posture, including on-board instrumentation that accurately measures tilt angles during dynamic sitting to be used for balance assessment and training. We developed a sitting device attached to a curved base that continuously destabilizes seated posture in two rotational dimensions. Near their limits of stability, individuals rely on reactive control strategies to maintain upright sitting, allowing the integrity of these strategies to be assessed. For example, stroke survivors exhibit significantly higher center of pressure (COP) velocities than non-disabled, older adults *only* while sitting on an unstable surface; no differences in COP velocities between groups can be observed during unperturbed sitting [26]. Analogous devices exist to simultaneously perturb and assess standing posture. For example, the Equitest (NeuroCom International, Clackamas, OR, USA) alters the standing support surface and visual surround, and has been used to quantify the effects of novel balance aids [56], evaluate balance training programs [16], and identify sensorimotor deficiencies [16] via COP analyses. While the passive perturbations elicited by the curved base of the wobble board do not afford the luxury of prescribing a known perturbation to the upright sitting posture [73], it holds the advantage of eliciting continuous instability in all horizontal directions while requiring no external power or additional equipment. On the one hand, continuity of the perturbations allows the long-term performance of the postural control system to be assessed (as opposed to the assessment of postural response to transient perturbations); on the other hand, the multidirectional aspect of the unstable surface facilitates the assessment of the full directional range of reactive control that may be required to maintain upright sitting during everyday challenges, and the identification of those directions that may be particularly challenging for the user.

A key feature of the design is the modularity of bases with varying radii of curvature. The bases can be interchanged to adjust the difficulty of maintaining upright sitting. This feature makes the device suitable for users of ranging abilities and those that improve abilities over time – as the stability level can be modulated to continuously, but safely challenge seated balance. When comparing this method to others published in the literature, it can be seen that similar protocols used curved bases of various sizes [29]–[39], [43]–[45] or a sitting surface attached to a central

pivot [23], [24], [40], [46] to passively and continuously elicit seated instability. A major advantage of the wobble board considered in this study is its accessibility; unlike most other unstable sitting devices described in the literature [24], [29]–[46], an-onboard IMU quantifies seated stability, thus, eliminating the need for a force plate or motion capture system. It has been shown that correlation coefficients between tilt angles measured via classical motion capture and those measured via an IMU are higher than 0.88 during unstable sitting [23]. The same study observed that, during unstable sitting, support surface tilt angles and COP displacements are highly correlated [23]; thus, many of the established methods for summarizing and interpreting COP behavior (e.g., posturographic measures) are valid for analyzing tilt angles as measured by the wobble board. The technical experiment performed in this study revealed correlation coefficients higher than 0.96, verifying that the device in this study can accurately measure *AP* and *ML* tilt angles during multidirectional perturbations to seated posture. One limitation of this approach is that it may fail to distinguish between different balance strategies that control the upper body differently to achieve the same support surface tilt [24]. To address this limitation, additional IMUs could be placed on body segments to characterize their motion during assessment tasks. However, this would significantly increase the complexity of the assessment protocol. As is, the wobble board is a completely portable device capable of obtaining assessment metrics in any convenient environment, with accuracy comparable to a gold-standard motion capture system.

Other methods of quantitative sitting assessment exist [1], including: (1) the comparison of foot and trunk contributions to the balancing task, by measuring support surface reactions on the floor *and* seat during sitting [136]; or (2) the identification of transfer functions between directional perturbations [73] and kinematic [60] or COP and electromyographic responses [75]. These methods are well suited for fundamental investigations of neuromuscular mechanisms, but are complex and restricted to laboratory settings. In the future, the wobble board device could also be used to replicate aspects of other unstable sitting studies, or devise new studies to help characterize underlying mechanisms of seated postural control, without requiring a force plate or motion capture system.

### 3.4.2 Potential of Vibrotactile Feedback Device

Besides its conceivable use as a postural assessment tool, the wobble board has a significant potential to train seated balance in clinical populations, consistent with a main objective of the overall thesis research project. The postural perturbations elicited by the curved base challenge the user to maintain upright sitting, which may strengthen the muscles required for sitting and decrease reaction times to restore seated stability [137], [138]. Additionally, the wobble board uses vibrating tactors, activated intermittently based on kinematic feedback and within the responsive frequency range of cutaneous receptors in the skin [134], to display sensory cues. Concurrent sensory feedback during functional task training could reinforce movement proficiency by repetition [139], increase motivation to successfully perform training tasks [118], [139], relieve therapists from a coaching role during training sessions [52], and induce plasticity of somatosensory pathways for improved sensorimotor function [52], [118]. Note that many feedback modalities, including visual displays [98], [119], auditory tones [124], vibrotactile stimulation [49], [56]–[63], and multimodal [88] or other approaches [140] have been used for displaying feedback during standing balance. However, vibrotactile feedback has been favored for its compact, non-invasive nature as well as its effectiveness in reducing postural sway during stance [49], [56]–[63] and improving sensorimotor function during a wide range of other functional tasks [54]. Decreased tactile sensitivity, as in some older adults [141], could, however, restrict the effectiveness of vibrotactile feedback for balance training. In these cases, visual feedback on support surface tilt shown on the guided user interface could be used for sensory augmentation.

The vibrating tactors in the wobble board deliver repulsive feedback cues based on the weighted sum of tilt angle and tilt velocity. This proportional-derivative control scheme has been used by other vibrotactile feedback devices [56], [60]–[62] due to the notion that position and velocity feedback are important variables for the CNS when controlling balance [59], [142]. When placebo feedback (not based on direction) was delivered to standing balancers, stability decreased [56], refuting the notion that balance is improved purely by sub-sensory vibration or attentiveness effects [143]. However, the natural tendency to move towards a torso vibration when no instruction is provided suggests that attractive cueing may be more compatible with postural response dynamics than repulsive cueing [144]. Many other schemes have been considered [142], [145], and the optimal tuning of feedback parameters for training seated

balance remains to be determined. The Arduino-LabView interface used in this study allows the feedback parameters (control signal formula, feedback thresholds) to be easily adjusted, whereas the use of eight equally-spaced factors facilitates further spatial resolution of the feedback (up to 8 directions) if deemed necessary [56].

Since vibrotactile cues are based on wobble board tilt, the user must be able to maintain balance on the easiest base. For people who struggle to maintain upright sitting on a stable surface, this paradigm fails to provide measurements that can be converted into feedback cues. In this case, COP displacements or body kinematics could be used to generate vibrotactile feedback cues during quiet sitting. However, the presence of postural perturbations may be necessary for effective training via sensory augmentation, since concurrent feedback is less effective, or even detrimental, when the training task is too simple [146].

Vibrotactile feedback has been used in a closely related application, to correct sitting posture during static sitting in a chair [147]. In contrast to dynamic balance training, where vibrotactile cues are delivered concurrently to alert reactive response mechanisms to correct an impending loss of balance, vibrotactile cues in the device designed by Cohen et al. are delivered intermittently, with the intent to alert the user of a change from the preferred posture. Here, the response is a voluntary adjustment of posture. While posture-correcting vibrotactile feedback aims to mitigate effects of poor posture, balance-training vibrotactile feedback aims to mitigate the effects of postural instability and restore or improve reactive balance control. Our sensory augmentation device is completely self-contained and relies only on a laptop computer if recording of the training session is desired.

### 3.5 Conclusions

The wobble board's curved bases elicit the response of reactive control strategies required to maintain upright sitting. The stand-alone device is portable and requires no additional equipment to quantitatively assess and train seated balance. The device bears the potential to improve diagnosis and prognosis of balance-deficient individuals; however, extensive testing is required. The assessment technique is only useful if it can reliably identify specific deficiencies in seated

balance that can lead to more effective treatments. The sensory feedback technique is only useful if unstable sitters benefit compared to simpler training methods.

## 4 Utility of Instrumented Wobble Board for Balance Assessment and Sensory Augmentation during Balance Training

### 4.1 Introduction

The ‘instrumented wobble board’ described in Chapter 3 was developed to quantify postural stability and deliver vibrotactile feedback cues during unstable sitting. The desired functions of the wobble board were validated in an experiment involving human participants. The main objective of the present study was to evaluate the feasibility of using the device to assess and train sensorimotor function during continuous, multidirectional perturbations. To meet this goal, we tested the sensitivity of posturographic measures in non-disabled individuals to conditioned settings, including a vibrotactile feedback paradigm.

Non-disabled participants sat on the wobble board and tried to maintain balance while three variables were systematically altered: balance difficulty via base curvature, elimination of visual input, and status of the vibrotactile feedback system. Posturographic measures were calculated from angular displacements of the wobble board measured by the on-board IMU during each experimental condition, and statistical methods identified significant explanatory variables.

### 4.2 Methods

#### 4.2.1 Participants

A total of 27 non-disabled volunteers (Table 4-1) were recruited to participate in preliminary testing of the wobble board functions. Each participant provided informed consent and had no history of neurological or musculoskeletal disorders, nor was experiencing back pain chronically or acutely at time of testing. This study was approved by the ethics committee of the University of Alberta (HREB Pro00039437).

## 4.2.2 Experimental Protocol

A preliminary protocol was completed by twelve individuals. Following refinements to the protocol, another fifteen participants completed the revised protocol. The preliminary protocol and reasons for its revision are discussed in Appendix D. In this chapter, the materials and methods, analysis, result, and interpretation associated with the second protocol are presented.

Table 4-1: Participant characteristics.

<b>Dataset</b>	<b>Gender</b>	<b>Age</b>	<b>Weight (kg)</b>	<b>Height (cm)</b>
Preliminary Experiments	M	19	79	180
	M	20	60	175
	M	24	85	184
	M	23	69	174
	M	18	85	190
	M	20	61	167
	M	23	76	156
	M	22	86	184
	M	30	82	182
	M	24	83	182
	M	21	102	188
	M	22	73	182
Mean (Standard Deviation)		22.4 (2.9)	75.4 (12.9)	177 (10)
Validation Experiments	F	25	55.3	156
	F	21	55.8	173
	F	28	56.4	157
	F	25	61.5	159
	F	23	61.1	163
	M	20	69.8	171
	M	20	85.5	177
	M	24	86.7	174
	M	24	67.9	167
	M	24	69.2	181
	M	24	85.3	186
	M	24	72.6	177
	M	24	92.8	185
	M	28	86.2	183
	M	25	92.8	178
Mean (Standard Deviation)		23.9 (2.3)	73.2 (13.7)	172 (10)
<b>Grand Mean (Standard Deviation)</b>		<b>23.1 (2.7)</b>	<b>74.4 (13.1)</b>	<b>175 (10)</b>

For each of forty attempted 30-s balance trials [148], each participant was asked to maintain, as much as possible, an upright posture while sitting on the wobble board without foot support. Each trial started after the participant donned noise-cancelling headphones, folded his or her arms across the chest, and verbally cued the experimenter of being ready. The experimenter monitored the participant for safety and noted any loss-of-balance events. Note that participants were allowed to take rests as long as needed between balance trials.

Three task conditions were tested: eyes were either open or closed (EO or EC), base curvature was either 20 cm or 15 cm (B2 or B3), and vibrotactile feedback cues were provided intermittently or not at all (ON or OFF). Four blocks of ten consecutive trials were randomly assigned a unique combination of base and eye conditions. Within each block, the first four trials (familiarization trials) were used for the participant to mitigate the confounding effect of learning the dynamic sitting task [23], [44], [110], and for the experimenter to determine the thresholding control scheme for the vibrating factors in the surface of the seat. In the final six trials per block (balance trials), three were randomly selected as control trials; during these trials, the factors remained inactive (Table 4-2).

Table 4-2: Schedule of 30-s trials in one exemplary block of ten trials (shown: base #2 with eyes closed). In random order, four blocks were attempted: one for each unique combination of base and eye conditions. The horizontal line between trials 4 and 5 represents the end of the familiarization trials. In trials 5 through 10, the vibration condition was randomized so that exactly 3 trials were control (no feedback) trials.

<b>Trial</b>	<b>Base Condition</b>	<b>Eye Condition</b>	<b>Vibration Condition</b>
1	B2	EC	OFF
2	B2	EC	OFF
3	B2	EC	ON
4	B2	EC	ON
5	B2	EC	RANDOM
6	B2	EC	RANDOM
7	B2	EC	RANDOM
8	B2	EC	RANDOM
9	B2	EC	RANDOM
10	B2	EC	RANDOM

For the feedback trials, direction-specific vibrating factors were activated when the control signal, defined as the tilt angle of the wobble board plus one half its tilt velocity, exceeded a two-sided threshold in one or both of the *AP* or *ML* directions [57], [59]. If the *AP* signal passed the *anterior* threshold, the three *anterior* vibrators turned on. Similarly, the three factors in the *posterior*, *left* and *right* directions were activated if the control signal in the corresponding direction passed respective threshold. Thus, the feedback scheme is *repulsive cueing* [55]. The experimenter informed the participant of the upcoming feedback condition and set the thresholding control scheme for the eight vibrating factors in the surface of the seat. Previous studies of feedback devices have shown that balance function is improved when feedback is optimized for each individual [142], [145], while providing too much feedback may detriment learning [52]. Therefore, the thresholds for feedback were set to equal the third quartile of the positive (and third quartile of the negative) feedback control signal for each tilt direction (*AP*, *ML*) during an initialization trial, resulting in the vibrators being active approximately 50 percent of the time. During each trial, the wobble board tilt was sampled at a frequency of 32 Hz.

### 4.2.3 Data Processing

The kinematic data recorded from each participant were analyzed using MATLAB 2017a. The first two seconds of data were discarded to mitigate confounding effects of beginning the trial [38]. The *AP* and *ML* time series were then demeaned and filtered using a fourth-order, low-pass Butterworth filter with a cutoff frequency of 5 Hz, considering that higher frequency components are generally attributed to noise artifacts rather than balance characteristics [64]. See Appendix E for details of the filter design. An additional time series, tilt magnitude (TM), was derived from the vector sum of *AP* and *ML* measurements:

$$TM = \sqrt{AP^2 + ML^2}$$

Data from balance trials were omitted if the participant lost balance during the trial. The entire block of trials was omitted if the participant lost balance during at least half of the trials for the given eye and base condition.

#### 4.2.4 Posturographic Analysis

To quantify and compare sitting performance in each of the experimental conditions, *time domain*, *frequency domain*, and *stabilogram diffusion* analyses were performed with each of the tilt angle time series (*AP*, *ML*, *TM*) for each trial. From the categories of analyses above, six commonly used posturographic measures were selected on the basis of linear independence from other posturographic measures [37] and reliability [23], [37]. In the time domain, the root-mean-square (*RMS*), and the mean velocity (*MVELO*) were calculated from each time series [25]. In the frequency domain, the centroidal frequency (*CFREQ*) and the frequency dispersion (*FREQD*); were calculated in accordance with [25]. To do so, first the spectral density function for each time series was estimated using Welch's method (five windows with 50% overlap). Finally, the short-term diffusion coefficient (*DS*) and short-term scaling exponent (Hurst exponent; *HS*) were calculated from a stabilogram diffusion plot (SDP) as described in [95]. The former was expressed on a logarithmic scale to meet assumptions of the linear model discussed below. Further details regarding the selection and calculation of posturographic measures are provided in Appendix A.

#### 4.2.5 Statistical Analysis

The posturographic measures were tested for linear independence by calculating the matrix of correlation coefficients. Correlation coefficients were also calculated to quantify the relationship between weight, height, and the average posturographic measures for each participant. A linear mixed model was used to explore the relationship between posturographic measures from each trial and explanatory variables (Table 4-3): base condition (BASE; B2 or B3), eye condition (EYE; EO or EC), vibration condition (VIB; ON or OFF), and trial number since last rest (TR, 1-6). In addition to these fixed-effects factors, the model included random-effects factors that vary by participant (PP; 1-15); this method accounts for the correlation of repeated measures obtained from the same participant and allows unbalanced trials to be included [132]. The linear model assumes that the residual error is normally distributed with constant variance. Histograms and plots of residuals were inspected to ensure that the assumptions were reasonable. Post hoc, subgroups of trials were fit to the linear mixed-effects model to explore the BASE, EYE, and VIB effects within each condition and combination of conditions (Table 4-3). The significance of fixed effects factors in the linear mixed model was analyzed by an F-test of the ratio between the

variance between group means and the variance of residuals (ANOVA). F-tests with Bonferroni adjustments were performed to identify which of the multiple comparisons between explanatory variables were significant.

Table 4-3: Summary of explanatory variables used in mixed linear model of balance trials.

<b>Sample</b>	<b>Explanatory Variables</b>	<b>Degrees of freedom</b>
ALL	Eye, base, and vibration condition (EYE, BASE, VIB)	255
B2	EYES, VIB	164
B3	EYES, VIB	89
EC	BASE, VIB	107
EO	BASE, VIB	146
B2, EC	VIB	81
B2, EO	VIB	82
B3, EC	VIB	25
B3, EO	VIB	63
ALL	Trial number since last rest (TR)	257

## 4.3 Results

### 4.3.1 Response of Vibrotactile Display

Figure 4-1 shows the magnitude of the *AP* (top) and *ML* (bottom) control signals (gray lines) from one exemplary balance trial. Horizontal lines represent the two-sided threshold; bold lines represent actively vibrating factors in the corresponding direction: front for positive *AP*, rear for negative *AP*, right for positive *ML*, and left for negative *ML* (in accordance with Figure 3-5). In all cases where a control signal exceeded a threshold, the corresponding vibrators were activated with negligible onset latency. At least once during the depicted balance trial, the wobble board exceeded *AP* and *ML* thresholds simultaneously (see, e.g., data segment from 20 seconds on), resulting in activation of tactors in both corresponding directions (in accordance with Figure 3-5). The vibrators were active (in at least one direction) for approximately 4.8 seconds, or 15.1% of the depicted balance trial.

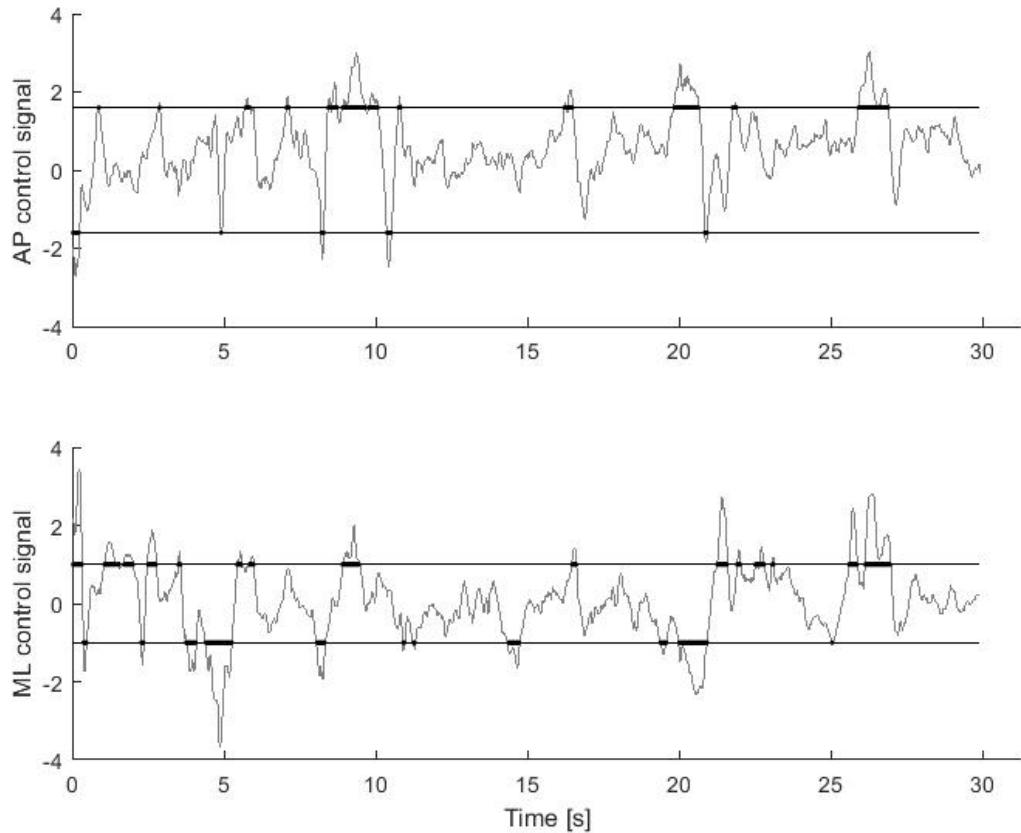


Figure 4-1: Control signal time series in *AP* (top) and *ML* (bottom) directions during one 30-s balance trial (Participant 4, base #2, eyes open) with vibrotactile feedback. The gray time series represent the control signals (tilt angle plus one half of tilt velocity), whereas the black horizontal lines represent the two-sided thresholds for vibrotactile feedback. Bold lines indicate that factors were active in the corresponding direction (front for positive *AP*, rear for negative *AP*, right for positive *ML*, left for negative *ML*). The vibrators were active (in at least one direction) for approximately 4.8 seconds, or 15.1% of the depicted balance trial.

### 4.3.2 Sample Characteristics

In total, 259 balance trials were analyzed (Table 4-4). Five of the fifteen participants completed balance trials under all four base and eye combinations. The other ten participants could not maintain balance on base #3 with eyes closed. Four of these ten participants could not maintain balance on base #3, regardless of eye condition.

Table 4-4: Summary of completed balance trials in each task condition. Trials in bold were excluded from the analysis because the participant lost balance in half or more of the balance trials for that task condition (in the case of Participant 11, all trials were excluded because the participant lost balance in half or more trials in all but one of the task conditions, so comparisons between conditions were unreliable).

Participant	Base #2		Base #3		Total
	Eyes Open	Eyes Closed	Eyes Open	Eyes Closed	
1	6	6	<b>0</b>	<b>0</b>	12
2	6	6	6	<b>0</b>	18
3	6	6	6	<b>0</b>	18
4	6	6	5	<b>0</b>	17
5	6	6	6	5	23
6	6	6	6	5	23
7	6	6	6	6	24
8	6	6	6	5	23
9	6	6	6	<b>0</b>	18
10	6	6	6	<b>0</b>	18
11	<b>6</b>	<b>2</b>	<b>3</b>	<b>0</b>	0
12	6	6	6	<b>1</b>	18
13	6	5	<b>2</b>	<b>0</b>	11
14	6	6	6	6	24
15	6	6	<b>0</b>	<b>0</b>	12
Total	84	83	65	27	259

### 4.3.3 Correlation of Posturographic Measures

As shown in Table 4-5, measures based on *TM* time series were highly correlated with their *AP* and *ML* counterparts; only *FREQD* of *TM* tilts appeared to be independent. Furthermore, *TM*-based measures were only sensitive to the manipulated conditions when one (or both) of the corresponding *AP*- and *ML*-based measures were significant. Therefore, results of *TM* measures were omitted from the following sections in favor of the more interesting *AP* and *ML* results. Most of the remaining measures are linearly independent ( $r < 0.6$ ) as shown in Table 4-5. The *AP* measures correlate to *ML* measures of the same type (except *FREQD*). The *RMS* and *MVELO* measures are highly correlated. The *DS* measures also correlate to the *RMS* and *MVELO* measures. The *HS* and *CFREQ* measures are negatively correlated.



#### 4.3.4 Effects of Participant Anthropometry on Posturographic Measures

Correlations between participant weights and heights and their average posturographic measures are shown in Table 4-6. Only trials performed on base #2 were considered, to maintain a balanced sample of posturographic measures (Table 4-4). Heavier and taller participants swayed faster (*MVELO*) and with greater variance (*RMS*) with greater diffusion (*DS*) in both directions. In the *AP* direction, taller participants swayed less frequently (*CFREQ*) but with higher frequency dispersion (*FREQD*). None of the correlation coefficients were greater than 0.5 in magnitude.

Table 4-6: Correlation coefficients for the weight and height of each participant and the average of their posturographic measures from trials on base #2.

Posturographic measure	Tilt direction	Weight	Height
RMS	AP	0.30	0.33
	ML	0.33	0.38
MVELO	AP	0.35	0.24
	ML	0.37	0.35
CFREQ	AP	-0.16	-0.47
	ML	-0.18	-0.25
FREQD	AP	0.03	0.44
	ML	-0.39	-0.14
DS	AP	0.44	0.29
	ML	0.49	0.41
HS	AP	0.18	0.20
	ML	0.36	0.30

#### 4.3.5 Effects of Base Curvature on Posturographic Measures

Table 4-7 shows the average posturographic measures obtained from all successful trials in each combination of conditions. Table 4-8 shows the estimated change in each posturographic measure when seat instability is increased (BASE). In both *AP* and *ML* directions, *RMS* and *MVELO* were higher in trials with the less stable base (Figure 4-2). Also in the less stable base condition, *FREQD* was lower in the *AP* direction (Figure 4-3). *DS* increased due to increasing

seat instability, in both tilt directions (Figure 4-4). HS also increased due to increasing seat instability, but only in the *AP* direction for eyes closed. This particular effect was only significant according to the post-hoc test of trials with eyes closed (figure not shown).

Table 4-7: Posturographic measures derived from *AP* and *ML* tilts during upright sitting trials under each experimental condition. Average measures and their standard deviation were calculated for each participant, then averaged per condition across all participants. Shown in brackets is the average of within-participant standard deviations.

HS [-]		DS [degrees <sup>2</sup> /s]		FREQD [-]		CFREQ [Hz]		MVELO [degrees/s]		RMS [degrees]		Dependent Variable			
												Experimental Condition			
												Base #2		Base #3	
												Eyes Open		Eyes Closed	
Vibration Off		Vibration On		Vibration Off		Vibration On		Vibration Off		Vibration On					
ML	AP	ML	AP	ML	AP	ML	AP	ML	AP	ML	AP	ML	AP		
0.87 (0.02)	0.86 (0.02)	-1.23 (0.60)	-1.10 (0.43)	0.65 (0.05)	0.71 (0.04)	0.47 (0.06)	0.43 (0.06)	1.30 (0.34)	1.39 (0.25)	0.70 (0.19)	0.87 (0.19)	1.30 (0.34)	1.39 (0.25)		
0.85 (0.02)	0.84 (0.03)	-1.48 (0.56)	-1.34 (0.43)	0.66 (0.05)	0.71 (0.04)	0.52 (0.07)	0.45 (0.08)	1.13 (0.26)	1.22 (0.22)	0.55 (0.11)	0.71 (0.17)	1.13 (0.26)	1.22 (0.22)		
0.86 (0.02)	0.86 (0.02)	-0.02 (0.48)	-0.01 (0.50)	0.66 (0.04)	0.68 (0.04)	0.48 (0.07)	0.44 (0.06)	2.36 (0.56)	2.36 (0.52)	1.28 (0.20)	1.37 (0.36)	2.36 (0.56)	2.36 (0.52)		
0.86 (0.02)	0.87 (0.01)	0.16 (0.43)	0.16 (0.42)	0.66 (0.04)	0.66 (0.05)	0.48 (0.05)	0.47 (0.06)	2.48 (0.47)	2.55 (0.44)	1.32 (0.27)	1.34 (0.31)	2.48 (0.47)	2.55 (0.44)		
0.86 (0.02)	0.85 (0.03)	-0.12 (0.55)	-0.18 (0.52)	0.65 (0.04)	0.69 (0.04)	0.52 (0.09)	0.45 (0.06)	2.14 (0.54)	2.02 (0.41)	1.07 (0.22)	1.24 (0.32)	2.14 (0.54)	2.02 (0.41)		
0.85 (0.03)	0.85 (0.02)	-0.25 (0.73)	-0.35 (0.58)	0.66 (0.05)	0.68 (0.04)	0.52 (0.07)	0.49 (0.06)	2.10 (0.72)	1.90 (0.52)	1.06 (0.39)	1.06 (0.34)	2.10 (0.72)	1.90 (0.52)		
0.84 (0.03)	0.87 (0.02)	1.19 (0.41)	1.02 (0.40)	0.70 (0.03)	0.65 (0.05)	0.50 (0.06)	0.47 (0.04)	4.54 (0.83)	4.00 (0.56)	2.25 (0.40)	1.98 (0.39)	4.54 (0.83)	4.00 (0.56)		
0.84 (0.03)	0.88 (0.01)	1.15 (0.48)	1.07 (0.43)	0.68 (0.04)	0.64 (0.03)	0.49 (0.05)	0.45 (0.05)	4.35 (0.98)	4.10 (0.92)	2.18 (0.47)	2.13 (0.51)	4.35 (0.98)	4.10 (0.92)		

#### 4.3.6 Effects of Eye Condition on Posturographic Measures

Table 4-8 includes the estimated effect of eliminating visual input on each posturographic measure. Removing visual input had a similar effect on posturographic measures as increasing seat instability: *RMS*, *MVELO*, *DS* in both *AP* and *ML* directions, whereas *HS* increased in the *AP* direction only (Figure 4-2, Figure 4-4). In addition, *FREQD* decreased in the *AP* direction only (Figure 4-3).

#### 4.3.7 Effects of Vibrotactile Feedback on Posturographic Measures

At least one of the control signals (*AP*, *ML*) was above the given threshold for feedback during  $25.6 \pm 9.5$  % of each ON trial and during  $32.6 \pm 10.8$  % of each OFF trial (grand mean  $\pm$  average of within-participant standard deviations). Table 4-8 shows that posturographic measures were generally less sensitive to the addition of vibrotactile feedback (VIB) than changes in base or eye condition, showing no significant differences between conditions (Figure 4-2 to Figure 4-4). However, the post-hoc analysis revealed the following significant effects: with eyes open on base #2, vibration significantly decreased *RMS* measures in both directions, increased *CFREQ* in the *ML* direction, and decreased *HS* in the *ML* direction.

Table 4-8: Estimated effect of experimental conditions on posturographic measures derived from tilt angles in each direction. Effects include: base (BASE: the estimated change in the posturographic measure when the radius of curvature is decreased, i.e., when the surface is less stable), eye (EYE: the estimated change in the posturographic measure when visual input is removed, i.e., when eyes are closed), vibration (VIB: the estimated change in the posturographic measure when the vibrotactile feedback is provided, i.e., compared to control trials with no feedback), and trials since last rest (TR: the estimated change in the posturographic measure when progressing from one trial to the next). Shown are the estimated coefficients of the linear mixed models, their standard error, and the probability that the F-statistic derived from the ANOVA in the mixed-effects model is observed under the hypothesis that the factor has no effect on the posturographic measure. Effects in bold are considered significant after a Bonferroni correction for multiple comparisons ( $\alpha_{\text{adjusted}} = 0.0014$ ).

Posturographic Measure	Direction	Effect	Estimate	Standard Error	Pr > F
RMS [degrees]	AP	<b>BASE</b>	0.72	0.12	<0.0001
		<b>EYE</b>	0.75	0.15	<0.0001
		<b>VIB*</b>	-0.12	0.05	<0.05
		TR	-0.01	0.02	0.54
	ML	<b>BASE</b>	0.80	0.14	<0.0001
		<b>EYE</b>	0.89	0.20	<0.0001
		<b>VIB*</b>	-0.08	0.05	0.09
		TR	0.01	0.03	0.79
MVELO [degrees/s]	AP	<b>BASE</b>	1.27	0.19	<0.0001
		<b>EYE</b>	1.51	0.27	<0.0001
		VIB	-0.03	0.08	0.72
		TR	-0.04	0.04	0.35
	ML	<b>BASE</b>	1.59	0.21	<0.0001
		<b>EYE</b>	1.59	0.24	<0.0001
		VIB	-0.07	0.09	0.45
		TR	-0.04	0.05	0.43
CFREQ [Hz x10 <sup>-3</sup> ]	AP	BASE	6.80	12.25	0.58
		EYE	7.75	11.03	0.48
		VIB	28.94	13.85	<0.05
		TR	-7.00	2.73	<0.05
	ML	BASE	2.95	14.38	0.84
		EYE	-23.52	12.05	0.05
		<b>VIB*</b>	20.74	9.80	<0.05
		TR	-7.51	2.95	<0.05

*table continues on next page*

Posturographic Measure	Direction	Effect	Estimate	Standard Error	Pr > F
FREQD [x10-3]	AP	<b>BASE</b>	-27.31	7.72	<0.001
		<b>EYE</b>	-39.16	6.22	<0.0001
		VIB	-12.63	5.95	<0.05
		TR	-1.17	1.91	0.54
	ML	BASE	5.77	7.17	0.42
		EYE	11.77	8.15	0.15
		VIB	2.25	6.16	0.72
		TR	2.59	1.83	0.16
log DS [-]	AP	<b>BASE</b>	1.39	0.16	<0.0001
		<b>EYE</b>	1.44	0.15	<0.0001
		VIB	-0.08	0.08	0.32
		TR	-0.03	0.04	0.38
	ML	<b>BASE</b>	1.63	0.15	<0.0001
		<b>EYE</b>	1.53	0.14	<0.0001
		VIB	-0.09	0.08	0.29
		TR	-0.03	0.04	0.48
HS [x10-3]	AP	<b>BASE**</b>	11.34	5.05	<0.05
		<b>EYE</b>	15.93	3.68	<0.0001
		VIB	-3.91	4.65	0.40
		TR	2.88	1.08	<0.01
	ML	BASE	-0.55	4.31	0.90
		EYE	-1.10	4.36	0.80
		<b>VIB*</b>	-8.94	3.29	<0.01
		TR	1.79	0.99	0.07

\* significant when considering only trials on base #2 with eyes open

\*\* significant when considering only trials with eyes closed

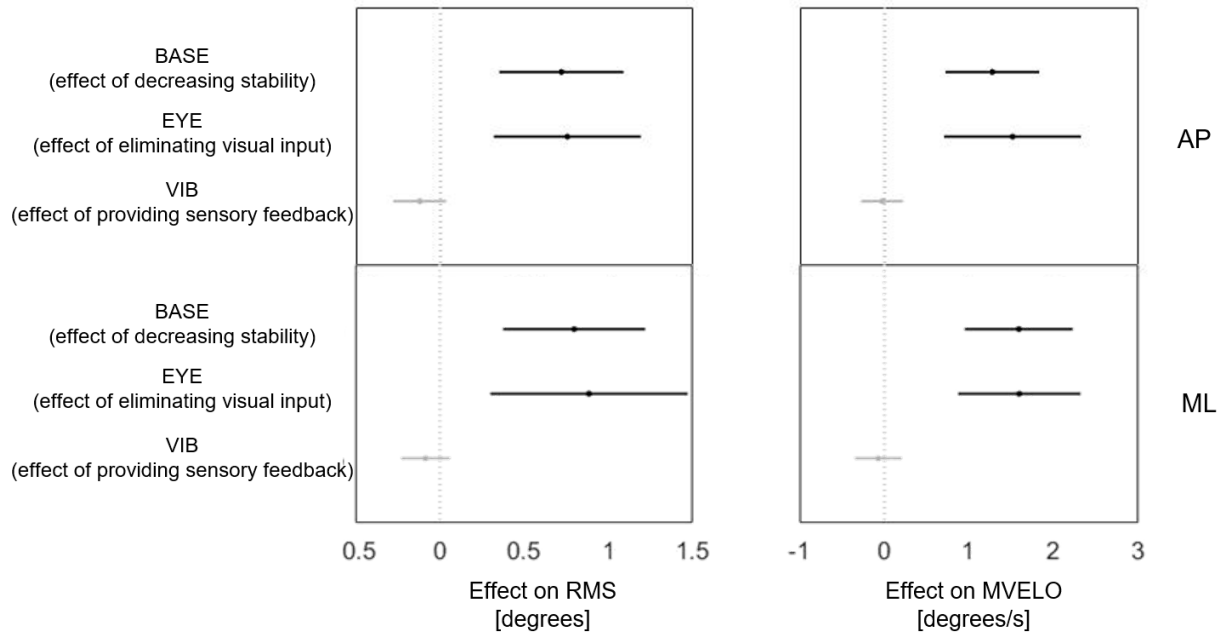


Figure 4-2: Response of time-domain measures derived from *AP* (top) and *ML* (bottom) tilts to changes in base (decreased stability), eye (elimination of visual input), and vibration (addition of vibrotactile feedback) conditions. Circles indicate the estimated effect. Bars indicate the confidence intervals for effects, based on the Bonferroni-corrected confidence level ( $1 - \alpha_{\text{adjusted}} = 0.9986$ ). Black bars represent measures that are significantly different between conditions.

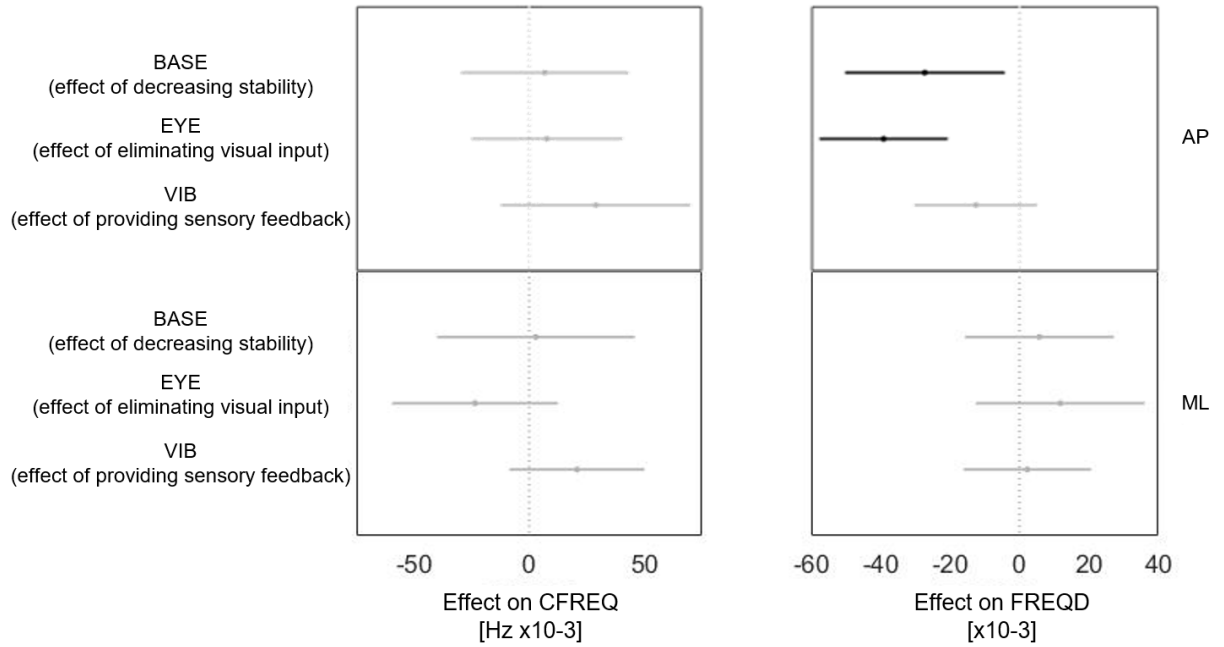


Figure 4-3: Response of frequency-domain measures derived from *AP* (top) and *ML* (bottom) tilts to changes in base (decreased stability), eye (elimination of visual input), and vibration (addition of vibrotactile feedback) conditions. Circles indicate the estimated effect. Bars indicate the confidence intervals for effects, based on the Bonferroni-corrected confidence level ( $1 - \alpha_{\text{adjusted}} = 0.9986$ ). Black bars represent measures that are significantly different between conditions.

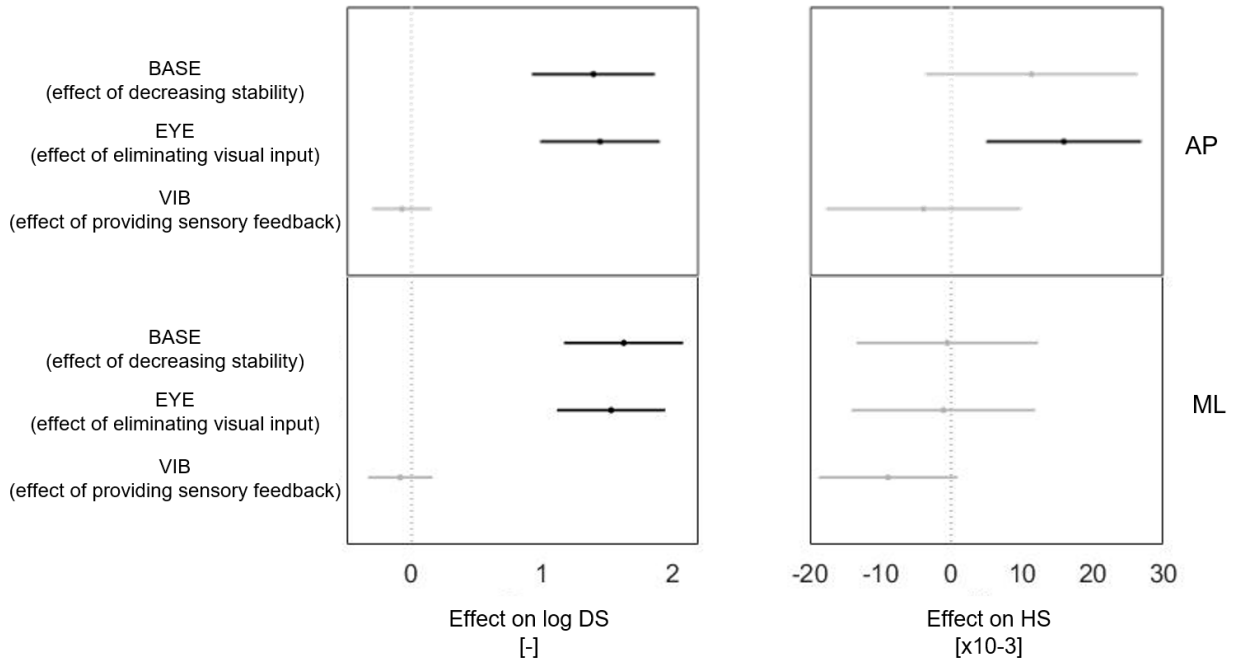


Figure 4-4: Response of stabilogram diffusion measures derived from *AP* (top) and *ML* (bottom) tilts to changes in base (decreased stability), eye (elimination of visual input), and vibration (addition of vibrotactile feedback) conditions. Circles indicate the estimated effect. Bars indicate the confidence intervals for effects, based on the Bonferroni-corrected confidence level ( $1 - \alpha_{\text{adjusted}} = 0.9986$ ). Black bars represent measures that are significantly different between conditions.

#### 4.3.8 Effects of Learning and Fatigue on Posturographic Measures

In both tilt directions, *HS* increased and *CFREQ* decreased as trials progressed from the first to the sixth trial within a given base and eye condition (Table 4-8). After correcting for multiple comparisons, there were no significant linear trends in posturographic measures.

### 4.4 Discussion

The main objective of the present study was to evaluate the feasibility of using a portable sitting device to assess and train sensorimotor function during continuous, multidirectional perturbations. The main findings of the present study were that (1) the wobble board assessment

technique provides quantitative metrics that correlate with physical characteristics of non-disabled individuals and manipulations of balance conditions; (2) the degree of instability elicited by the portable wobble board can be modulated, with predictable effects on the assessment metrics; (3) the assessment metrics are also sensitive to the condition of visual input, i.e., changes in the postural control system of non-disabled individuals; and (4) vibrotactile feedback can enhance the performance of non-disabled individuals during dynamic sitting.

#### 4.4.1 Sensitivity and Independence of Posturographic Measures

In this study, posturographic measures were used to summarize deviations in tilt angle of the support surface during unstable sitting trials under manipulated experimental conditions. *RMS* and *MVELO*, known to reliably quantify unstable sitting kinematics [44], were sensitive to base, eye, and vibration condition. *FREQD*, *DS*, and *HS* were also sensitive to all three conditions, but only in certain trials and tilt directions. *CFREQ* was the least sensitive to the experimental conditions, affected only by vibration, but was the most sensitive to the progression of trials between rests; it may be more sensitive to characteristics of balance control that are affected by fatigue.

The measures used in this study were selected to be independent of each other [37], although the observed correlation between measures suggests that some of these measures might still be redundant within the present context. *DS* correlates with *RMS* and *MVELO* (which are highly correlated in both directions); and *HS* correlates negatively with *CFREQ*. Significant changes in *DS* were only observed in cases where *RMS* and *MVELO* also changed significantly; therefore, computing all three of *DS*, *RMS*, and *MVELO* was probably redundant. Clinicians may consider omitting certain metrics for simplicity during balance assessments. The correlation between *RMS* and *MVELO* (0.87 and 0.90 for *AP* and *ML* directions, respectively) was much higher than observed in a study of COP-based posturographic measures during unstable sitting (0.27, 0.28) [37]. This discrepancy could be attributed to differences in measurement methods (tilt angles versus COP), or to differences in protocols: e.g., our 20 and 15 cm radii-hemispherical bases versus their 39 cm radius; our lack of foot support versus their attached footplate; and our participants were instructed to maintain an upright posture and keep the board as level as possible with arms crossed over the chest while their participants were instructed to grab a safety rail if needed to maintain balance, with those trials being included in their analysis). It is possible

that any of the posturographic measures included here or in other works may quantify some unique characteristic of balance control that would only be observed when individuals with a specific impairment perform a certain balance protocol. As such, posturographic measures can give insight into the underlying mechanisms of postural control, improving the specificity of assessment of balance-impaired individuals.

Each combination of base and eye conditions included four 30-s practice trials followed by six 30-s assessment trials, meant to mitigate the confounding effect of learning that has been detected for this type of assessment [110]. From the first to the sixth trial in each condition, linear trends were observed in *CFREQ* of *AP* and *ML* tilts (both decreasing) and *HS* of *AP* tilts (increasing); however, none of the effects were statistically significant. This result suggests that either the training protocol is sufficient to mitigate learning from affecting the balance assessment, or learning improvements are counterbalanced by the effect of fatigue. To improve the reliability and repeatability of within-participant measures, the training period could be increased [44] or a calibration procedure used [23]; however, the potential of fatigue to confound the assessment should also be considered. The position of the participants' limbs during sitting should also be paid special attention to, since different configurations can significantly affect sitting performance [100].

Posturographic measures varied significantly among participants in the non-disabled sample, but were mostly uncorrelated with weight and height characteristics. The increased speed and decreased frequency of wobble board tilt in taller participants could have biomechanical causes; e.g., according to an inverted-pendulum model of upright sitting, increasing the height of the center of mass (COM) above the hip joint decreases the stability just as increasing the radius of curvature of the base does [29]. The inter-participant variability could also be attributed to differences in strength, endurance, anticipatory postural adjustments, proprioception, reflexes, prior training, and flexibility [24]. The potential for inter-participant comparisons of posturographic measures is, therefore, limited. To validate the wobble board assessment method for clinical use, test-retest reliability of posturographic measures and their relationship to potential balance impairments should be investigated.

#### 4.4.2 Modularity of Unstable Sitting Task

As discussed in Chapter 3, an unstable support surface can enhance assessment paradigms by provoking reactive balance control mechanisms, and manipulating the degree of instability allows the assessment to be tailored to individuals of ranging abilities. All but one of the non-disabled participants in the present study were able to maintain upright sitting with base #2 attached. Note that easier (base #1) and more difficult (base #4, base #5) conditions are available. Similar apparatuses have been described [18], [29], [32], [33], [37] and other techniques that perturb seated balance using prescribed motion [73] or continuously modulated passive mechanisms [111]; our method holds the advantage of accessibility and portability, as its design was tailored for clinical assessment and training paradigms rather than laboratory-restricted research. The task can also be modulated by attaching a footrest that restricts any counterbalancing motions of the legs. Other unstable sitting assessments have used attached foot supports to constrain the influence of the lower limbs [29], [37], or measured the COP exerted by one foot on a floor-mounted force plate and, thus, identified the contribution of leg and trunk control to dynamic sitting balance [36], [110]. In the present study, omitting the foot support saved time during experimental setup, but confounds the comparison of the results to other unstable sitting studies. A balance therapist could choose to attach the wobble board's modular foot support and any curved base, depending on the needs or goals of the individual being trained or assessed.

#### 4.4.3 Quantitative Assessment of Conditioned Responses

The observation of balance trials on base #3 compared to those on base #2 revealed differences in the posturographic measures derived from the tilt angles measured during these trials. The significant increase in *RMS* and *MVELO* suggests decreased postural proficiency and increased neuromuscular control, respectively [19], [25], [149], indicating that the curved bases can indeed be modulated to decrease mechanical support, and thereby demand additional active control to maintain upright sitting, consistent with the study objectives. Also in base #3 trials, *CFREQ* was unchanged in both directions and *FREQD* was lower in the *AP* direction compared to base #2 trials. Decreased *FREQD* could be the result of increased stiffness of the trunk via co-contraction of agonist-antagonist pairs during challenging balance conditions [105]; however, this result warrants further investigation. *HS* measures were also sensitive in the *AP* direction only,

showing a significant increase that suggests greater persistence of wobble board tilts in the less stable condition. The observed values of *HS* remained well above 0.5 in all conditions, indicating that tilt angles move persistently away from equilibrium in the short term [95]. The reported values of *HS* (0.84-0.87) are consistent with those derived from COP displacements during sitting on a similar support surface (0.79 – 0.81) [29] and those derived from angular displacements of a sitting surface that uses a central pivot and springs to modulate support (0.76-0.77) [34].

Similar patterns in posturographic measures were observed when comparing trials with eyes closed to trials with eyes open as when comparing base #3 trials with base #2 trials (both reveal increases in *DS* and time-domain measures), suggesting that lack of visual input has a similar effect on postural performance in non-disabled individuals as a decrease in mechanical support. The response of *RMS* and *DS* measures is consistent with the findings of Silfies et al., who investigated the relative effects of increasing seat instability and elimination of visual input by measuring COP displacements of non-disabled individuals during unstable sitting (*MVELO* and frequency domain measures were not reported) [30]. The observed decrease in *FREQD* of *AP* tilts indicates that the power spectrum of the tilt signal varies over a narrower range of frequencies, i.e., the frequency of tilt is less variable in more challenging conditions (base #3, eyes closed). In these conditions, we also observed a significant increase in *HS* derived from *AP* tilts, whereas no change was observed in COP-based posturographic measures between eye conditions [30]. This discrepancy could be attributed to differences in measured variables or other methodological aspects (e.g., trial schedule, support surface characteristics, or participant instructions).

It has been shown that the observed short-and long-term regions of SDP curves can be reproduced by a simple model of time-delayed feedback control [150]. In the current study, the elimination of visual input presumably degrades the quality of the feedback signal, which decreases the overall stability (*RMS*, *MVELO*) and increases the short-term persistence of tilts (*DS*, *HS*). Since proprioception of support surface tilt is thought to trigger co-contraction in the early response to support surface tilt, with multisensory integration (including visual, if present) triggering precise muscle activation later [74], it is possible that the observed increase in *HS* is a result of adaptations of the controller strategy to the absence of visual input [151]. In other words, an increased co-contraction during eyes closed conditions may lead to more persistent

tilts in the short term. Since there is a redundant set of control strategies that may stabilize the upper body in any given environment [76], effective assessment techniques must be able to identify potential compensatory changes in the postural control system. The response of time- and frequency-domain measures as well as of stabilogram diffusion measures to the stability and visual conditions presented to non-disabled participants in this study reflects their potential use as quantitative measures of dynamic seated balance stability. Further research is warranted to explore whether these and other measures are also sensitive to changes in postural characteristics of certain clinical populations during dynamic sitting.

#### 4.4.4 Potential for Enhancement of Training by Vibrotactile Feedback

The results of the balance assessment and training study show that the vibrating tactors deliver kinematics-encoded feedback to the wobble board surface. The vibrotactile feedback control signal was based on tilt angle and velocity, leading to decreased tilt variance (*RMS*) and velocity (*MVELO*) in non-disabled participants. The effect of vibrotactile feedback on *RMS* and *MVELO* indicates that seated balance is more stable during the balance trials where vibrotactile feedback was provided. The corresponding increase in *CFREQ* suggests that the neuromuscular control system makes postural adjustments more frequently to maintain the increased stability. Feedback only significantly improved time domain measures in the easiest balance conditions (base #2, eyes open). As such, it is possible that the feedback is only useful to refine performance of an already simple task, and may not be useful to non-disabled individuals when challenged near the limits of their stability. In other words, the non-disabled participants used as many postural adjustments as were necessary to maintain stable position and velocity combinations during seated balance, and, when feedback was provided, used more frequent postural adjustments only if the neuromuscular control system was not already fully engaged [69]. Or, it is possible that significance of feedback effects is obscured by the increased variability and smaller sample size of posturographic measures in more difficult balance conditions. In either case, the potential for the feedback to be used in balance training paradigms is clear: for individuals who struggle to achieve the proper neuromuscular coordination required to maintain upright sitting, vibrotactile feedback could provide cues to establish proper coordination of muscular output during training. Consider individuals with hemispatial neglect (a common symptom post-stroke) who may be free of sensory impairments, yet unaware of an impending loss of balance [152]. In such cases,

prompts from a vibrotactile feedback system could relieve therapists from a coaching role during training sessions [52] and increase motivation to maintain consistent sitting posture. In fact, the eight vibrotactile tactors in the surface of the wobble board and their activation thresholds can be easily re-configured to address specific directional limitations in balance-impaired individuals. The efficacy of training with this vibrotactile feedback system should be explored in more detail, including longitudinal effects and further characterization of the postural response [60].

## 4.5 Conclusions

The balance assessment test in this study was designed to demonstrate the sensitivity of posturographic measures derived from wobble board tilt angles to the conditioned response of non-disabled individuals. Moreover, the protocol was designed to explore assessment and training techniques for potential use in a clinical setting. The basic functions of the wobble board have been demonstrated on a sample of non-disabled individuals. The wobble board's curved bases elicit the response of reactive control strategies required to maintain upright sitting. Posturographic measures calculated from the on-board IMU are sensitive to changes in eye conditions and level of seat instability. Vibrating tactors display balance cues during dynamic sitting, and facilitate improved balance performance in non-disabled individuals. More extensive testing is required to determine whether the device can be more effective than current techniques for assessing and training seated balance.

## 5 Conclusion

For balance-impaired individuals, optimizing rehabilitation outcomes relies on assessment and training techniques that should be based on ever-expanding evidence of human sensorimotor control mechanisms. Quantitative assessment protocols exist to provide reliable insight into the integrity of mechanisms that control balance. Sensory augmentation techniques are proven to enhance standing balance training. However, there are currently no clinical tools that provide quantitative assessment and vibrotactile feedback during dynamic seated balance (Chapter 2).

The first objective of this thesis was to engineer such a tool. The wobble board combines elements of previous biomedical devices (interchangeable bases to elicit modular instability, an on-board IMU to measure displacement of the support surface, and vibrating tactors to facilitate tilt-based sensory augmentation) into one novel device. The device design sets a new standard for passively perturbed sitting assessments: the wobble board is portable, modular, and instrumented to meet the specific goals of clinical assessment and training paradigms (Chapter 3).

The second objective of this thesis was to evaluate the feasibility of using the device to assess and train sensorimotor function during continuous, multidirectional perturbations by assessing and training a sample of non-disabled volunteers under experimental conditions. The assessment technique, i.e., measurement and analysis of support surface tilt angles during unstable sitting, can distinguish eyes-closed sitting from eyes-open sitting and two different instability levels in a sample of non-disabled participants (Chapter 4). The vibrotactile feedback technique, i.e., real-time directional stimulation of lower-body cutaneous receptors based on support surface tilt angle and velocity, can facilitate improved performance of dynamic sitting in a sample of non-disabled participants (Chapter 4). This information is critical for the development of seated balance assessment and training techniques in the future.

## 5.1 Future Directions

To be considered for clinical use, the wobble board assessment technique requires further investigation. There are several clinical functions that should be explored, including the ability of the outcome measures to provide differential diagnosis, predict risk of falling, and measure therapeutic effects in individuals with impaired seated balance. Clinical validation of the posturographic measures requires investigation of their repeatability, reproducibility, and test-retest reliability. The assessment technique is only useful when it can reliably identify specific deficiencies in seated balance that lead to more effective treatments.

The wobble board could be used to validate aspects of other assessment techniques that involve passive perturbation methods. In some cases, this would require certain modifications to the method, such as: adding a safety rail at approximately elbow height for participants to keep themselves from losing balance, attaching springs beneath the wobble board surface to provide continuous modulation of the degree of instability, placing the wobble board on a force plate to measure reaction forces during seated balance, or adding one or more IMUs that can attach to the participant's body and measure its tilt angles with respect to the wobble board. These additions could make the wobble board assessment technique more robust and adaptable, but may subtract from its portability and accessibility.

Further development and investigation is required to optimize the vibrotactile feedback provided by the wobble board for enhanced balance training. As discussed in Chapter 2, there are several means by which vibrotactile feedback may train upright sitting in balance-impaired individuals. The potential training benefits warrant further investigation of vibrotactile feedback during dynamic sitting as a training tool for balance-impaired individuals. Future research should explore whether the technique can benefit clinical populations in real-world sitting conditions, and whether this benefit is greater than that of simpler training methods. For example, longitudinal training sessions could be studied to investigate the retention of performance enhancement and the response of clinically-significant outcomes (e.g. quality of life, occurrence of falls), with vibrotactile feedback trainees practicing in parallel with wobble board trainees and traditional balance therapies.

As shown in the literature, the vibrotactile feedback scheme could be optimized to provide feedback cues with direction and timing that are optimized for a given task or goal. Identification

of these optimal parameters requires further experimentation. For example, the EMG response to directional vibrotactile stimuli could be measured during quiet sitting to identify automatic body response to such stimuli. Furthermore, the feedback signal can comprise different weights of position and velocity, and the threshold can be designed to reflect the limits of stability or other standards. In addition, a body-based IMU could provide tilt measurements to the feedback controller, which would facilitate vibrotactile feedback training during quasi-static sitting (i.e., for individuals who cannot maintain balance on even the flattest base curvature).

In summary, a tool for assessing and training seated balance has been developed and validated. While there are many alterations and improvements to the technique that may be further investigated, its current functions have been demonstrated to assess and train non-disabled individuals. This preliminary validation step is expected to provide a foundation for future investigations involving assessment and training of clinical populations with impaired seated balance.

## References

- [1] T. Paillard and F. Noé, “Techniques and Methods for Testing the Postural Function in Healthy and Pathological Subjects,” *Biomed Res. Int.*, vol. 2015, 2015.
- [2] K. D. Anderson, “Targeting recovery: priorities of the spinal cord-injured population.,” *J. Neurotrauma*, vol. 21, no. 10, pp. 1371–1383, 2004.
- [3] J. L. Minkel, “Seating and mobility considerations for people with spinal cord injury.,” *Phys. Ther.*, vol. 80, no. 7, pp. 701–709, 2000.
- [4] C. V Oleson, I. Sie, and R. L. Waters, “Outcomes Following Spinal Cord Injury,” in *Spinal Cord Medicine: Principles & Practice*, Second., Springer Publishing Company, 2010, pp. 136–152.
- [5] S. F. Tyson, M. Hanley, J. Chillala, A. Selley, and R. C. Tallis, “Balance disability after stroke.,” *Phys. Ther.*, vol. 86, no. 1, pp. 30–38, 2006.
- [6] L. Nyberg and Y. Gustafson, “Patient Falls in Stroke Rehabilitation,” *Stroke*, vol. 26, pp. 838–842, 1995.
- [7] C. J. Partridge, M. Johnston, and S. Edwards, “Recovery From Physical Disability After Stroke: Normal Patterns As a Basis for Evaluation,” *Lancet*, vol. 329, pp. 373–375, 1987.
- [8] A. D. Goodworth and R. J. Peterka, “Influence of Bilateral Vestibular Loss on Spinal Stabilization in Humans,” *J. Neurophysiology*, vol. 103, pp. 1978–1987, 2010.
- [9] M. E. Tinetti, “Performance-oriented assessment of mobility problems in elderly patients.,” *J. Am. Geriatr. Soc.*, vol. 34, no. 2, pp. 119–126, 1986.
- [10] K. Berg, “Measuring balance in the elderly: Development and validation of an instrument.,” *Can. J. Public Heal.*, vol. 83, pp. S7–S11, 1992.
- [11] N. Hart *et al.*, “Respiratory effects of combined truncal and abdominal support in patients with spinal cord injury,” *Arch. Phys. Med. Rehabil.*, vol. 86, no. 7, pp. 1447–1451, 2005.

- [12] A. Nieuwboer, H. Feys, W. De Weerd, G. Nuyens, and E. De Corte, "Developing a Clinical Tool to Measure Sitting Balance after Stroke: A reliability study," *Physiotherapy*, vol. 81, no. 8, pp. 439–445, 1995.
- [13] K. J. Sandin and B. S. Smith, "The measure of balance in sitting in stroke rehabilitation prognosis.," *Stroke.*, vol. 21, no. 1, pp. 82–86, 1990.
- [14] S. E. Fife, L. A. Roxborough, R. W. Armstrong, S. R. Harris, J. L. Gregson, and D. Field, "Development of a clinical measure of postural control for assessment of adaptive seating in children with neuromotor disabilities.," *Phys. Ther.*, vol. 71, no. 12, pp. 981–993, 1991.
- [15] U. Hohtari-Kivimäki, M. Salminen, T. Vahlberg, and S. L. Kivelä, "Short Berg Balance Scale, BBS-9, as a predictor of fall risk among the aged: A prospective 12-month follow-up study," *Aging Clin. Exp. Res.*, vol. 25, no. 6, pp. 645–650, 2013.
- [16] K. M. Guskiewicz and D. H. Perrin, "Research and clinical applications of assessing balance," *J. Sport Rehabil.*, vol. 5, no. 51, pp. 45–63, 1996.
- [17] J. E. Visser, M. G. Carpenter, H. van der Kooij, and B. R. Bloem, "The clinical utility of posturography," *Clin. Neurophysiol.*, vol. 119, no. 11, pp. 2424–2436, 2008.
- [18] A. Radebold, J. Cholewicki, G. K. Polzhofer, and H. S. Greene, "Impaired postural control of the lumbar spine is associated with delayed muscle response times in patients with chronic idiopathic low back pain," *Spine (Phila. Pa. 1976).*, vol. 26, no. 7, pp. 724–730, 2001.
- [19] N. Genthon, N. Vuillerme, J. P. Monnet, C. Petit, and P. Rougier, "Biomechanical assessment of the sitting posture maintenance in patients with stroke," *Clin. Biomech.*, vol. 22, no. 9, pp. 1024–1029, 2007.
- [20] S. Perlmutter, F. Lin, and M. Makhsous, "Quantitative analysis of static sitting posture in chronic stroke," *Gait Posture*, vol. 32, no. 1, pp. 53–56, 2010.
- [21] C. L. Chen, K. T. Yeung, L. I. Bih, C. H. Wang, M. I. Chen, and J. C. Chien, "The relationship between sitting stability and functional performance in patients with paraplegia," *Arch. Phys. Med. Rehabil.*, vol. 84, no. 9, pp. 1276–1281, 2003.

- [22] R. A. Preuss, S. G. Grenier, and S. M. McGill, "Postural control of the lumbar spine in unstable sitting," *Arch. Phys. Med. Rehabil.*, vol. 86, no. 12, pp. 2309–2315, 2005.
- [23] C. Larivière, H. Mecheri, A. Shahvarpour, D. Gagnon, and A. Shirazi-Adl, "Criterion validity and between-day reliability of an inertial-sensor-based trunk postural stability test during unstable sitting," *J. Electromyogr. Kinesiol.*, vol. 23, no. 4, pp. 899–907, 2013.
- [24] C. Larivière, D. H. Gagnon, and H. Mecheri, "Trunk postural control in unstable sitting: Effect of sex and low back pain status," *Clin. Biomech.*, vol. 30, no. 9, pp. 933–939, 2015.
- [25] T. E. Prieto, J. B. Myklebust, R. G. Hoffmann, E. G. Lovett, and B. M. Myklebust, "Measures of postural steadiness: Differences between healthy young and elderly adults," *IEEE Trans. Biomed. Eng.*, vol. 43, no. 9, pp. 956–966, 1996.
- [26] I. J. W. Van Nes, B. Nienhuis, H. Latour, and A. C. H. Geurts, "Posturographic assessment of sitting balance recovery in the subacute phase of stroke," *Gait Posture*, vol. 28, no. 3, pp. 507–512, 2008.
- [27] E. Maaswinkel, M. Griffioen, R. S. G. M. Perez, and J. H. van Dieën, "Methods for assessment of trunk stabilization, A systematic review," *J. Electromyogr. Kinesiol.*, vol. 26, pp. 18–35, 2016.
- [28] F. B. Horak, S. M. Henry, and A. Shumway-Cook, "Postural perturbations: new insights for treatment of balance disorders," *Phys. Ther.*, vol. 77, no. 5, pp. 517–533, 1997.
- [29] J. Cholewicki, G. K. Polzhofer, and A. Radebold, "Postural control of trunk during unstable sitting," *J. Biomech.*, vol. 33, no. 12, pp. 1733–1737, 2000.
- [30] S. P. Silfies, J. Cholewicki, and A. Radebold, "The effects of visual input on postural control of the lumbar spine in unstable sitting," *Hum. Mov. Sci.*, vol. 22, no. 3, pp. 237–252, 2003.
- [31] N. P. Reeves, V. Q. Everding, J. Cholewicki, and D. C. Morrisette, "The effects of trunk stiffness on postural control during unstable seated balance," *Exp. Brain Res.*, vol. 174, no. 4, pp. 694–700, 2006.

- [32] N. P. Reeves, J. Cholewicki, and K. S. Narendra, "Effects of reflex delays on postural control during unstable seated balance," *J. Biomech.*, vol. 42, no. 2, pp. 164–170, 2009.
- [33] W. Sung, M. Abraham, C. Plastaras, and S. P. Silfies, "Trunk motor control deficits in acute and subacute low back pain are not associated with pain or fear of movement," *Spine J.*, vol. 15, no. 8, pp. 1772–1782, 2015.
- [34] H. Lee, K. P. Granata, and M. L. Madigan, "Effects of trunk exertion force and direction on postural control of the trunk during unstable sitting," *Clin. Biomech.*, vol. 23, no. 5, pp. 505–509, 2008.
- [35] G. P. Slota, K. P. Granata, and M. L. Madigan, "Effects of seated whole-body vibration on postural control of the trunk during unstable seated balance," *Clin. Biomech.*, vol. 23, no. 4, pp. 381–386, 2008.
- [36] U. Van Daele, F. Hagman, S. Truijen, P. Vorlat, B. Van Gheluwe, and P. Vaes, "Differences in balance strategies between nonspecific chronic low back pain patients and healthy control subjects during unstable sitting," *Spine (Phila. Pa. 1976)*, vol. 34, no. 11, pp. 1233–1238, 2009.
- [37] J. H. van Dieën, L. L. J. Koppes, and J. W. R. Twisk, "Postural sway parameters in seated balancing; their reliability and relationship with balancing performance," *Gait Posture*, vol. 31, no. 1, pp. 42–46, 2010.
- [38] J. H. van Dieën, L. L. J. Koppes, and J. W. R. Twisk, "Low back pain history and postural sway in unstable sitting," *Spine (Phila. Pa. 1976)*, vol. 35, no. 7, pp. 812–817, 2010.
- [39] N. W. Willigenburg, I. Kingma, and J. H. Van Dieën, "Center of pressure trajectories, trunk kinematics and trunk muscle activation during unstable sitting in low back pain patients," *Gait Posture*, vol. 38, no. 4, pp. 625–630, 2013.
- [40] M. Freddolini, S. Strike, and R. Y. W. Lee, "Stiffness properties of the trunk in people with low back pain," *Hum. Mov. Sci.*, vol. 36, pp. 70–79, 2014.
- [41] D. A. Pérennou, C. Leblond, B. Amblard, J. P. Micallef, C. Hérisson, and J. Y. Péliissier, "Transcutaneous electric nerve stimulation reduces neglect-related postural instability

- after stroke,” *Arch. Phys. Med. Rehabil.*, vol. 82, no. 4, pp. 440–448, 2001.
- [42] D. A. Pérennou, C. Leblond, B. Amblard, J. P. Micallef, E. Rouget, and J. Pélissier, “The polymodal sensory cortex is crucial for controlling lateral postural stability: Evidence from stroke patients,” *Brain Res. Bull.*, vol. 53, no. 3, pp. 359–365, 2000.
- [43] J. C. E. van der Burg, E. E. H. van Wegen, M. B. Rietberg, G. Kwakkel, and J. H. van Dieën, “Postural control of the trunk during unstable sitting in Parkinson’s disease,” *Park. Relat. Disord.*, vol. 12, no. 8, pp. 492–498, 2006.
- [44] D. Barbado, J. Moreside, and F. J. Vera-Garcia, “Reliability and Repetition Effect of the Center of Pressure and Kinematics Parameters That Characterize Trunk Postural Control During Unstable Sitting Test,” *Pm&R*, vol. 9, no. 3, pp. 1–12, 2016.
- [45] D. Barbado, A. Lopez-Valenciano, C. Juan-Recio, C. Montero-Carretero, J. H. Van Dieën, and F. J. Vera-Garcia, “Trunk stability, trunk strength and sport performance level in judo,” *PLoS One*, vol. 11, no. 5, pp. 1–12, 2016.
- [46] M. Freddolini, S. Strike, and R. Y. W. Lee, “The role of trunk muscles in sitting balance control in people with low back pain,” *J. Electromyogr. Kinesiol.*, vol. 24, no. 6, pp. 947–953, 2014.
- [47] L. M. Nashner, “Brain Adapting Reflexes Controlling the Human Posture,” *Exp. Brain Res.*, vol. 26, pp. 59–72, 1976.
- [48] T. Ikai *et al.*, “Dynamic Postural Control in Patients with Hemiparesis,” *Am. J. Phys. Medicin Rehabil.*, vol. 6, no. 82, pp. 463–469, 2003.
- [49] C. Wall and E. Kentala, “Control of sway using vibrotactile feedback of body tilt in patients with moderate and severe postural control deficits,” *J. Vestib. Res.*, vol. 15, pp. 313–325, 2005.
- [50] N. Y. Harel, P. K. Asselin, D. B. Fineberg, T. J. Pisano, W. A. Bauman, and A. M. Spungen, “Adaptation of computerized posturography to assess seated balance in persons with spinal cord injury,” *J. Spinal Cord Med.*, vol. 36, no. 2, pp. 127–133, 2013.

- [51] R. Cabanas-Valdés, G. U. Cuchi, and C. Bagur-Calafat, “Trunk training exercises approaches for improving trunk performance and functional sitting balance in patients with stroke: A systematic review,” *NeuroRehabilitation*, vol. 33, no. 4, pp. 575–592, 2013.
- [52] L. Marchal-Crespo and D. J. Reinkensmeyer, “Review of control strategies for robotic movement training after neurologic injury,” *J. Neuroeng. Rehabil.*, vol. 6, no. 1, pp. 20–35, 2009.
- [53] A. U. Alahakone and S. M. N. A. Senanayake, “A real-time system with assistive feedback for postural control in rehabilitation,” *IEEE/ASME Trans. Mechatronics*, vol. 15, no. 2, pp. 226–233, 2010.
- [54] A. U. Alahakone and S. M. N. A. Senanayake, “Vibrotactile feedback systems: Current trends in rehabilitation, sports and information display,” *IEEE/ASME Int. Conf. Adv. Intell. Mechatronics, AIM*, pp. 1148–1153, 2009.
- [55] P. B. Shull and D. D. Damian, “Haptic wearables as sensory replacement, sensory augmentation and trainer – a review,” *J. Neuroeng. Rehabil.*, vol. 12, no. 1, p. 59, 2015.
- [56] K. H. Sienko, M. D. Balkwill, L. I. E. Oddsson, and C. Wall, “Effects of multi-directional vibrotactile feedback on vestibular-deficient postural performance during continuous multi-directional support surface perturbations,” *J. Vestib. Res.*, vol. 18, pp. 273–285, 2008.
- [57] K. H. Sienko, V. V. Vichare, M. D. Balkwill, and C. Wall, “Assessment of vibrotactile feedback on postural stability during pseudorandom multidirectional platform motion,” *IEEE Trans. Biomed. Eng.*, vol. 57, no. 4, pp. 944–952, 2010.
- [58] E. Kentala, J. Vivas, and C. Wall III., “Reduction of Postural Sway By Use of a Vibrotactile Balance Prosthesis Prototype in Subjects With Vestibular Deficits,” *Ann. Otol. Rhinol. Laryngol.*, vol. 112, no. 5, pp. 404–409, 2003.
- [59] C. Wall and E. Kentala, “Effect of displacement, velocity, and combined vibrotactile tilt feedback on postural control of vestibulopathic subjects,” *J. Vestib. Res.*, vol. 20, pp. 61–

69, 2010.

- [60] R. J. Peterka, C. Wall, and E. Kentala, “Determining the effectiveness of a vibrotactile balance prosthesis.,” *J. Vestib. Res.*, vol. 16, pp. 45–56, 2006.
- [61] K. H. Sienko, M. D. Balkwill, and C. Wall, “Biofeedback improves postural control recovery from multi-axis discrete perturbations.,” *J. Neuroeng. Rehabil.*, vol. 9, no. 1, pp. 53–64, 2012.
- [62] C.-C. Lin *et al.*, “The effect of age on postural and cognitive task performance while using vibrotactile feedback.,” *J. Neurophysiol.*, vol. 113, no. 7, pp. 2127–2136, 2015.
- [63] S. Haggerty, L. T. Jiang, A. Galecki, and K. H. Sienko, “Effects of biofeedback on secondary-task response time and postural stability in older adults,” *Gait Posture*, vol. 35, no. 4, pp. 523–528, 2012.
- [64] A. H. Vette, K. Masani, V. Sin, and M. R. Popovic, “Posturographic measures in healthy young adults during quiet sitting in comparison with quiet standing.,” *Med. Eng. Phys.*, vol. 32, no. 1, pp. 32–38, 2010.
- [65] M. Grangeon, C. Gauthier, C. Duclos, J. F. Lemay, and D. Gagnon, “Unsupported eyes closed sitting and quiet standing share postural control strategies in healthy individuals,” *Motor Control*, pp. 10–24, 2014.
- [66] S. M. McGill, S. Grenier, N. Kavcic, and J. Cholewicki, “Coordination of muscle activity to assure stability of the lumbar spine,” *J. Electromyogr. Kinesiol.*, vol. 13, pp. 353–359, 2003.
- [67] J. Cholewicki and J. J. VanVliet Iv, “Relative contribution of trunk muscles to the stability of the lumbar spine during isometric exertions,” *Clin. Biomech.*, vol. 17, no. 2, pp. 99–105, 2002.
- [68] D. A. Winter, *Biomechanics and Motor Control of Human Movement*, Fourth Edi. New Jersey: John Wiley & Sons, 2009.
- [69] M. L. Tanaka, S. D. Ross, and M. A. Nussbaum, “Mathematical modeling and simulation

- of seated stability,” *J. Biomech.*, vol. 43, no. 5, pp. 906–912, 2010.
- [70] K. M. Moorhouse and K. P. Granata, “Role of reflex dynamics in spinal stability: Intrinsic muscle stiffness alone is insufficient for stability,” *J. Biomech.*, vol. 40, no. 5, pp. 1058–1065, 2007.
- [71] R. J. Peterka, “Postural control model interpretation of stabilogram diffusion analysis.,” *Biol. Cybern.*, vol. 82, no. 4, pp. 335–343, 2000.
- [72] P. J. Lee, E. L. Rogers, and K. P. Granata, “Active trunk stiffness increases with co-contraction,” *J. Electromyogr. Kinesiol.*, vol. 16, pp. 51–57, 2006.
- [73] A. H. Vette, E. Sanin, A. Bultmann, A. Morris, K. Masani, and M. R. Popovic, “A Portable and Automated Postural Perturbation System for Balance Assessment, Training, and Neuromuscular System Identification,” *J. Med. Device.*, vol. 2, no. 4, pp. 1–9, 2008.
- [74] H. Forssberg and H. Hirschfeld, “Postural adjustments in sitting humans following external perturbations: muscle activity and kinematics,” *Exp. Brain Res.*, vol. 97, no. 3, pp. 515–527, 1994.
- [75] H. van der Kooij, E. van Asseldonk, and F. C. T. van der Helm, “Comparison of different methods to identify and quantify balance control,” *J. Neurosci. Methods*, vol. 145, pp. 175–203, 2005.
- [76] Y. Xu, J. Choi, N. P. Reeves, and J. Cholewicki, “Optimal control of the spine system,” *J. Biomech. Eng.*, vol. 132, no. 5, p. 51004, 2010.
- [77] M. Vanoncini, W. Holderbaum, and B. Andrews, “Development and experimental identification of a biomechanical model of the trunk for functional electrical stimulation control in paraplegia,” *Neuromodulation*, vol. 11, no. 4, pp. 315–324, 2008.
- [78] R. J. Peterka *et al.*, “Sensorimotor Integration in Human Postural Control,” pp. 1097–1118, 2002.
- [79] R. A. Schmidt and T. D. Lee, *Motor Control and Learning: A Behavioural Emphasis*, Fifth. Champaign, IL: Human Kinetics, 2011.

- [80] D. Engelhart *et al.*, “Impaired Standing Balance in Elderly: A New Engineering Method Helps to Unravel Causes and Effects,” *J. Am. Med. Dir. Assoc.*, vol. 15, no. 3, pp. 1–6, 2014.
- [81] D. N. Lee and E. Aronson, “Visual proprioceptive control of standing in human infants ;,” *Percept. Psychophys.*, vol. 15, no. 3, pp. 529–532, 1974.
- [82] L. Nashner and A. Berthoz, “Visual contribution to rapid motor responses during postural control,” *Brain Res.*, vol. 150, no. 2, pp. 403–407, 1978.
- [83] F. B. Horak, “Postural compensation for vestibular loss and implications for rehabilitation,” *Restor. Neurol. Neurosci.*, vol. 28, no. 1, pp. 57–68, 2010.
- [84] D. A. Winter, “Human balance and posture control during standing and walking,” *Gait Posture*, vol. 3, no. 4, pp. 193–214, 1995.
- [85] R. J. Peterka and M. S. Benolken, “Role of somatosensory and vestibular cues in attenuating visually induced human postural sway,” *Exp. Brain Res.*, vol. 105, no. 1, pp. 101–110, 1995.
- [86] J. Richman and J. Moorman, “Physiological time-series analysis using approximate entropy and sample entropy,” *Am. J. Physiology*, vol. 278, pp. 2039–2049, 2000.
- [87] S. F. Donker, M. Roerdink, A. J. Greven, and P. J. Beek, “Regularity of center-of-pressure trajectories depends on the amount of attention invested in postural control,” *Exp. Brain Res.*, vol. 181, no. 1, pp. 1–11, 2007.
- [88] L. L. Verhoeff, C. G. C. Horlings, L. J. F. Janssen, S. A. Bridenbaugh, and J. H. J. Allum, “Effects of biofeedback on trunk sway during dual tasking in the healthy young and elderly,” *Gait Posture*, vol. 30, no. 1, pp. 76–81, 2009.
- [89] S. F. Tyson and L. A. Connell, “How to measure balance in clinical practice. A systematic review of the psychometrics and clinical utility of measures of balance activity for neurological conditions.,” *Clin. Rehabil.*, vol. 23, no. 9, pp. 824–840, 2009.
- [90] Y. L. Tsang and M. K. Mak, “Sit-and-Reach Test can Predict Mobility of Patients

- Recovering from Acute Stroke,” *Arch. Phys. Med. Rehabil.*, vol. 85, no. 1, pp. 94–98, 2004.
- [91] S. Sprigle, C. Maurer, and M. Holowka, “Development of Valid and Reliable Measures of Postural Stability,” *J Spinal Cord Med*, vol. 30, no. May, pp. 40–49, 2007.
- [92] S. F. Tyson and L. H. DeSouza, “Reliability and validity of functional balance tests post stroke.,” *Clin. Rehabil.*, vol. 18, no. 8, pp. 916–923, 2004.
- [93] G. Verheyden, A. Nieuwboer, J. Mertin, R. Preger, C. Kiekens, and W. De Weerd, “The Trunk Impairment Scale: a new tool to measure motor impairment of the trunk after stroke.,” *Clin. Rehabil.*, vol. 18, no. 3, pp. 326–334, 2004.
- [94] S. F. Tyson and L. H. DeSouza, “Development of the Brunel Balance Assessment: a new measure of balance disability post stroke.,” *Clin. Rehabil.*, vol. 18, no. 7, pp. 801–810, 2004.
- [95] J. J. Collins and C. J. De Luca, “Open-loop and closed-loop control of posture: A random-walk analysis of center-of-pressure trajectories,” *Exp. Brain Res.*, vol. 95, no. 2, pp. 308–318, 1993.
- [96] P. Serra-Añó, M. Pellicer-Chenoll, X. Garcia-Massó, G. Brizuela, C. García-Lucerga, and L. M. González, “Sitting balance and limits of stability in persons with paraplegia.,” *Spinal Cord*, vol. 51, no. 4, pp. 267–72, 2013.
- [97] D. Delignieres, T. Deschamps, A. Legros, and N. Caillou, “A methodological note on nonlinear time series analysis: Is the open- and closed-loop model of Collins and De Luca (1993) a statistical artifact?,” *J Mot Behav*, vol. 35, no. 1, pp. 86–96, 2003.
- [98] D. G. Sayenko *et al.*, “Positive effect of balance training with visual feedback on standing balance abilities in people with incomplete spinal cord injury.,” *Spinal Cord*, vol. 48, no. 12, pp. 886–93, 2010.
- [99] H. G. Kang and J. B. Dingwell, “A direct comparison of local dynamic stability during unperturbed standing and walking,” *Exp. Brain Res.*, vol. 172, no. 1, pp. 35–48, 2006.

- [100] M. Grangeon, D. Gagnon, C. Gauthier, G. Jacquemin, K. Masani, and M. R. Popovic, "Effects of upper limb positions and weight support roles on quasi-static seated postural stability in individuals with spinal cord injury," *Gait Posture*, vol. 36, no. 3, pp. 572–579, 2012.
- [101] S. P. Gombatto, D. R. Collins, S. A. Sahrman, J. R. Engsberg, and L. R. Van Dillen, "Patterns of Lumbar Region Movement During Trunk Lateral Bending in 2 Subgroups of People with Low Back Pain," vol. 87, no. 4, 2007.
- [102] H. M. Kerr and J. J. Eng, "Multidirectional measures of seated postural stability," *Clin. Biomech.*, vol. 17, no. 7, pp. 555–557, 2002.
- [103] K. Masani *et al.*, "Postural reactions of the trunk muscles to multi-directional perturbations in sitting," *Clin. Biomech. (Bristol, Avon)*, vol. 24, no. 2, pp. 176–82, 2009.
- [104] T. A. Thrasher, V. W. Sin, K. Masani, A. H. Vette, B. C. Craven, and M. R. Popovic, "Responses of the trunk to multidirectional perturbations during unsupported sitting in normal adults," *J. Appl. Biomech.*, pp. 1–25, 2009.
- [105] A. H. Vette, K. Masani, N. Wu, and M. R. Popovic, "Multidirectional quantification of trunk stiffness and damping during unloaded natural sitting," *Med. Eng. Phys.*, vol. 36, no. 1, pp. 102–109, 2014.
- [106] M. Zedka, S. Kumar, and Y. Narayan, "Electromyographic response of the trunk muscles to postural perturbation in sitting subjects," *J. Electromyogr. Kinesiol.*, vol. 8, pp. 3–10, 1998.
- [107] A. D. Goodworth, Y. H. Wu, D. Felmlee, E. Dunklebarger, and S. Saavedra, "A Trunk Support System to Identify Posture Control Mechanisms in Populations Lacking Independent Sitting," *IEEE Trans. Neural Syst. Rehabil. Eng.*, vol. 25, no. 1, pp. 19–26, 2016.
- [108] R. F. Kirsch, D. Boskov, and W. Z. Rymer, "Muscle Stiffness During Transient and Continuous Movements of Cat Muscle: Perturbation Characteristics and Physiological Relevance," *IEEE Trans. Biomed. Eng.*, vol. 41, no. 8, pp. 758–770, 1994.

- [109] B. E. Maki and G. Ostrovski, "Do postural responses to transient and continuous perturbations show similar vision and amplitude dependence?," *J. Biomech.*, vol. 26, no. 10, pp. 1181–1190, 1993.
- [110] U. Van Daele, S. Huyvaert, F. Hagman, W. Duquet, B. Van Gheluwe, and P. Vaes, "Reproducibility of postural control measurement during unstable sitting in low back pain patients," *BMC Musculoskelet. Disord.*, vol. 8, no. 1, pp. 44–53, 2007.
- [111] M. Freddolini, S. Strike, and R. Lee, "Dynamic Stability of the Trunk During Unstable Sitting in People With Low Back Pain," *Spine (Phila. Pa. 1976)*, vol. 39, no. 10, pp. 785–790, 2014.
- [112] G. Cimadoro, C. Paizis, G. Alberti, and N. Babault, "Effects of different unstable supports on EMG activity and balance," *Neurosci. Lett.*, vol. 548, pp. 228–232, 2013.
- [113] A. S. Aruin, N. Kanekar, Y. J. Lee, and M. Ganesan, "Enhancement of anticipatory postural adjustments in older adults as a result of a single session of ball throwing exercise," *Exp. Brain Res.*, vol. 233, pp. 649–655, 2015.
- [114] M. H. Mudie, U. Winzeler-Mercay, S. Radwan, and L. Lee, "Training symmetry of weight distribution after stroke: a randomized controlled pilot study comparing task-related reach, Bobath and feedback training approaches," *Clin. Rehabil.*, vol. 16, pp. 582–592, 2002.
- [115] J. J. Jeka, R. D. Easton, B. L. Bentzen, and J. R. Lackner, "Haptic cues for orientation and postural control in sighted and blind individuals," *Percept. Psychophys.*, vol. 58, no. 3, pp. 409–23, 1996.
- [116] L. Johannsen, A. Wing, and M. S. Redfern, "Tactile Control of Balance," in *Scholarpedia of Touch*, T. Prescott, E. Ahissar, and E. Izhikevich, Eds. Paris: Atlantis Press, 2016, pp. 263–277.
- [117] R. D. Gilson and R. E. Fenton, "Kinesthetic-Tactual Information Presentations: Inflight Studies," *IEEE Trans. Syst. Man Cybern.*, vol. 4, no. 6, pp. 531–535, 1974.
- [118] H. Huang, S. L. Wolf, and J. He, "Recent developments in biofeedback for neuromotor rehabilitation," *J. Neuroeng. Rehabil.*, vol. 3, no. 1, p. 11, 2006.

- [119] Z. Hirjaková, J. Lobotková, K. Bučková, D. Bzdúšková, and F. Hlavačka, “Age-related differences in efficiency of visual and vibrotactile biofeedback for balance improvement,” *Act. Nerv. Super. Rediviva*, vol. 57, no. 3, 2015.
- [120] G. Wulf, J. Mercer, N. McNevin, and M. A. Guadagnoli, “Reciprocal influences of attentional focus on postural and suprapostural task performance,” *J Mot Behav*, vol. 36, no. 2, pp. 189–199, 2004.
- [121] R. G. Hamman, I. Mekjavic, A. I. Mallinson, and N. S. Longridge, “Training effects during repeated therapy sessions of balance training using visual feedback,” *Arch. Phys. Med. Rehabil.*, vol. 73, no. 8, pp. 738–744, 1992.
- [122] A. Shumway-Cook, D. Anson, and S. Haller, “Postural sway biofeedback: its effect on reestablishing stance stability in hemiplegic patients,” *Arch. Phys. Med. Rehabil.*, vol. 69, no. 6, pp. 395–400, 1988.
- [123] S. W. Lee, D. C. Shin, and C. H. Song, “The Effects of Visual Feedback Training on Sitting Balance Ability and Visual Perception of Patients with Chronic Stroke,” *J. Phys. Ther. Sci.*, vol. 25, no. 5, pp. 635–639, 2013.
- [124] M. Dozza, L. Chiari, and F. B. Horak, “Audio-biofeedback improves balance in patients with bilateral vestibular loss,” *Arch. Phys. Med. Rehabil.*, vol. 86, no. 7, pp. 1401–1403, 2005.
- [125] C. G. C. Barros, R. S. M. Bittar, and Y. Danilov, “Effects of electrotactile vestibular substitution on rehabilitation of patients with bilateral vestibular loss,” *Neurosci. Lett.*, vol. 476, no. 3, pp. 123–126, 2010.
- [126] C. Wall, M. S. Weinberg, P. B. Schmidt, and D. E. Krebs, “Balance prosthesis based on micromechanical sensors using vibrotactile feedback of tilt,” *IEEE Trans. Biomed. Eng.*, vol. 48, no. 10, pp. 1153–1161, 2001.
- [127] P. P. Kadmade, B. J. Benda, P. B. Schmidt, and C. Wall, “Vibrotactile Display Coding for a Balance Prosthesis,” *IEEE Trans. Neural Syst. Rehabil. Eng.*, vol. 11, no. 4, pp. 392–399, 2003.

- [128] K. E. Bechly, W. J. Carender, J. D. Myles, and K. H. Sienko, "Determining the preferred modality for real-time biofeedback during balance," *Gait Posture*, vol. 37, no. 3, pp. 391–396, 2013.
- [129] M. Dozza, C. 3rd Wall, R. J. Peterka, L. Chiari, and F. B. Horak, "Effects of practicing tandem gait with and without vibrotactile biofeedback in subjects with unilateral vestibular loss.," *J. Vestib. Res.*, vol. 17, no. 4, pp. 195–204, 2007.
- [130] L. J. F. Janssen, L. L. Verhoeff, C. G. C. Horlings, and J. H. J. Allum, "Directional effects of biofeedback on trunk sway during gait tasks in healthy young subjects," *Gait Posture*, vol. 29, pp. 575–581, 2009.
- [131] K. H. Sienko, M. D. Balkwill, L. I. E. Oddsson, and C. W. Iii, "The effect of vibrotactile feedback on postural sway during locomotor activities," *J. Neuroeng. Rehabil.*, vol. 10, pp. 1–6, 2013.
- [132] B. Lee, J. Kim, S. Chen, and K. H. Sienko, "Cell phone based balance trainer," *J. Neuroeng. Rehabil.*, vol. 9, pp. 1–14, 2012.
- [133] R. W. Lindeman, Y. Yanagida, K. Hosaka, and S. Abe, "The TactaPack: A wireless sensor/actuator package for physical therapy applications," in *IEEE Virtual Reality*, 2006.
- [134] E. Ribot-Ciscar, J. P. Vedel, and J. P. Roll, "Vibration sensitivity of slowly and rapidly adapting cutaneous mechanoreceptors in the human foot and leg," *Neurosci. Lett.*, vol. 104, no. 1–2, pp. 130–135, 1989.
- [135] J. J. Craig, *Introduction to Robotics: Mechanics and Control*, 3rd ed. Upper Saddle River: Pearson Education, Inc, 2005.
- [136] M. Milosevic *et al.*, "Trunk control impairment is responsible for postural instability during quiet sitting in individuals with cervical spinal cord injury," *Clin. Biomech.*, vol. 30, no. 5, pp. 507–512, 2015.
- [137] S. Karthikbabu *et al.*, "Comparison of physio ball and plinth trunk exercises regimens on trunk control and functional balance in patients with acute stroke: a pilot randomized controlled trial.," *Clin. Rehabil.*, vol. 25, no. 8, pp. 709–719, 2011.

- [138] D. G. Behm, T. Muehlbauer, A. Kibele, and U. Granacher, “Effects of Strength Training Using Unstable Surfaces on Strength, Power and Balance Performance Across the Lifespan: A Systematic Review and Meta-analysis,” *Sport. Med.*, vol. 45, no. 12, pp. 1645–1669, 2015.
- [139] R. Loureiro, F. Amirabdollahian, S. Coote, E. Stokes, and W. Harwin, “Using haptics technology to deliver motivational therapies in stroke patients: Concepts and initial pilot studies,” in *EuroHaptics 2001 Conference*, 2001, pp. 1–6.
- [140] N. Vuillerme, O. Chenu, J. Demongeot, and Y. Payan, “Controlling posture using a plantar pressure-based, tongue-placed tactile biofeedback system,” *Exp. Brain Res.*, vol. 179, no. 3, pp. 409–414, 2007.
- [141] J. Bear-Lehman, A. SM, and A. Burkhardt, “Cutaneous sensitivity and functional limitation.,” *Top. Geriatr. Rehabil.*, vol. 22, no. 1, pp. 61–69, 2006.
- [142] A. D. Goodworth, C. Wall, and R. J. Peterka, “Influence of feedback parameters on performance of a vibrotactile balance prosthesis,” *IEEE Trans. Neural Syst. Rehabil. Eng.*, vol. 17, no. 4, pp. 397–408, 2009.
- [143] A. A. Priplata, J. B. Niemi, J. D. Harry, L. A. Lipsitz, and J. J. Collins, “Vibrating insoles and balance control in elderly people.,” *Lancet (London, England)*, vol. 362, pp. 1123–1124, 2003.
- [144] B. C. Lee, B. J. Martin, and K. H. Sienko, “Directional postural responses induced by vibrotactile stimulations applied to the torso,” *Exp. Brain Res.*, vol. 222, no. 4, pp. 471–482, 2012.
- [145] P. Loughlin, A. Mahboobin, and J. Furman, “Designing vibrotactile balance feedback for desired body sway reductions,” in *Annual International Conference of the IEEE Engineering in Medicine and Biology Society*, 2011, pp. 1310–1313.
- [146] R. Sigrist, G. Rauter, R. Riener, and P. Wolf, “Augmented visual, auditory, haptic, and multimodal feedback in motor learning: A review,” *Psychon. Bull. Rev.*, vol. 20, no. 1, pp. 21–53, 2013.

- [147] O. Cohen, E. Eliachar, and N. Lilach, "Posture detection device." Google Patents, 2015.
- [148] H. Lee and K. P. Granata, "Process stationarity and reliability of trunk postural stability," *Clin. Biomech.*, vol. 23, no. 6, pp. 735–742, 2008.
- [149] B. E. Maki, P. J. Holliday, and G. R. Fernie, "Aging and Postural Control: A Comparison of Spontaneous- and Induced-Sway Balance Tests," *J. Am. Geriatr. Soc.*, vol. 38, no. 1, pp. 1–9, 1990.
- [150] C. Maurer and R. J. Peterka, "A new interpretation of spontaneous sway measures based on a simple model of human postural control," *J. Neurophysiology*, vol. 93, pp. 189–200, 2005.
- [151] R. J. Peterka and P. J. Loughlin, "Dynamic regulation of sensorimotor integration in human postural control.," *J Neurophysiol*, vol. 91, pp. 410–423, 2004.
- [152] G. Kerkhoff, "Spatial hemineglect in humans," *Prog. Neurobiol.*, vol. 63, no. 1, pp. 1–27, 2001.
- [153] M. Roerdink, M. De Haart, A. Daffertshofer, S. F. Donker, A. C. H. Geurts, and P. J. Beek, "Dynamical structure of center-of-pressure trajectories in patients recovering from stroke," *Exp. Brain Res.*, vol. 174, no. 2, pp. 256–269, 2006.
- [154] M. T. Rosenstein, J. J. Collins, and C. J. De Luca, "A practical method for calculating largest Lyapunov exponents from small data sets," *Phys. D*, vol. 65, pp. 117–134, 1993.
- [155] R. T. Harbourne and N. Stergiou, "Nonlinear analysis of the development of sitting postural control," *Dev. Psychobiol.*, vol. 42, no. 4, pp. 368–377, 2003.
- [156] L. Baratto, P. G. Morasso, C. Re, and G. Spada, "A new look at posturographic analysis in the clinical context: sway-density versus other parameterization techniques.," *Motor control*, vol. 6, no. 3. pp. 246–270, 2002.
- [157] N. Marwan, M. Carmen Romano, M. Thiel, and J. Kurths, "Recurrence plots for the analysis of complex systems," *Phys. Rep.*, vol. 438, no. 5–6, pp. 237–329, 2007.
- [158] K. M. Newell, S. M. Slobounov, E. S. Slobounova, and P. C. M. Molenaar, "Stochastic

processes in postural center-of-pressure profiles,” *Exp. Brain Res.*, vol. 113, no. 1, pp. 158–164, 1997.

[159] G. Robertson, G. Caldwell, J. Hamill, G. Kamen, and S. Whittlesey, *Research methods in biomechanics, 2E*. Human Kinetics, 2013.

[160] N. R. Crawford, G. T. Yamaguchi, and C. A. Dickman, “Methods for determining spinal flexion/extension, lateral bending, and axial rotation from marker coordinate data: Analysis and refinement,” *Hum. Mov. Sci.*, no. 15, pp. 55–78, 1996.

# Appendices

## Appendix A: Selection and Calculation of Posturographic Measures

Many posturographic measures, derived from various analytic methodologies, have been used to summarize kinematic or kinetic time series and gain understanding of the mechanisms that maintain stability during balance tasks. Eight categories of posturographic analysis and their associated posturographic measures are listed in Table A1 and overviewed below.

Time domain measures estimate the deviation of the COP or body segment from its average position. The mean tilt (*MEAN*) is the average of the absolute displacement values. The root-mean-square (*RMS*) is the average of the squared displacement values, or the standard deviation of the zero-mean time series. The mean velocity (*MVELO*) is the total excursion of the COP trajectory divided by the duration of the measurement. The sway area (*AREA-SW*) is the area enclosed by the COP path per unit of time. The area of the 95% confidence circle (*AREA-CC*) and ellipse (*AREA-CE*) are expected to enclose 95% of the bivariate COP or body segment distribution of displacements. The fractal dimension measures the degree to which a planar curve fills the metric space as calculated from the planar diameter of the curve (*FDPD*), the 95% confidence circle (*FDCC*) or the 95% confidence ellipse (*FDCE*). Mean frequency (*MNFREQ*) is proportional to the ratio of the mean velocity to the mean distance. It is typically presumed that smaller values of time domain measures are representative of a more stable system.

Frequency domain measures aim to characterize the power spectral density of the COP or body segment displacement. The median frequency (*MDFREQ*) and 95% power frequency (*UPFREQ*) are the smallest frequencies below which 50% and 95% of the respective total power is found. According to [25], the centroidal frequency (*CFREQ*) is the square root of the ratio of second spectral moments to corresponding spectral densities between 0 and 5 Hz. An increase in quantile or centroidal frequencies indicates that kinematic or COP variable was displaced with greater amplitude at higher frequencies. The frequency dispersion (*FREQD*) is a unitless measure of the variability of the frequency content. Frequency measures are generally expected

to increase with the responsiveness of the system, since control that is more responsive produces more frequent movements of the system.

The stabilogram diffusion plot (SDP) computes the square of the displacements between all pairs of points that are separated by a certain time interval; these squared displacements are averaged, and the process repeated for increasing intervals [95]. The short- and long-term diffusion coefficients ( $DS$ ,  $DL$ ) are calculated from the slope of mean square COP displacement plotted against time intervals, and measures of the behaviour of the mean square displacement relative to random walk in a straight line or plane. The critical point ( $CP$ ) is calculated as the intersection of these two slopes. Scaling exponents ( $HS$ ,  $HL$ ) can be estimated from log-log plots of the same curves. Other exponential scaling exponents, as derived from detrended fluctuation analysis (DFA) or rescaled range analysis (RRA) [97], can also quantify postural stability [153].

Finite-time estimates of the largest Lyapunov exponents [154] parametrize the divergence of states in a dynamic system. These parameters can characterize the stability of seated posture [69], [155].

Sway density plots (SDPs) are used to identify the characteristics of stable regions in COP or segment displacements [156]. A sway density curve (SDC) indicates how many consecutive measurements lie within a certain radius. For a given SDC, seven parameters can be extracted: the mean number of SDC peaks per second ( $MNUM$ ), the mean time between consecutive SDC peaks ( $MDUR$ ), the standard deviation of times between consecutive peaks ( $SDUR$ ), the mean of the spatial distance between consecutive SDC peaks ( $MDIST$ ), the standard deviation of the spatial distance between consecutive peaks ( $SDIST$ ), the mean duration of the SDC peaks ( $MPEAKS$ ), and the standard deviation of the mean duration of SDC peaks ( $SPEAKS$ ). The mean duration of these peaks describes how long the displacement variable stays within a certain radius.

Recurrence quantification analysis ( $RQA$ ) identifies recurrent points in a time series. From a recurrence plot in which each data point on the x-axis is plotted against each other data point on the y-axis, the percentage of recurrent data points (RECUR), the percentage determinism ( $DET$ ), the mean diagonal length ( $DIAG$ ), and the entropy ( $RENTR$ ) are calculated [157]. Entropy estimates level of chaos in the dynamical system, and can also be calculated using the sample entropy ( $SENTR$ ) of the COP or segment displacement time series [86].

The number of dimensions required to describe a dynamic system indicate how complex the system is. Dimensionality analysis can estimate dimensionality ( $D2$ ) for standing [153] and sitting [155].

Table A1: Posturographic measures derived from various methods for summarizing time-varying kinematic and kinetic variables during balance tasks. Typical abbreviations and units are included for some measures.

<b>Posturographic Measure</b>	<b>Abbreviation</b>	<b>Units</b>
<i>Time Domain Analysis</i> [25]		
Mean displacement of COP or body segment	MEAN	° or cm
Root-mean-square distance	RMS, VAR	° or cm
Mean velocity	MVELO	°/s or cm/s
Root-mean-square velocity	VARVELO	°/s or cm/s
Sway area	AREA-SW	deg <sup>2</sup> /s or cm <sup>2</sup> /s
Area of 95% confidence circle	AREA-CC	deg <sup>2</sup> /s or cm <sup>2</sup> /s
Area of 95% confidence ellipse	AREA-CE	deg <sup>2</sup> /s or cm <sup>2</sup> /s
Mean frequency	MNFREQ, MFREQ	Hz
Fractal dimension based on planar diameter	FDPD	
Fractal dimension based on the 95% confidence circle	FDCC	
Fractal dimension based on the 95% confidence ellipse	FDCE	
<i>Frequency Domain Analysis</i> [25]		
50% power frequency or median power frequency	MDFREQ, FREQ50	Hz
95% power frequency	UPFREQ, FREQ95	Hz
Centroidal Frequency	CFREQ	Hz
Frequency Dispersion	FREQD	
<i>Stabilogram Diffusion Analysis</i> [95]		
Diffusion coefficient for the short-term region	DS	deg <sup>2</sup> /s or cm <sup>2</sup> /s
Diffusion coefficient for the long-term region	DL	deg <sup>2</sup> /s or cm <sup>2</sup> /s
Short term scaling exponent	HS	

Long term scaling exponent	HL	
Critical point	CP	s
<i>Fractal Analysis</i> [97]		
Hurst exponent by rescaled range analysis	RRAH	
Hurst exponent by detrended fluctuation analysis	DFAH	
<i>Lyapunov Exponents</i> [154]		
Lyapunov exponent corresponding to the short interval	Ls	
Lyapunov exponent corresponding to the long interval	Ll	
<i>Sway Density Analysis</i> [156]		
Mean number of SDC peaks per second	MNUM	Hz
Mean time between consecutive SDC peaks	MDUR	s
SD of times between consecutive peaks	SDUR	s
Mean of the spatial distance between consecutive SDC peaks	MDIST	deg or cm
SD of the spatial distance between consecutive peaks	SDIST	deg or cm
Mean duration of the SDC peaks	MPEAKS	s
SD of the duration of the SDC peaks	SPEAKS	s
<i>Recurrence Quantification Analysis</i> [157]		
Percentage of recurrent data points	RECUR	%
Percentage determinism	DET	%
Mean diagonal length	DIAG	deg or cm
Entropy	RENTR	
<i>Sample Entropy</i> [86]		
Entropy	SENTR	
<i>Dimensionality Analysis</i> [153]		
Correlation dimension	D2	

## Selecting Posturographic Measures

Posturographic measures were selected based on three criteria: (1) linear independence from other posturographic measures (2) reliability, and (3) sensitivity to changes in postural dynamics. Previous studies of sitting balance have selected posturographic measures using one or more of these criteria: van Dieën et al. and Bardbado et al. calculated posturographic measures from COP

displacements during unstable sitting on a hemispherical seat [37], [44]; Larivière et al. calculated posturographic measures from COP displacements during unstable sitting on a seat with a central pivot and calibrated springs [23].

The first study found that *UPFREQ*, *DI*, *HI*, *CP*, *MNUM*, *MDUR*, *SDUR*, had low reliability; *HS*, *SDPEAKS*, and *MVELO* correlated with only one or none of other parameters; and the remaining measures could be explained by linear combinations of *RMS*, *MDFREQ*, or *DS* (*FD*, *CFREQ*, *FREQD*, and *D2* were not calculated) [37]. The second calculated only *RMS* and *MVELO*, and found that both had high test-retest reliability after a familiarization period (their correlation was not tested) [44]. The third study found that *FD*, *FREQD*, *RRAH*, *MNUM*, *MDIST*, and *SDIST*, and *DET* were the most reliable measures of postural sway (correlations were not tested, *DFAH*, *D2*, and *CFREQ* were not calculated) [23].

Previous research has explored interrelationships among posturographic measures derived from model simulations of upright standing, showing that ; the results are represented schematically in Figure A1 [150]. In the wobble board assessment demonstration (Chapter 4), we calculated *RMS* and *MVELO* from time domain analysis, *CFREQ* and *FREQD* from frequency domain analysis, and *HS* and *DS* from stabilogram diffusion analysis. Admittedly, exponential scaling exponents calculated by DFA or RRA may provide more precise estimates of long term correlations [97]. Additionally, it is possible that *SDPEAKS* or other measures could provide additional, unique information pertaining to seated stability [37]. However, DFA, RRA, SDP, and other analyses were omitted for the sake of brevity. Moreover, the present study aims to demonstrate the potential of the wobble board to be used as an assessment tool; it is beyond the scope of this study to determine which posturographic measures are ideal for unstable sitting assessment. In Chapter 4, Pearson's correlation coefficients were calculated to quantify the linear relationship between the selected posturographic measures.

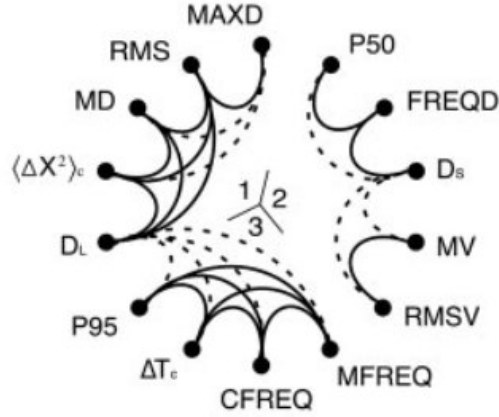


Figure A1: A schematic representation of 3 aggregated groups of posturographic measures obtained from model simulations of upright standing. Solid lines connect sway measures with correlation coefficients above 0.9, dashed lined connect posturographic measures with a correlation above 0.8 [150].

## Calculating Selected Measures

In the following section:

$x_i$  denotes  $AP_i$ ,  $ML_i$ , or  $TM_i$ , corresponding to the anteroposterior, mediolateral, or resultant displacement of the COP or segment at time frame  $i$

$n$  denotes the number of samples in the measurement

$T$  denotes the time span of the measurement

$\mu_i$  denotes the  $i^{\text{th}}$  spectral moment

## Time-Domain Measures

The mean tilt (*MEAN*) is the average of the absolute tilt values.

$$MEAN = \frac{1}{n} \sum_{i=1}^n |x_i|$$

The root-mean-square (*RMS*) is the average of the squared tilt values. For a zero-mean time series, this measure is equivalent to the standard deviation (*SD*).

$$RMS = SD = \sqrt{\frac{1}{n} \sum_{i=1}^n [x_i]^2}$$

The mean velocity (*MVELO*) is the total excursion divided by the duration of the trial.

$$MVELO = \frac{\sum_{n=1}^{N-1} |x_{i+1} - x_i|}{T}$$

## Frequency-Domain Measures

The centroidal frequency (*CFREQ*) is the square root of the ratio of second spectral moments to corresponding spectral densities between 0 and 5 Hz.

$$CFREQ = [\mu_2 / \mu_0]^{1/2}$$

The frequency dispersion (*FREQD*) is calculated from the ratio of first spectral moments to second and zero spectral moments between 0 and 5 Hz.

$$FREQD = \left[ 1 - \mu_1^2 / \mu_0 \mu_2 \right]^{1/2}$$

The  $k^{th}$  spectral moment is defined as the sum of the discrete power estimates, each multiplied  $k$  times by the corresponding frequency.

## Estimating power spectral density

The frequency of a postural response variable (e.g., COP, body segment displacement, or support surface tilt angles) may contain valuable information about the postural response. Consider the kinematic data recorded in Chapter 4: after the initial processing of wobble board tilt angles (resampling, demeaning, truncating), the time series to be analyzed are each 28-s in length, sampled at 32 Hz; yielding 896 samples per series. The periodogram can be estimated using a fast fourier transform. To decrease the variance of this power spectrum estimate, modified periodograms (Hamming windowed) are calculated for segments of the time series and averaged (this is known as Welch's method). Using more windows decreases the variance but also decreases the resolution. Some choices for window length and overlap are shown in Figure A2. Using 4 windows (358 samples each) with 179 sample overlap reduces the variance and

maintains a resolution of 0.09 Hz. This method was used to obtain power spectrum estimates for calculating frequency-domain posturographic measures (Chapter 4).

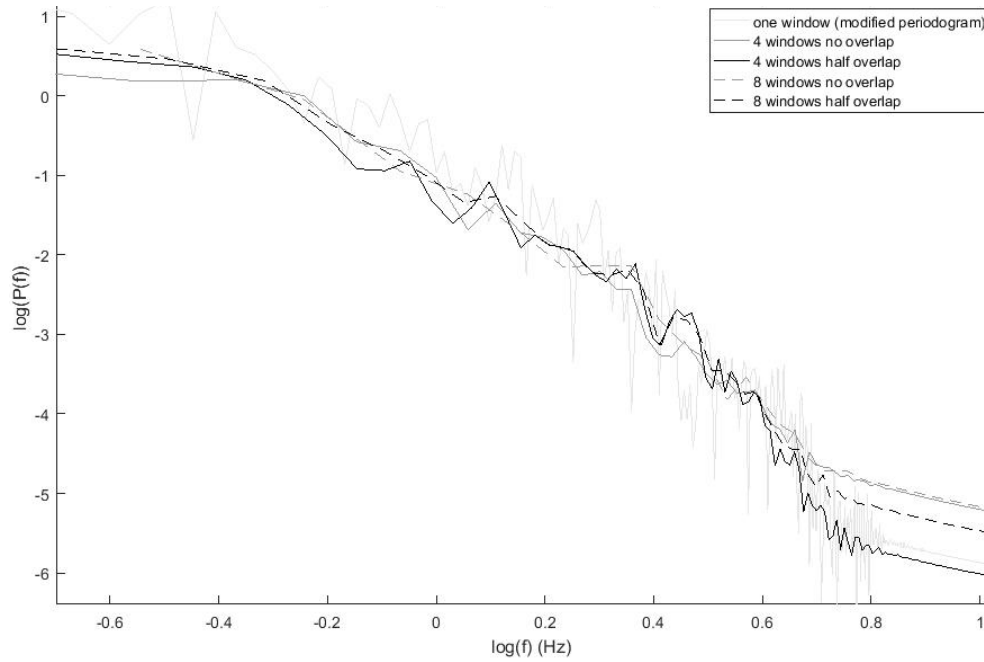


Figure A2: Single-sided amplitude spectrum of a 28-s tilt angle recording plotted on a log-log scale. The light gray line represents the estimate obtained from one modified periodogram. The remaining lines represent estimates according to Welch's method, with parameters described in the legend.

## Stabilogram Diffusion Plots

According to [95], the stabilogram diffusion plot (SDP), computes the square of the displacements between all pairs of points ( $\Delta x$ ) that are separated by a certain time interval ( $\Delta t$ ); these squared displacements are averaged, and the process repeated for increasing values of  $\Delta t$  [95]. For a COP or angular trajectory made up of  $N$  data points where  $\Delta t$  spans  $m$  sampling intervals, this computation is expressed as:

$$\langle \Delta x^2 \rangle_{\Delta t} = \frac{\sum_{i=1}^{N-m} (x_{i+m} - x_i)^2}{N - m}$$

where  $\langle \cdot \rangle$  indicates a calculation of the mean value. The diffusion coefficient ( $D$ ) is a measure of the behaviour of the mean square displacement relative to random walk in a straight line or plane. This relation is expressed as:

$$\langle \Delta x^2 \rangle = 2D\Delta t$$

The parameter  $D$  can be calculated from the slope of mean square COP displacement plotted against time intervals. Similarly, scaling exponents ( $H$ ) can be estimated from log-log scaled plots of the same data. When the stabilogram diffusion plot exhibits a different slope for short time intervals that for long time intervals, the critical point ( $CP$ ) is calculated as the intersection of these two slopes as shown in Figure A3. Then,  $D$  and  $H$  can be calculated for each region ( $DS$ ,  $DL$ ,  $HS$ ,  $HL$ ). Model simulations have suggested that parameters derived from stabilogram diffusion analysis should be more sensitive to changes in postural dynamics than most other sway measures [150].

Cholewicki et al. used stabilogram diffusion analysis to demonstrate that COP displacements exhibit antipersistent behaviour in the long term during dynamic sitting. [29]. In this study, an unstable sitting apparatus was placed on a force plate, and hemispheres with decreasing diameters were attached to the apparatus to achieve increasing levels of instability. The stabilogram diffusion plots feature long and short term regions similar to those seen in quiet standing [95]. In contrast to the open-loop interpretation of short term diffusion coefficients presented by [95], when users of the seat closed their eyes (i.e., removed visual feedback), short term diffusion coefficients were increased compared to trials with visual feedback, indicating that visual feedback affects the open-loop control system, which it should not according to the definition of open loop control [30]. This finding supports the alternative hypothesis that postural control is a continuously regulated feedback system, without open-loop systems [158].

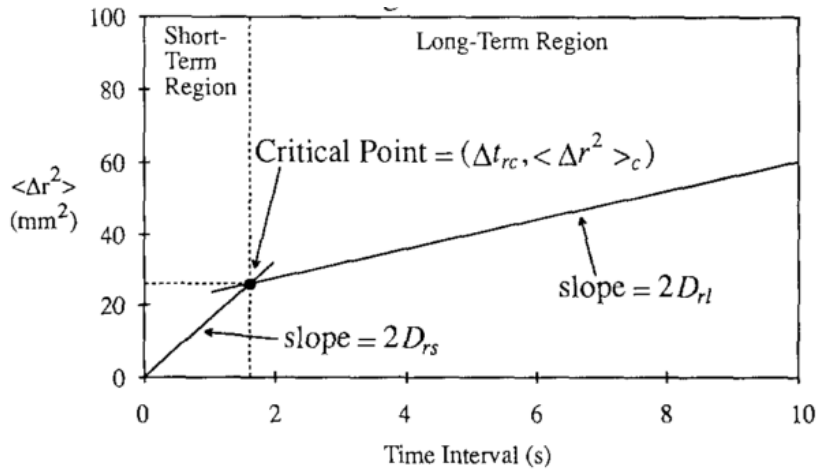


Figure A3: Schematic representation of stabilogram-diffusion plot and associated parameters [95].

## Appendix B: Bill of Materials

Table B1: Bill of materials for wobble board

<b>Component</b>	<b>Manufacturer</b>	<b>Part number</b>	<b>Cost per part (\$CAD)</b>	<b>Estimated mass per part (g)</b>	<b>Quantity</b>	<b>Total cost (\$CAD)</b>	<b>Total mass (g)</b>
Platform base	In-house <sup>(a)</sup>	8657K414	22.74	1071	1	22.74	1071
Platform filler	In-house	8657K421	135.38	4791	1	135.38	4791
Platform lid	In-house	8657K414	22.74	1571	1	22.74	1571
Hitch	In-house	6582K433	46.57	341	1	46.57	341
Leg Bar	In-house	6545K7	22.15	1008	1	22.15	1008
Foot Bar	In-house	4931T31	19.03	97	2	38.06	194
Adjustable							
Torque Knob	Vlier	TH103A			1		
Aluminum							
5/16-18 Rivet Nut	McMaster-Carr	93482A810	15.80		1	15.80	
3" 5/16-18 Threaded Rod	McMaster-Carr	90575A593	10.38		1	10.38	
Square Finishing Plug	McMaster-Carr	9565K51	16.10		1	16.10	
Clevis Pin	McMaster-Carr	97245A616	5.10		2	10.20	
Cotter Pin	McMaster-Carr	97245A616	5.10		2	10.20	
Counterbalance	In-house	8910K67	39.71	3623	1	39.71	3623
Curved Base	In-house						
Base stud	In-house	90596A039	7.58	92	1	7.58	92
Base extrusion	In-house	9546K43	4.03	28	1	4.03	28
2.5" 5/8-11 Threaded Rod	McMaster-Carr	90322A170	4.45	100	1	4.45	100

1/4" Washer	McMaster-Carr	91081A129	3.63	6	21.78	
3/8" Washer	McMaster-Carr	91081A131	7.68	2	15.36	
1/4" Hex Nut	McMaster-Carr	90499A029	3.80	6	22.80	
3/8" Hex Nut	McMaster-Carr	93827A225	17.70	2	35.40	
3/8-16x1x1 CS Bolt	McMaster-Carr	90911A624	19.37	2	38.74	
1/4-20x1.5x1.5 CS Bolt	McMaster-Carr	91858A546	7.86	2	15.72	
1/4-20x5/8x5/8 CS Bolt	McMaster-Carr	91500A538	9.67	4	38.68	
<b>Total</b>					<b>594.57</b>	<b>12819</b>

(a) In-house manufacturing and consulting was provided by the University of Alberta Mechanical Engineering machine shop, for a combined total of 63 hours at a rate of \$25 per hour.

Table B2: Bill of Materials for wobble board instrumentation

<b>Component</b>	<b>Manufacturer</b>	<b>Part number</b>	<b>Printing time (min)</b>	<b>Cost per part (\$CAD)</b>	<b>Quantity</b>	<b>Total cost (\$CAD)</b>
microprocessor board	Arduino	MEGA 2560		45.99	1	45.99
inertial measurement unit	x-io Technologies Limited	x-IMU with enclosure		504.56 <sup>(a)</sup>	1	504.56
IMU enclosure	in-house <sup>(b)</sup>	n/a	25		1	
Vibrational tactors	Sparkfun Electronics	LilyPad Vibe Board		8.35 <sup>(c)</sup>	8	66.80
Tactor enclosure	in-house	n/a	5		8	
Wiring and connectors	in-house	n/a				
<b>Total</b>						<b>617.35</b>

(a) conversion made using 1.63 CAD to 1.00 GBP as of July 30, 2017; costs do not include shipping, taxes, or fees

(b) 3D printing and electronics wiring was completed by the author at the Glenrose Research Centre.

(c) conversion made using 1.31 CAD to 1.00 USD as of June 19, 2017; costs do not include shipping, taxes, or fees

## Appendix C: Estimating Tilt Angles from Motion Capture Measurements

In trunk biomechanics and many other applications, we often want to convert the measured locations of reflective markers into angles that represent the orientation of the body segment or support surface being marked. Methods for doing so are described below.

In the context of rigid body biomechanics, a local coordinate system (LCS) is an orthonormal basis of vectors attached to a rigid body in 3D space. Any rotation of the rigid body is reflected in the direction of the vectors that comprise the LCS. Any translation of the rigid body is reflected in the location of the origin of the LCS.

In the technical validation study, the location of four reflective markers on the wobble board surface (*ANT*, *POST*, *LEFT*, *RIGHT*) were measured and used to determine a LCS defining the time-varying orientation of the wobble board with respect to the global coordinate system (GCS) of the laboratory. In particular, the LCS was defined as

$$\vec{r}_y = ANT - POST \quad 6$$

$$\vec{r}_z = \vec{r}_y \times (RIGHT - LEFT) \quad 7$$

$$\vec{r}_x = \vec{r}_z \times \vec{r}_y \quad 8$$

A rotation matrix is a matrix that postmultiplies one LCS to give the vectors coordinates of another, thus defining the relative orientation of two LCSs. Note that the rotation matrix ( $R$ ) between the global frame (an identity matrix) and the wobble board LCS is just the LCS (Equation 10). This is not true for, say, the rotation matrix between LCSs defining trunk orientation and pelvic orientation.

$$R = \{\vec{r}_x, \vec{r}_y, \vec{r}_z\} \quad 9$$

$$[LCS] = [R][GCS] \quad 10$$

The tilt angles obtained from a 3-dimensional rotation matrix depend on the sequence of planar rotations assumed to comprise it. For example, rotating by  $\gamma$  about the x-axis, then  $\beta$  about the y-axis, then  $\alpha$  about the z-axis gives a different result than rotating about by the same angles about the y-, then z-, then x-axis. Furthermore, the rotations could be performed about the new axes as

they are formed (moving axes), and about the same axis more than once. Rotations about consecutive moving axes produce Euler angle sets, while rotations about fixed axes produce Cardan angle sets. This procedure is detailed in p 44-52 of [159] and p 39-51 of [135].

## Cardan Angle Method

According to a suggested procedure for calculating human joint angles [160], a Cardan sequence was selected: rotation about the fixed axes z-y-x (yaw, then roll, then pitch), which is equivalent to rotating sequentially about the moving axes x-y-z. The derivation of the of the angle set is shown in equations 11 and 12. Equations 13 and 14 show how the tilt angles in the *AP* and *ML* planes can be extracted from this matrix according to [135], noting that the *ML* axis coincides with the y-axis, and the *AP* axis with the x-axis of the wobble board LCS. Note that *atan2* is the four-quadrant inverse tangent, and  $r_m$  are the column vectors of the wobble board rotation matrix, i.e., the normalized position vectors of the wobble board LCS in the global reference frame. There will be some systematic bias introduced by the selection of rotation choice of order.

$$R_{yaw}R_{roll}R_{pitch} = [\vec{r}_x \ \vec{r}_y \ \vec{r}_z] \quad 11$$

$$\begin{bmatrix} c\alpha & -s\alpha & 0 \\ s\alpha & c\alpha & 0 \\ 0 & 0 & 1 \end{bmatrix} \begin{bmatrix} c\beta & 0 & s\beta \\ 0 & 1 & 0 \\ -s\beta & 0 & c\beta \end{bmatrix} \begin{bmatrix} 1 & 0 & 0 \\ 0 & c\gamma & -s\gamma \\ 0 & s\gamma & c\gamma \end{bmatrix} = \begin{bmatrix} cac\beta & cas\beta s\gamma - sac\gamma & cas\beta c\gamma + sas\gamma \\ sac\beta & -sas\beta s\gamma + cac\gamma & -sas\beta c\gamma - cas\gamma \\ -s\beta & c\beta s\gamma & c\beta c\gamma \end{bmatrix} \quad 12$$

$$\angle ML = \beta = atan2\left(r_x \vec{k}, \sqrt{r_x \vec{i}^2 + r_x \vec{j}^2}\right) \quad 13$$

$$\angle AP = \gamma = atan2(r_y \vec{k}, r_z \vec{k}) \quad 14$$

## Projection Method

The *ML* and *AP* tilts can also be calculated as the angle between each local coordinate vector (x,y) and its projection onto the z-plane, after normalizing the LCS vectors to unit length.

$$\angle ML = \sin^{-1}(r_x \vec{k})$$

$$\angle AP = \sin^{-1}(r_y \vec{k})$$

This method neglects the dependency of rotations and their order; each rotation (*AP*, *ML*) is assumed to be the first rotation. Therefore, any component of *ML* tilt that could actually be resolved into *AP* tilt is neglected. An advantage of the projection method is that there is no bias introduced by sequence dependency. Therefore, comparisons between *AP* and *ML* tilts cannot be confounded by the chosen Cardan sequence. However, obtaining a three parameter description of the wobble board orientation using projection angles is not as straightforward as the use of Cardan or Euler angles [160].

## Comparison

The Cardan angle method and projection method produce nearly indistinguishable results for the range of tilt angles demonstrated in the technical validation study (Figure C1). Using either method, the results of the technical validation study (Chapter 3) were unchanged. We decided to use the Cardan method to maintain consistency with similar and future experiments where tilt angles are calculated not only for the wobble board, but also for the angle between body segments.

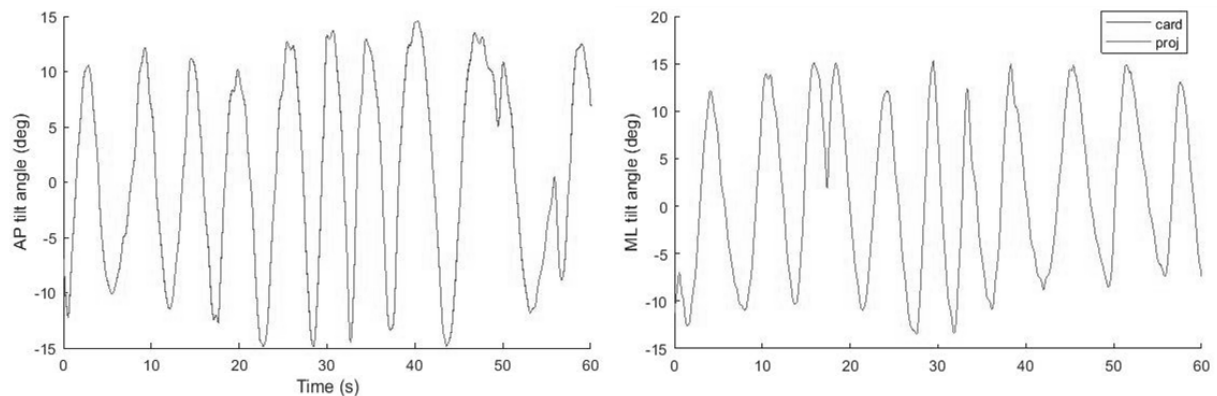


Figure C1: Comparison of *AP* (left) and *ML* (right) tilt angles calculated by Cardan angle method (black lines) and projection method (gray lines) showing the virtual indistinguishability of the resulting angles for an exemplary technical validation trial.

## Appendix D: Preliminary Protocol

This experimental protocol was designed for the same purposes as that described in Chapter 4, i.e., to validate the wobble board functions by assessing and training seated balance in a sample of non-disabled volunteers. For reasons discussed below, the protocol was revised; the second edition is described in Chapter 4.

### Method

#### Experimental Protocol

Each participant was asked to maintain upright sitting on the wobble board with no foot support and eyes open or eyes closed (randomly selected). Base #1 (the least curved, most stable base) was attached to the wobble board. The participant performed one 30-s balance trial in this condition. The trial started after the participant donned noise-cancelling headphones, folded arms across the chest, and verbally cued the experimenter of being ready. The experimenter monitored the participant for safety and noted any loss-of-balance events. If the control signal, defined as the tilt angle of the wobble board plus one half its tilt velocity, remained below the feedback threshold in both the AP and ML direction for more than 18 seconds (60 % of the initialization trial), the trial was repeated on the next-most curved base. This procedure was repeated until the 60 % criterion was met. If the participant failed to maintain balance for 30 seconds, the next-least curved base was selected. After selecting a base, the participant attempted six consecutive trials under the same base and eye condition. Three of the six trials were randomly selected as control trials; during these trials, the tactors remained inactive. The experimenter informed the participant of the upcoming feedback condition. For the feedback trials, direction-specific vibrating tactors were activated when the control signal exceeded a two-sided threshold in one or both of the *AP* or *ML* directions. If the *AP* signal passed the *anterior* threshold, the three *anterior* vibrators turned on. Similarly, the three tactors in the *posterior*, *left* and *right* directions were activated if the control signal in the corresponding direction passed respective threshold. Thus, the feedback scheme is *repulsive cueing*. The participant was allowed to rest for as long as needed between trials. Then, the eye condition was changed, and six more trials were performed after another series of initialization trials to select the base. The initialization procedure ensures that the task is neither so simple that the vibrotactile feedback is not used, nor so difficult that the

participant cannot maintain upright sitting. During each trial, the wobble board tilt was sampled at a frequency of 32 Hz.

## Analysis

The data were processed and posturographic measures were calculated as described in Chapter 4. Linear regression and paired t-test were performed using the posturographic measures from each trial as dependent variables. The linear regression used the trial number (1-6) as independent variable, thus testing for learning effects from the beginning to the end of each trial set. If learning effects are present, we expect a change in dependent variables as the participant progresses through the trials. A hypothesized zero-slope of a linear regression line was tested for all 6 trials, for the 3 feedback trials, and for the 3 control trials. The linear regression was performed for each participant's trials and for all trials together. We also fit these same three regression lines to averages from all participants for each eye condition.

The paired t-test used vibration status as the dependent variable, thus testing for significant differences between feedback trials and control (no feedback trials). In each eye condition group, there are 36 feedback trials and 36 control trials. These groups cannot be compared using t-tests (paired or unpaired) because this would violate the assumption of independence; measurements from the same participant are not independent from each other. To validate the assumption of independence, each set of 3 dependent measurements (from the same participant) are averaged. This reduces the sample group to 24 measurements that are assumedly independent (each comes from a unique participant's average for one of the feedback conditions). With this new sample group, a paired t-test was carried out.

## Results

All 12 participants completed 6 trials under each eye condition (eyes closed: EC; eyes open: EO) resulting in 72 trials available for analysis.

## Results of linear regression tests

As shown in Figure D1 and Figure D2 respectively, the regression lines with a significant slope were FREQDtm\_EO ( $p=0.048$ ) and CFREQml\_EC ( $p=0.040$ ). This suggests that certain kinematic measures were significantly affected by the progression of trials from start to finish.

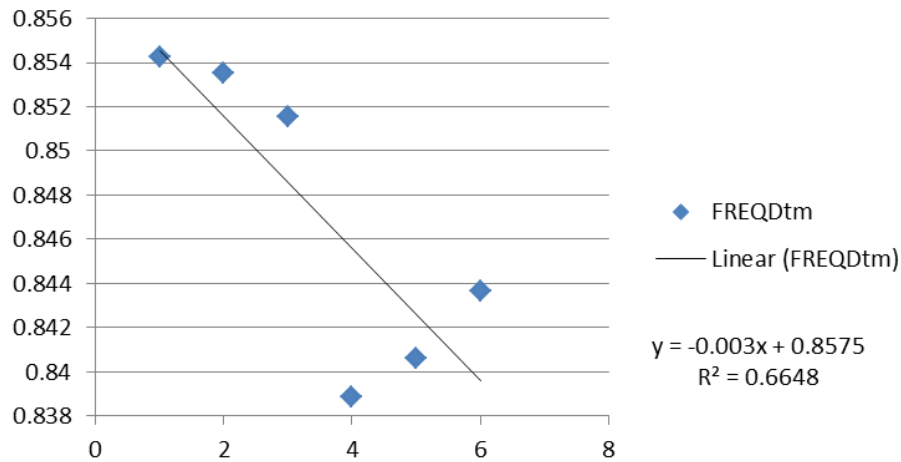


Figure D1: Average frequency dispersion of tilt angle in first to sixth trial under eyes open condition and a least-squares linear regression model

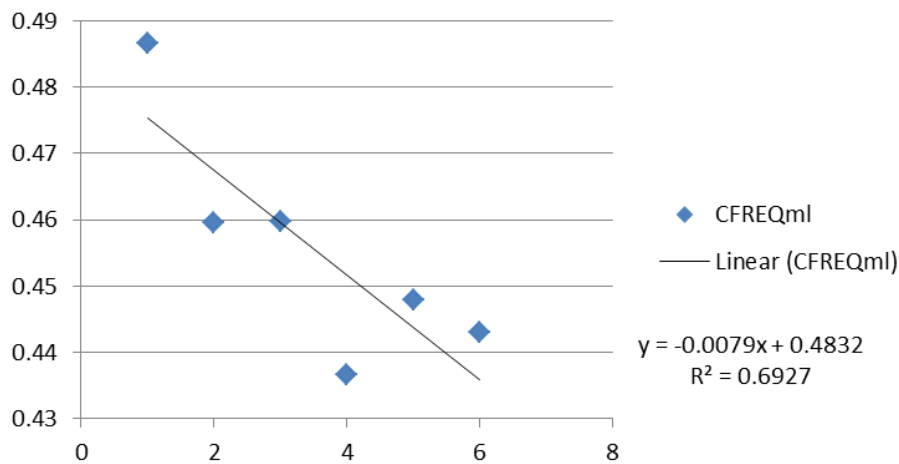


Figure D2: Average centroidal frequency of tilt angle in first to sixth trial under eyes closed condition and a least-squares linear regression model

## Results of paired t-test

This test revealed significant differences between feedback and control conditions for two of the kinematic measures: MEANap and FREQDap. Both measures were higher on average in control trials, suggesting that the vibrotactile feedback caused a reduction in the mean tilt angle and frequency dispersion of the tilt angles.

## Discussion

Within each participant, the base factor and eye factor are dependent, i.e., when one is changed, so is the other. This means that any comparison between eye conditions is confounded by the effect of changing the bases, and any comparison between base conditions is confounded by the effect of changing the eye condition. This experimental design only allows for statistical comparison between vibration conditions. This major shortcoming was addressed by separating the eye and base factors; in the refined protocol, each participant attempts to balance under each combination of eye and base conditions. Eye condition and base condition can then be considered independent factors and their effect on balance performance can be statistically analyzed. As a consequence, the number of trials was increased from 12 to 24. Additionally, four practice trials were mandated prior to each new combination of eye and base condition. Thus, the total number of trials in the refined protocol is 40 (16 practice trials, 24 experimental trials). Furthermore, the thresholds for feedback were set to equal the third quartile of the positive (and third quartile of the negative) feedback control signal for each tilt direction (*AP*, *ML*) during an initialization trial, resulting in the vibrators being active approximately 50 percent of the time.

Due to the major limitations of this protocol (dependence of manipulated factors, small sample size per participant, inconsistency of practice instructions and threshold calculation) the results were trivial; the refined protocol was designed to observe all and additional results presented in the preliminary protocol.

## Appendix E: Filtering Kinematic Time Series

High frequency components of the tilt angle measurements may be artifacts of noise in the measurement system. Since the dominant frequencies of movements during balance are generally less than 1 Hz [68], measurements of support surface tilt angles are typically filtered using low-pass digital Butterworth filters with cut-off frequencies between 2 Hz [40], and 20 Hz [110]. Butterworth filters have a nearly monotonic frequency response in the passband, so low-frequency components of the signal are maintained. In addition, the nonlinear phase response is accounted for by filtering in the forward direction and the reverse direction, which eliminates any phase distortion.

The built-in matlab function was used to design a fourth order, low-pass Butterworth filter with a cut-off frequency of 5 Hz, as used in [25], [64], [100]. The amplitude and phase response of this filter are shown in Figure E1 and Figure E2, respectively. The pole-zero plot is shown in Figure E3. Since all poles are within the unit circle, the filter is stable for any stable input.

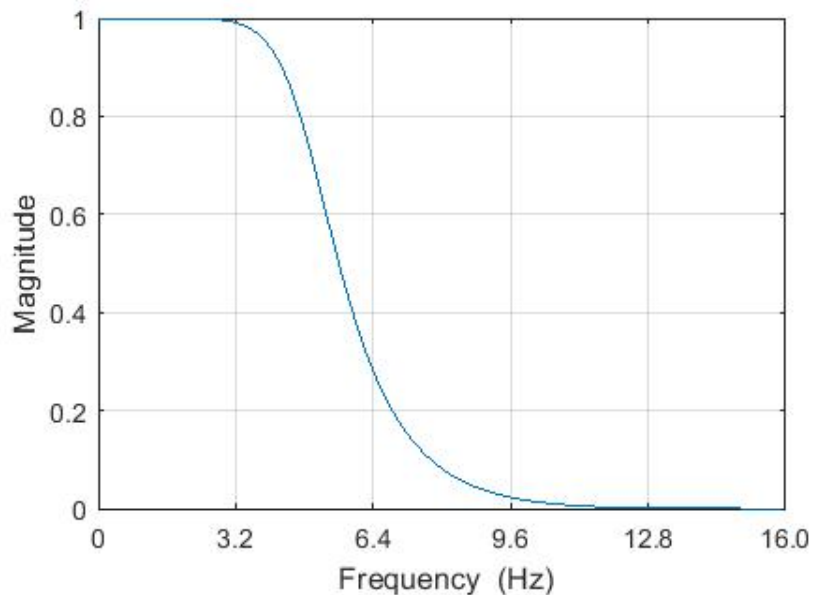


Figure E1: Magnitude response of a fourth-order, low-pass Butterworth filter

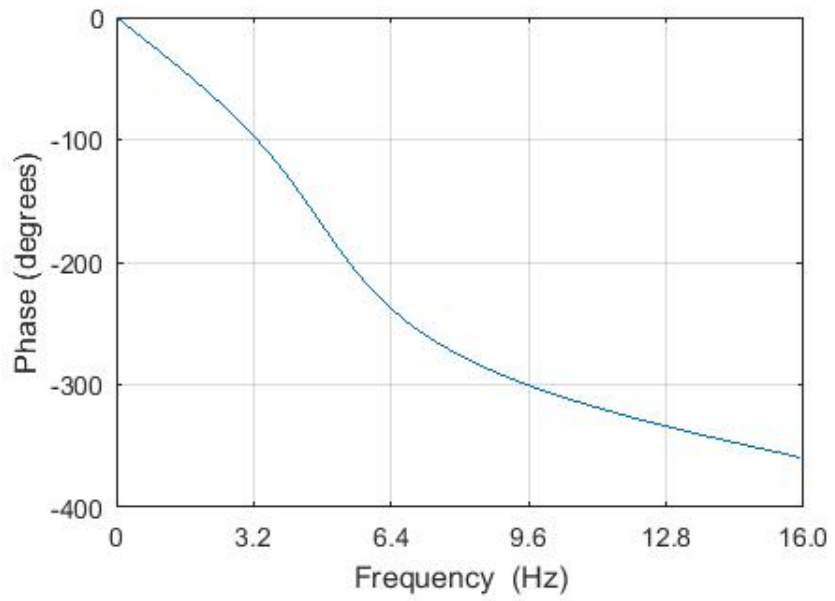


Figure E2: Phase response of a fourth-order, low-pass Butterworth filter

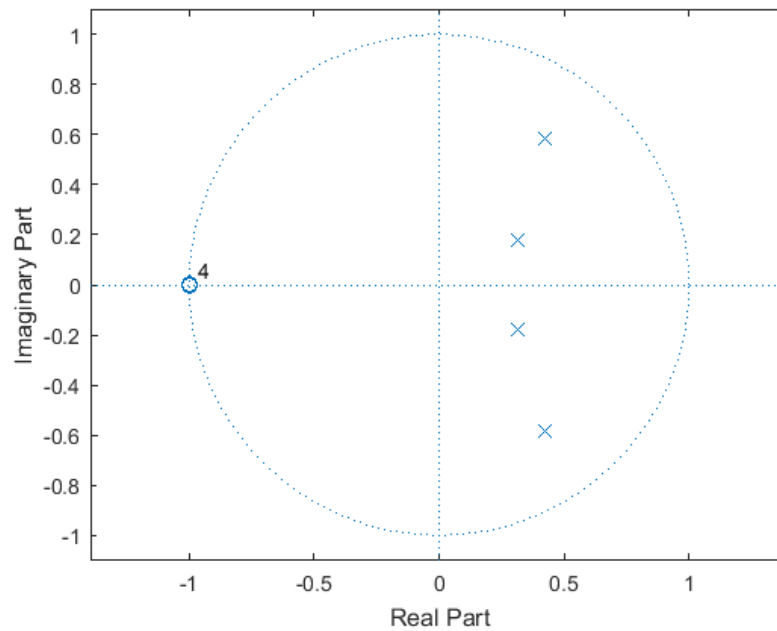


Figure E3: The poles (x's) and zeroes (o's) corresponding to a fourth-order, low-pass Butterworth filter.